personal buildup for

Force Motors Ltd.

MTZ worldwide 11/2009, as epaper released on 16.10.2009
http://www.mtz-worldwide.com

content:

Sampling of Engine Combustion Chamber Samples In High Temporal Resolution. p.46-53

MTZ
WORLDWIDE
11 | November 2009 Volume 70
www.MTZonline.com

The New 6 ¾ I-V8 Turbo Engine for the Bentley Mulsanne

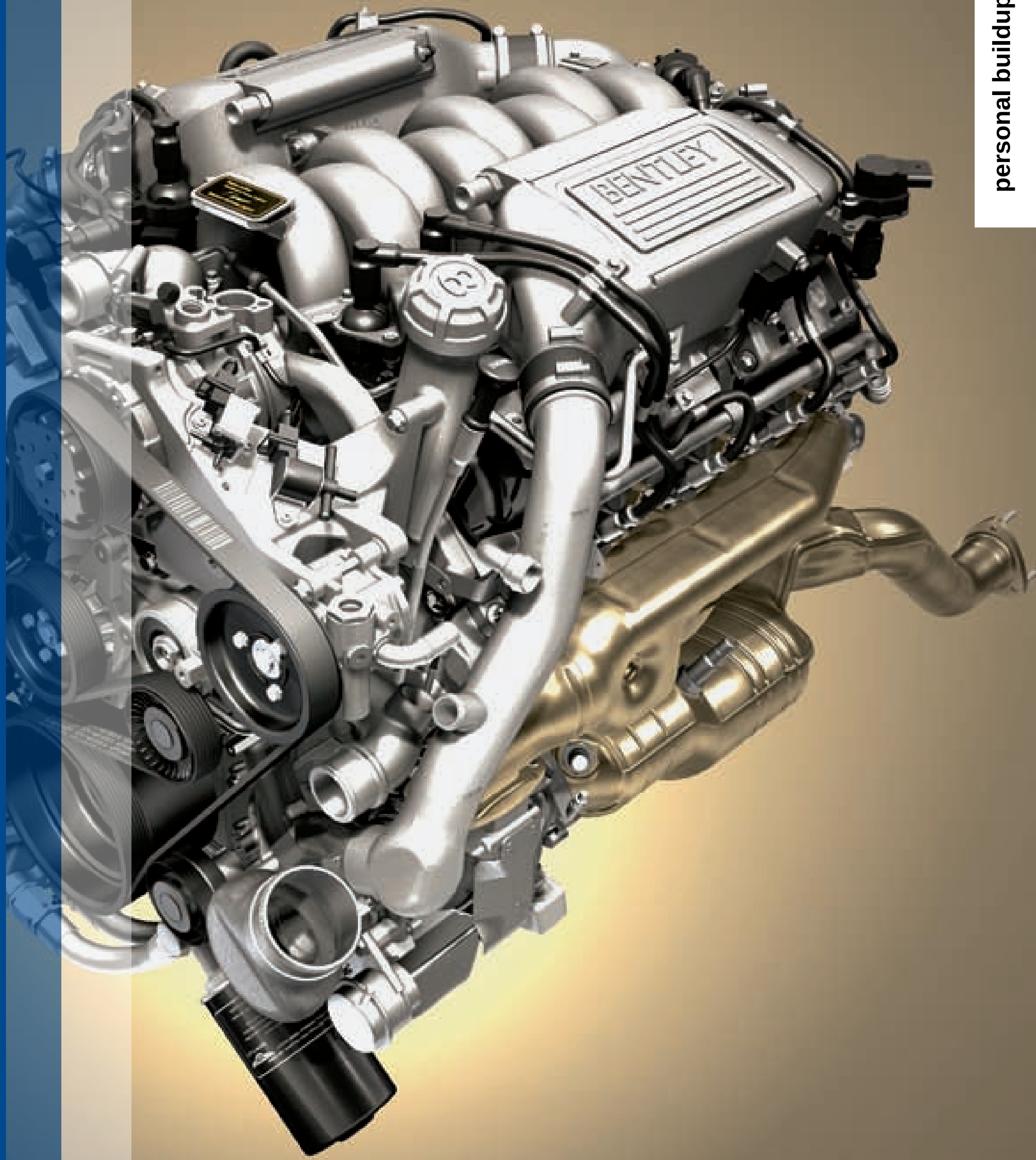

Reduction of Nitrogen Oxide Emission from Maritime Diesel Engines in Common Rail Operation

The New BMW V12 Gasoline Engine

Optimisation of Gasoline Engine Performance and Fuel Consumption through Combination of Technologies

KATsim – A Tool for Numerically Simulating Exhaust-gas Catalysts

Gas Sampling Probe for the Sampling of Engine Combustion Chamber Samples in High Temporal Resolution

For more information visit:
www.MTZonline.com

COVER STORY

The New 6 ¾ I-V8 Turbo Engine for the Bentley Mulsanne

4
The objective of the development for the Bentley Arnage successor, the Bentley Mulsanne, was to be the best vehicle in its class. The challenges for the new **6 ¾ I-V8 Turbo Engine** were to strengthen the brand values of performance, driveability, design and craftsmanship whilst optimising fuel consumption, emissions and quality.

COVER STORY

DEVELOPMENT

RESEARCH

RUBRICS

The Barometer is Rising

Dear Reader,

The doors to the IAA hadn‘t even closed when VDA President Matthias Wissmann announced that this year‘s show had been a success: With around 850,000 visitors, the drop in numbers was only 15 % and therefore less than the conservative estimates given before the event.

My personal conclusion regarding the show is also positive. Above all, because people are still clearly fascinated by cars. Whether it was the Mercedes SLS AMG, Audi R8 Spyder or Maserati Gran Cabrio, the visitors flocked to those stands that signalled automotive dynamics and driving enjoyment – features that were entirely lacking among most of the electric prototypes on show. But that‘s what people are like: Climate change is an abstract threat that we can avert only if efficiency does not mean austerity. Audi and BMW take this symbiosis to extremes with their “e-tron” and their „Vision Efficient Dynamics“. Breathtaking design coupled with intelligent technical solutions.

In my conversations with suppliers, many at top management level, I asked about their expectations for 2010. The relatively unanimous opinion: we will see single-digit percentage growth next year. This will, of course, not make up for the sharp falls in production volumes that we experienced at the end of last year. But it does mark a turning point from which, according to Bosch CEO Franz Fehrenbach, we can expect sustainable growth.

So let us bring this „annus horribilus“ to an end with dignity and the least possible losses. And then off to new horizons. Out there is a world in which many people in emerging economies can afford individual mobility for the very first time. A world that urgently requires solutions for using finite energy resources more efficiently.

I wish you all the best for the year-end rally.

Johannes Winterhagen
Cologne, 28 September 2009

Johannes Winterhagen
Editor-in-Chief

MTZ WORLDWIDE
11|2009

Founded 1939 by
Prof. Dr.-Ing. E. h. Heinrich Buschmann and
Dr.-Ing. E. h. Prosper L'Orange

Organ of the Fachverband Motoren und Systeme im VDMA, Verband Deutscher Maschinen- und Anlagenbau e.V., Frankfurt/Main, for the areas combustion engines and gas turbines

Organ of the Forschungsvereinigung Verbrennungskraftmaschinen e.V. (FVV)

Organ of the Wissenschaftliche Gesellschaft für Kraftfahrzeug- und Motorentechnik e.V. (WKM)

Organ of the Österreichischer Verein für Kraftfahrzeugtechnik (ÖVK)

Cooperation with the STG, Schiffbautechnische Gesellschaft e.V., Hamburg, in the area of ship drives by combustion engines

Heritage, Technology, Torque: The All-new 6 ¾ l-V8 Turbo Engine for the Bentley Mulsanne

The objective of the development for the Bentley Arnage successor, the Bentley Mulsanne, was to be the best vehicle in its class. The challenges for the engine were to strengthen the Bentley values of performance, driveability, design and craftsmanship whilst optimising fuel consumption, emissions and quality.

1 Introduction

With the completely revised V8, **Figure 1**, Bentley have created a new up to date engine, continuing 50 years of the basic layout, which is 6 ¾ litre engine displacement, 90° V8, two pushrod driven valves per cylinder and high torque at low engine speeds all combined with the latest technology.

The main objectives for the development of the new Bentley V8 engine were

- meet legislation for EU5/LEV2
- refinement to be “Best in class”
- fuel consumption/CO_2 reduction
- weight reduction
- retain Bentley quality standards
- improved performance feel.

2 Design and Development

During the 50 years development of the Bentley V8 engine many changes have taken place, but it has always retained its main characteristics according to the introduction, **Table**. For the development of this engine, Bentley stayed with this configuration as these characteristics define the Bentley V8 from other European high performance engines. These are the characteristics required to preserve the uniqueness and heritage of this classic British marque.

2.1 Crankcase and Main Bearing Caps

The crankcase design is a deep-skirted aluminium mono-block with wet cast iron liners. A new main bearing support system was developed, **Figure 2**, using a cast iron bearing cap with integrated cross beam to tie into the side skirts. The caps are made from spheroidal graphite iron. Because of the architecture of the crankcase it was not possible to include cross supports for the front and rear caps. The front cap does not take as much loading as the others and so was not deemed to be a problem. However the rear cap clearly takes much of the load from engine torque and support of the torque convertor. The solution here was to use a four bolt vertical arrangement with a much wider cap. With a new cast-

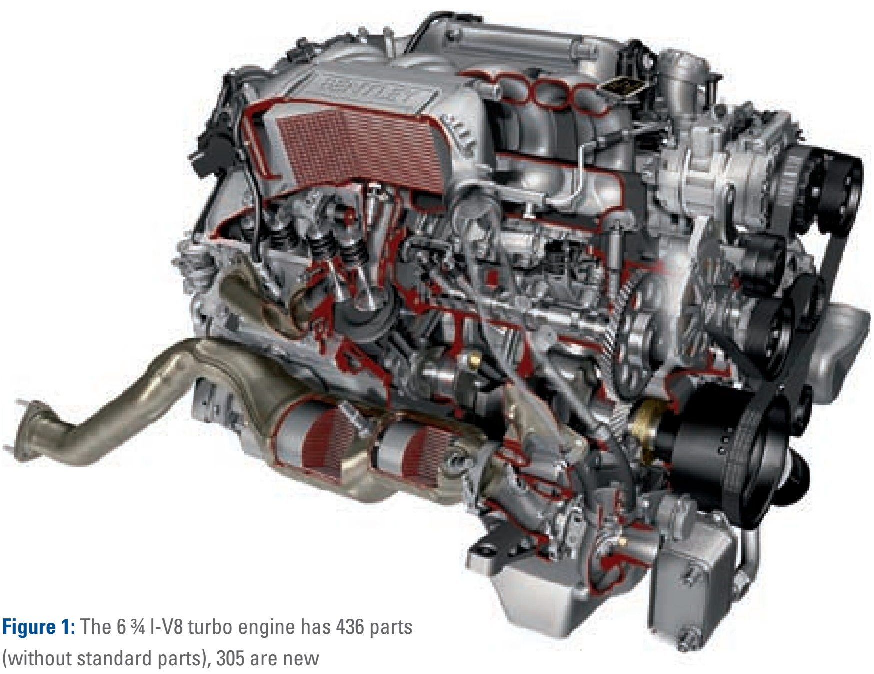

Figure 1: The 6 ¾ l-V8 turbo engine has 436 parts (without standard parts), 305 are new

The Authors

Brian Gush C.Eng FIMechE
is Director of Chassis, Powertrain and Motorsport at Bentley Motors Ltd. in Crewe (England).

Dipl.-Ing. Michael Fleiss
is Functional Manager of Engines and Test Centre at Bentley Motors Ltd. in Crewe (England).

Simon Baron-Oxberry B.Eng
is Senior Engineer for V8 and W12 Development at Bentley Motors Ltd. in Crewe (England).

John Humphries
is Senior Engineer for V8 Design at Bentley Motors Ltd. in Crewe (England).

Tim Seipel
is Senior Engineer for V8 Calibration at Bentley Motors Ltd. in Crewe (England).

Table: Engine data [1]

	1959	1999	2002	2006	2010
	S2	Arnage			Mulsanne
Model	S2	F1	F6	MY'07	MY'11
Engine design	V8 (90°)				V8 (90°)
Charging method	–	Single Turbo	Twin Turbo	Twin Turbo	Twin Turbo
Engine displacement [cm³]	6230	6750			6750
Bore [mm (inch)]	104.15 (4.1)				104.15 (4.1)
Stroke [mm (inch)]	91.44 (3.6)	99.06 (3.9)			99.06 (3.9)
Con-rod length [mm (inch)]	165.1 (6.5)				175,0
Cylinder spacing [mm (inch)]	120.65 (4.75)				120.65 (4.75)
Compression Ratio	8.0:1	7.8:1			7.8:1
Bank offset [mm (inch)]	25.4 (1)				25.4 (1)
Valves per cylinder	2				2
Inlet/Exhaust valve diameter [mm]	45.7 / 35.8	48.2 / 42.4			48.2 / 42.4
Main bearings	5				5
Main bearing diameter/width [mm]	63.5 / –	67.1 / 27.0			65.0 / 18.5
Con-rod bearing diameter/width [mm]	57.2 / 20.0				56.0 / 16.0
Maximum power [kW] (Engine speed [min⁻¹])	135 (4000)	300 (4000)	335 (4100)	373 (4200)	377 (4200)
Specific power [kW/l]	21,67	44,44	49,63	55,26	55,85
Maximum torque [Nm] (Engine speed [min⁻¹])	350 (1800)	835 (2100)	875 (3250)	1000 (3250)	1020 (1750-3250)
Brake mean effective pressure [bar]		15,49	16,29	18,61	19,03
Firing Order	1-5-4-8-6-3-7-2	1-3-7-2-6-5-4-8			1-3-7-2-6-5-4-8

ing and machining supplier further refinements were possible, which have reduced shrinkage porosity and mass.

2.2 Cranktrain

For the Mulsanne engine it was decided to renew the cranktrain, **Figure 3**, reducing mass whilst at the same time protecting for future performance increases. The scope was to make it "future-proof" for model year changes, both in terms of torque and engine speed. Cooperation with suppliers during the design and development stages helped to optimise quality and cost effectiveness.

2.2.1 Piston

The design remit for the piston was to reduce mass whilst at the same time allowing for an increase in cylinder loading (up to 85 bar) to protect for the future, **Figure 4**. In order to minimize mass, the compression height was reduced and a trapezoidal small end design was employed, allowing the pin to be shortened. Consequently, the side panels were brought closer together, resulting in a narrower skirt.

The pin diameter remained the same at 25.4 mm (one inch) and is now DLC Diamond Like Carbon coated. To prevent the piston from load concentration, the skirt profile was optimised and piston cooling jets were introduced. The ring pack was also raised to allow the reduction in compression height, although the ring spacing remained the same as the current engine. Due to the introduction of cam phasing a valve relief had to be added.

The crown and top ring land are hard anodised and the skirts graphite coated. A weight reduction of 130 g for each piston assembly was achieved.

2.2.2 Connecting Rod

The rod length was increased by 9.9 mm to account for the reduced compression height in the piston, **Figure 4**. The rod retained its I-beam section but was improved around the shoulder to the big end and the transition to the small end to increase strength. The bolting arrangement was changed to screws (as opposed to bolts and nuts), which attached through the cap into the rod fork. The cap alignment was controlled by spiral pins between the cap and fork.

The small end has a trapezoidal design, to remove unwanted mass and incorporates a lead free bushing with two oil holes for lubrication. The big end bearing shell (lead free) width was reduced by 20 % to reduce the friction losses.

The rod mass is reduced by 100 g over the previous design. Also, due to the better quality forging tool and manufacturing methods the mass variation between parts is within a 17 g range. To achieve excellent refinement the con-rods are supplied in weight matched sets.

Figure 2: Main bearing

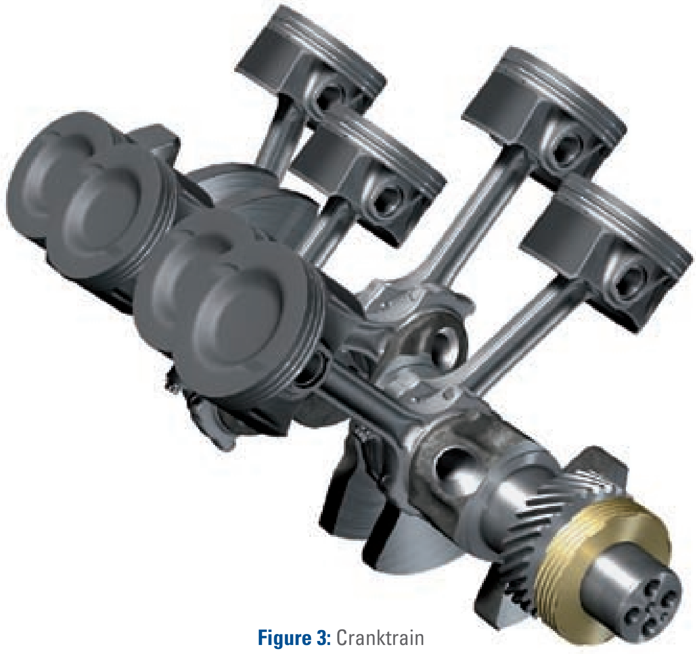

Figure 3: Cranktrain

2.2.3 Crankshaft

In the Arnage crankshaft, the oil feeds for the con-rods came from the main bearing journals, feeding into an angled cavity within the crank pin [2]. This crank pin then had cross drillings for each con-rod bearing intersecting this cavity. The purpose of the cavity was as a "sludge trap" to collect any sludge and oil contaminants which had managed to get to the con-rod oil feeds. The deposits would accumulate at the outer end of the cavity due to centrifugal forces. This was deemed necessary many years ago when oils did not have the detergent additives which are included in modern oil blends.

The design objectives for the crankshaft, **Figure 5**, were to retain its "dual plane" form to ensure good refinement for the vehicle occupants and to maintain the distinctive V8 "burble" associated with the large Bentley.

The design was carried out by utilising latest design software to produce an optimised crankshaft, which is 6000 g lighter than its predecessor. This was achieved with some careful profiling of the counterweights, optimising the web cheek areas and introducing lightening holes through each of the crank pins as well as along the length of the crankshaft (from the rear through the 2nd main journal).

The journal diameters were also reduced to nominal 65 mm for the mains (reduction of 2 mm) and 56 mm for the rods (reduction of 1.25 mm). This was to reduce bearing speed and also to allow the use of latest VW Group bearing technology. The lemon shaped bearings are lead free and have a MoS_2 coating.

The oil feeds for the con-rods are more typical of modern oiling systems, whereby there is a direct oil feed from the main bearing to the crank pin for each con-

Figure 4: Piston and connecting rod of Mulsanne (left) and Arnage (right)

Figure 5: Crankshaft, Mulsanne (left) and Arnage (right)

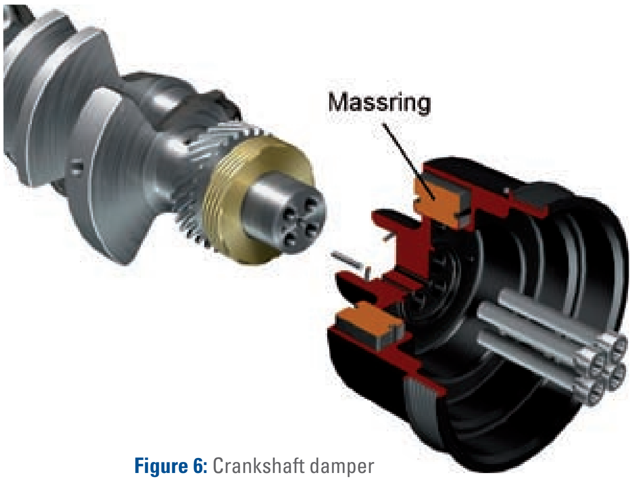

Figure 6: Crankshaft damper

rod. The sludge cavities have been deleted. The oil feeds deliver oil to the crank pin 37 degrees prior to TDC, ensuring a good lubrication condition just prior to the heaviest load.

The crank still carries the gears for driving the cam and oil pump. However, in order to simplify the manufacture and assembly processes, these gears are now shrink fitted – instead of a woodruff key with a fine threaded locknut – to the crankshaft at the crank supplier. The cam drive gear is aligned radially and axially to the crankshaft. This process eliminates an expensive machining operation and a difficult assembly process.

The bespoke Bentley rear crank seal was changed to a standard VW group part. This was done to reduce the running diameter and hence crankshaft mass.

2.2.4 Torsional Vibration Damper and Flywheel

Analysis showed that an elastomeric damper would overheat due to the torque and vibration input from the new cranktrain operating at the design limits for speed and output, therefore a visco-damper was designed, **Figure 6**. A number of potential design variants were considered before opting for a single inertia system, with the inertia ring mounted as close to the first main bearing as possible in order to minimise whirling about the crank nose. The new design resulted in a mass saving from the Arnage engine of 3000 g.

Another consideration for the Torsional Vibration damper was that the Mulsanne engine would be equipped with cylinder deactivation. This meant that the damper had to cope with high 2nd order vibrations as well as 4th order. The damper was designed with this in mind and test results show that it is a very effective part in all operating conditions and speeds. The mounting of the damper changed from a single stud arrangement to a four screw fixing arrangement. This improved the clamping load considerably and simplified the design. In order to further secure the connection between crank nose and TV damper, a diamond-coated washer is used between the parts for increased friction.

2.2.5 Engine Balancing

In order to improve refinement of the base engine, the cranktrain is "trim balanced" during the assembly process at Crewe. This process is fairly unique and continues for the Mulsanne engine. Whilst all the individual components are balanced and manufactured to tight tolerances, differences in mass between the piston/rod/bearing assemblies installed in the engine and the mass "assumed" during the balancing of the crankshaft assembly can become significant. The "short motor" assembly is installed on a balancing rig, which carries the engine in a special cradle that can move in any direction in the horizontal plane. Sensors detect the positional movement of the cradle at the front and rear of the engine. When the motion of the engine assembly is correlated to the crank angular position, the machine tells the operator how much correction (and where) to

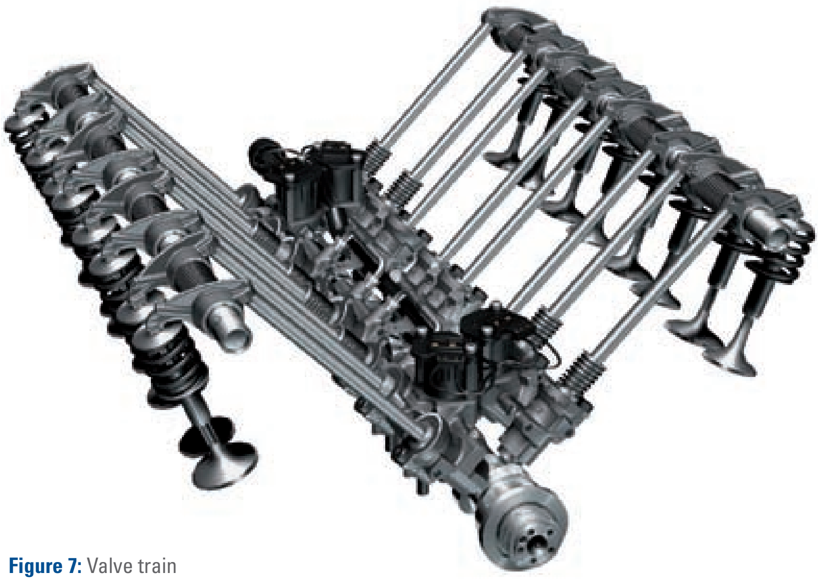

Figure 7: Valve train

Figure 8: Camshaft and phaser

make on the cranktrain. This process continues until the motion of the engine is less than 5 μm at 730 rpm.

2.3 Valvetrain

Camshaft phasing and cylinder deactivation have been introduced for the new Mulsanne V8, **Figure 7** and **Figure 8**. Together they bring about perhaps the most significant changes for the driver; a huge improvement in refinement, especially at idle, a large increase in low speed torque giving the car unparalleled performance and a reduction in the CO_2 emissions.

The requirement for a large improvement in idle speed refinement involved some detailed examination of combustion. It was determined that this process was variable at idle, between each cycle on individual cylinders and also between the cylinders on the engine. This led to a distinctive random "kick" felt under certain conditions. Key to improving combustion was the reduction in residual exhaust gas from the previous cycle, whilst maintaining a consistent charge between cycles. By testing it was proved that closing both the intake and exhaust valves sooner achieved both these conditions.

1D simulation modelling was used along with design of experiment techniques to derive a model of engine performance with varying inputs of valve lift, duration, separation between intake and exhaust and position relative to crankshaft for both intake and exhaust valves. The outputs from the model were residual exhaust gas in the cylinders and engine torque. From this model came the ability to determine not only the best compromise on lift, duration and separation across the engine speed, but also some starting points for the calibration team.

2.3.1 Camshaft

For the new engine the camshaft, Figure 8, is manufactured from steel billet and has roller followers.

The cam lobe profiles were designed to:
- optimise conditions for idle quality
- significantly increase low speed torque
- maintain high peak torque
- achieve the 505 bhp/1020 Nm target.

The camshaft has a hole gun drilled along almost its entire length for mass reduction. It also has features at its drive end to accommodate the oil feeds for the cam phaser.

2.3.2 Camphaser

The cam phaser, Figure 8, is a new component for the Mulsanne engine. It is attached to the camshaft drive gear. A mechanism to feed oil to the cam phaser was needed which reduced the amount of available gear width. In order to prevent durability issues the gear was made narrower and from steel. Lightening holes were incorporated to remove much of the extra mass incurred due to the material change.

A similar phaser is used on the Volkswagen V6 engine. As it is mounted on the rear of the chain driven V6 valvetrain, the direction of rotation was then correct for the front of the gear driven Bentley V8. The phaser has a range of 42° (crankshaft) and is infinitely variable across its entire range.

It also incorporates a locking pin mechanism to ensure the cam is in the most advanced position for start up whilst the engine has low oil pressure. An assistor spring on the phaser balances the forces from the valvetrain such that the oil pressure is used only to move the cam position and not to resist its drive torque.

A control solenoid sits in the crankcase above the phaser, in the main oil gallery feed for the cylinder heads. This solenoid directs oil to the advance/retard chambers of the phaser via a "cam closure plate'. This closure plate performs a number of functions: directing oil to the phaser; providing a thrust face for the camshaft and sealing the oil supply cavity at the front of the crankcase.

2.3.3 Cylinder Deactivation System

The system, **Figure 9**, works by disabling four of the cylinders during light load operation. When the system is active (cylinders disabled) not only is the fuelling to 4 of the cylinders cut, but also the valves of those cylinders are de-activated. This prevents energy waste from pumping air and also protects the catalysts from damage.

The cylinders which are deactivated are 2,3,5,8, which maintains a "V" configuration and hence crankshaft balance. The firing interval becomes 180° instead of 90°. By maintaining 2 working cylinders on each bank there is an added advantage of maintaining equal turbocharger speed which will assist in the event of a "step in" throttle demand.

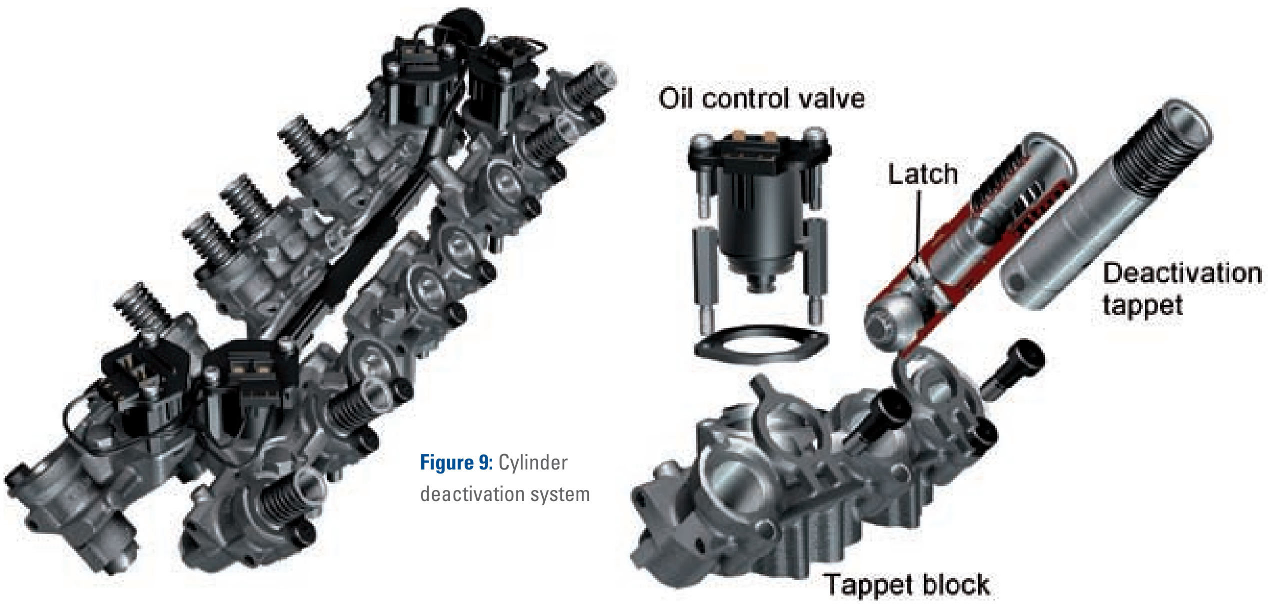

Figure 9: Cylinder deactivation system

The mechanism for deactivation is electronically controlled, via hydraulic actuation and mechanical operation. Four solenoid valves control oil flow to the intake and exhaust tappets at each of the deactivation cylinders. The solenoids fit into newly designed tappet blocks and are controlled via an electrical harness inside the tappet chest. When the high pressure oil flows to these tappets, internal latches are compressed allowing the inner body to collapse into the outer body. The outer body continues to follow the cam profile whilst the inner body remains motionless, hence the valve remains closed. De-activation and re-activation happen in the specific firing order within 2 revolutions of the crankshaft. Due to the finite time available for these events to occur, the maximum engine speed for cylinder deactivation to operate is limited to 2500 rpm. This equates to 40 ms to de-activate or re-activate the four cylinders.

Unlike an OHC engine, which has a complex hardware solution for cylinder deactivation, the pushrod valvetrain of the Mulsanne engine lends itself to a simpler solution.

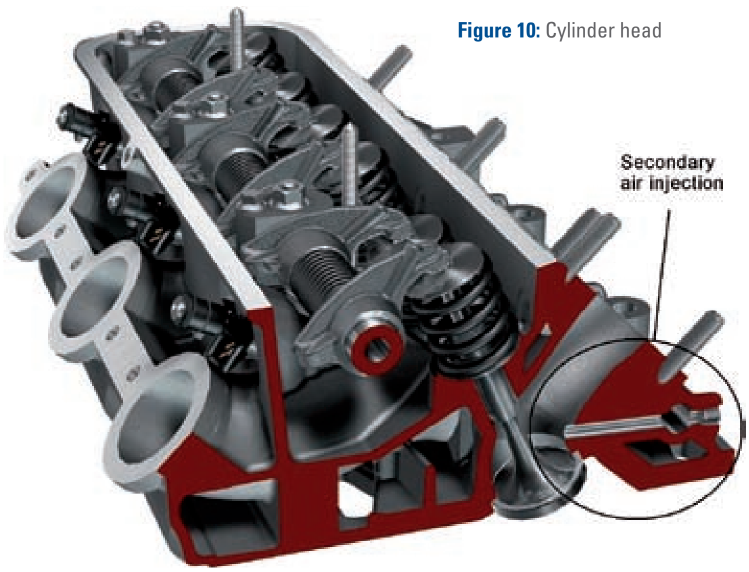

Figure 10: Cylinder head

2.4 Cylinder Head

Cylinder head changes for the new V8 engine were primarily to incorporate the secondary air injection rail into the cylinder head casting, **Figure 10**. The previous system used a separate pipe to connect the secondary air control valve with the injector nozzles inserted above each exhaust port in the cylinder head. The Euro 5 emission standards required a major improvement to the efficiency of the secondary air injection system. The design of the new system has dramatically reduced the operating pressure, as the injection is now in the area of the exhaust port with the lowest pressure. In addition injecting to the hottest area of exhaust gas has improved the conversion of the unburned hydrocarbons.

A 16 mm diameter rail was cast into the exhaust side of the cylinder head, between the inner and outer cylinder head bolts, which was connected to the exhaust ports by drilled injector ports near to the exhaust valve.

2.5 Water Cooling System

A considerable weight saving potential was identified with the Arnage water pump. Therefore a survey of likely pump specifications from group engines was conducted. The existing pump from the Bentley W12, **Figure 11**, engine was a likely candidate and the performance specification was similar to the original pump.

Testing showed that the pump output was less than with the original, but compensated by increasing the pump speed by 14 %. To mount the new water pump, a new volute housing was required, which replaced the complex 270°. volute of the original with a more easily manufactured 90° volute. This also gave the opportunity to design a new one piece crankcase front cover, which deleted the requirement to seal between the upper and lower parts. In addition the belt driven viscous fan for the radiator was replaced by electric motored fans.

3 Engine Management and Calibration

3.1 Electronic Management System, New Actuators and Sensors

A change in engine management system was required for several reasons; increased technical content of the engine requiring extra electrical pins, an increase in computational power and a new interface to vehicle systems. The change from the Bosch ME7 to the ME17 platform enabled the use of latest generation sensors and actuators for improved quality, reliability and cost. Indeed, some improvement in engine operation was possible due to these sensor changes resulting in faster and better controlled starts and improved fuel control.

Torque Structure in the common platform changed from the industry-known central relative torque coordinator to a physically based absolute system with sequential distribution along the torque path (wheel-gearbox-clutch-crankshaft). Not only was this compatible with the latest Bosch ESP Premium vehicle stability programme, Adaptive Cruise Control and the all new 8-speed transmission but protects for any future additional vehicle management concepts.

3.2 EU5/LEV2 Emission Specification

Europe's EU5 rules for emissions come into effect in January 2011. Moving the large Bentley from N1 class 3 to the M1 vehicle class resulted in another substantial reduction in emissions limits (approximately 50%) requiring major changes for this to be achieved. The key to meeting EU5 was to get the catalysts lit off as fast as possible whilst also precisely controlling the exhaust lambda.

Working with catalyst experts, the latest washcoat was selected giving a more tolerant gas conversion. Zoned loading of the precious metals enhanced the light-off at the front face of the brick. Where rapid heating wasn't required, at the rear face of the catalyst, the metal content was halved, ensuring good oxygen storage capacity for the life of the car. To maintain a low exhaust back-pressure and hence engine performance, a 400 cpsi metal matrix starter and 300 cpsi main catalyst was used.

To help catalyst light-off further improvements to the Secondary Air Injection system were made. High flow, bank individual, air pumps with self switching control valves replaced a single pump with vacuum operated control valves to simplify the system diagnosis.

During the after start condition, precise fuel/air mixture control was imperative. The LSU4.9 advanced Oxygen sensor from Bosch was specified which lights up in approximately half the time than the sensor used previously. These changes together with subtle changes to the engine speed after start and ignition timing used enabled the emissions targets to be met.

3.3 Cam Phasing

As described earlier, to reduce the compromises of fixed camshaft timing, a phaser was added to enable the optimum camshaft timing for all operating conditions. Investigations proved that there was little benefit in controlling the inlet and exhaust timing separately so a much simpler system with the single phaser was used. At part load conditions the timing is retarded. Delaying the overlap position reduces the pumping loses, improving fuel economy. This condition also increases residual gas content, reducing NO_x emissions. Due to the late exhaust valve opening HC emissions also reduce as more time is available for in-cylinder oxidation before the blow down event. For low speed performance, the camshaft is advanced to give an early inlet valve closing and consequent torque improvement. For best idle quality, the timing is also advanced reducing the residual gas fraction and improving cycle to cycle variation.

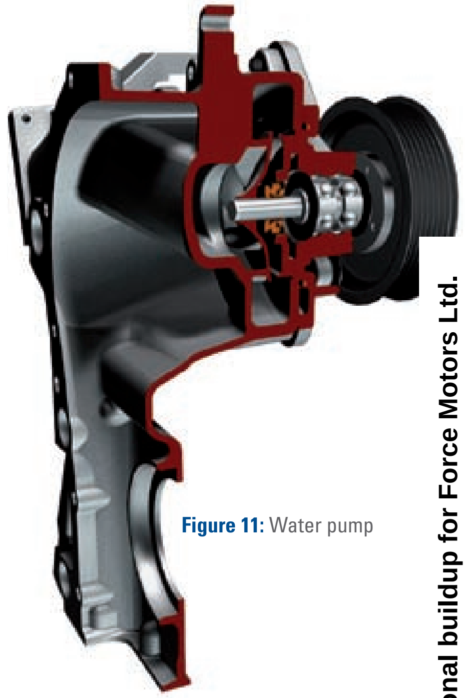

Figure 11: Water pump

3.4 Cylinder Deactivation

Because of the sudden change in engine capacity when switching from 4-8 or 8-4 cylinders, the torque delivery from the engine also changes abruptly. In order that the torque delivery remains smooth and constant, the throttle must also switch abruptly to compensate for the change in capacity. This is only achievable with latest engine management technology and electronic throttle control. The software to manage the cylinder deactivation was a new development by Bentley and Bosch Engineering.

The CDA system is operating during most of the "normal" driving conditions experienced by the driver, and even in cruise conditions on typical urban roads. The driver is unaware of the switching of the system, the only indication that he has of the system working is the reduction in "real world" fuel consumption.

The biggest advantage of operating in 4 cylinder mode is engine efficiency due to reduced pumping losses. Pumping losses are at their highest at the lowest load conditions. Although improvements can also be found at any part throttle condition, the improvements diminish as manifold conditions approach atmospheric pressure. Further limitations exist when the technology is

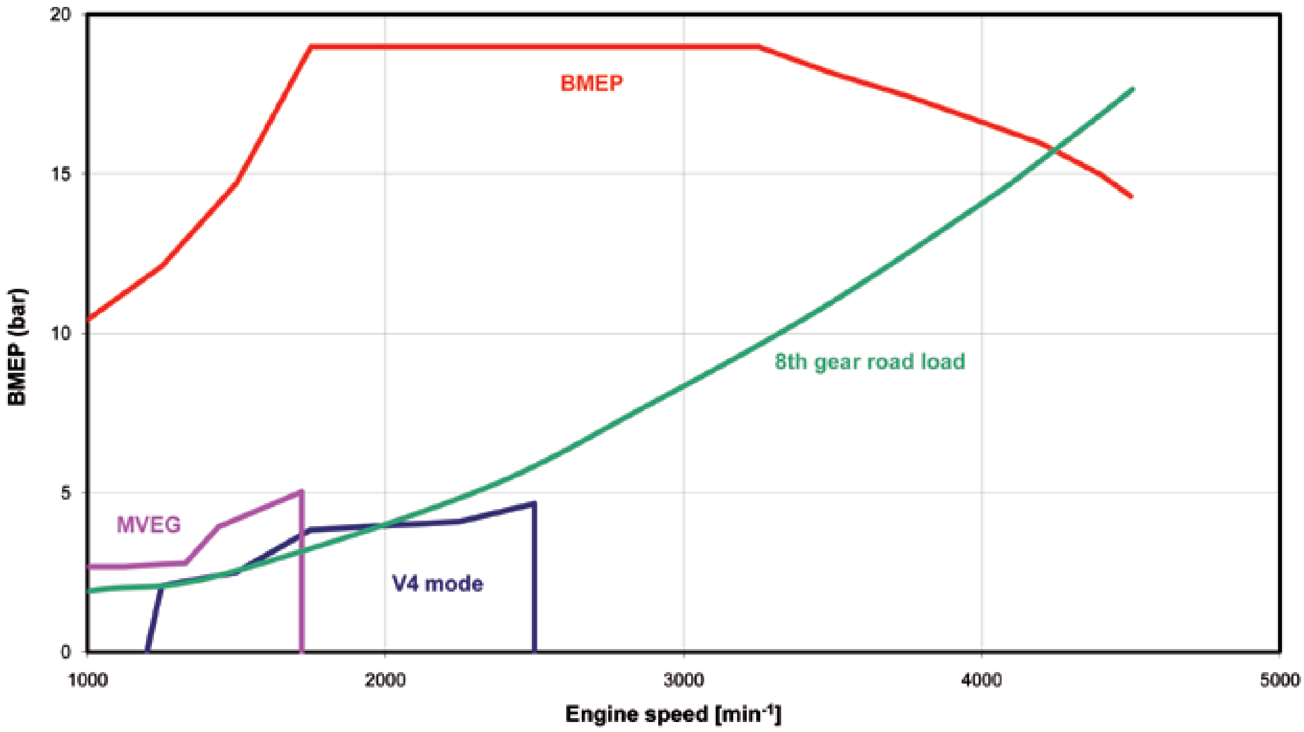

Figure 12: Cylinder deactivation window

applied in vehicle due to its effects on sound quality and vibration, mostly in the 2nd order mode. Changes to the vehicle to isolate this help to increase the load window of half engine mode.

Although the operating window, Figure 12, seems quite small, in the Bentley vehicle, this equates to both a significant amount of the MVEG drive cycle (33 %), improving the CO_2 emissions by approximately 8 % and also around 19 % in "real World" usage. The MVEG cycle, Figure 13, shows, the points at which the engine is in half engine mode and the cumulative time.

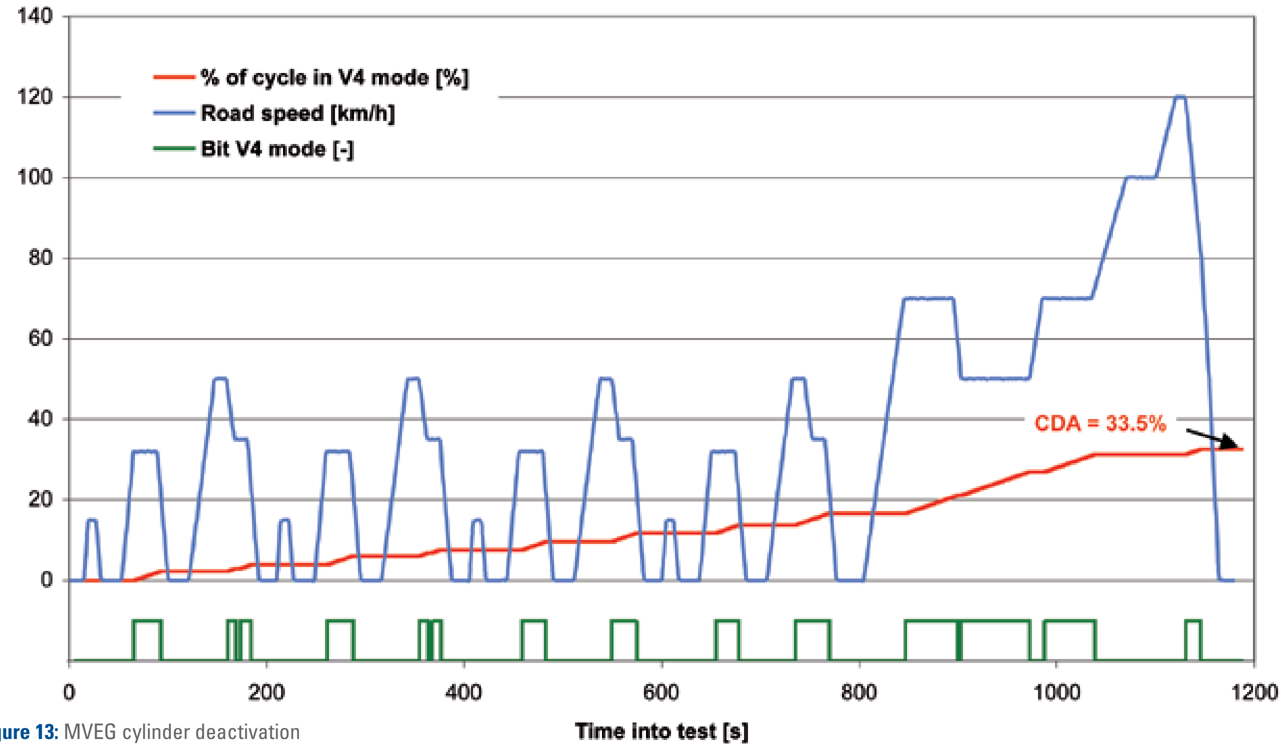

Figure 13: MVEG cylinder deactivation

It can be seen that the system is quick to operate after starting when a gear from 4th to 8th is selected. The system is not used below 4th gear as this would compromise vehicle refinement as lower gears are effectively transient conditions. When a demand is made to accelerate the vehicle, the engine instantly reverts back to full engine mode for seamless acceleration. Once this demand is reduced and the vehicle settles to a steady cruise condition at low load, half the engine is turned off again. To reduce any effects on NVH, a small amount of torque convertor slip is applied as a damper to 2nd order inputs to the drivetrain. This slip is increased during the transition into and out of the half engine mode.

4 Summary

The 377 kW (505 BHP) engine is a worldwide unique combination of traditional engineering art and the latest technology. Using known camphaser technology, excellent idle stability and huge torque of 1020 Nm at engine speeds have been achieved, **Figure 14**.

For the first time in the Volkswagen group, cylinder deactivation is being used. Thus the CO_2 emssions could be reduced by more than 15 %. A completely new cranktrain has been developed. Durability and quality have been optimised at the same time as significant weight and cost reductions.

With the new engine management system and the revised secondary air system, the V8 meets the EU5/LEV2 emission limits.

References

[1] Gush, B.; Becker, N.; Seipel, T.; Baron-Oxberry, S.: Der neue V8-Twin-Turbo-Motor im Bentley Arnage MTZ 01/2007

[2] Ludvigsen, K.: Bentley's great 8, 2009

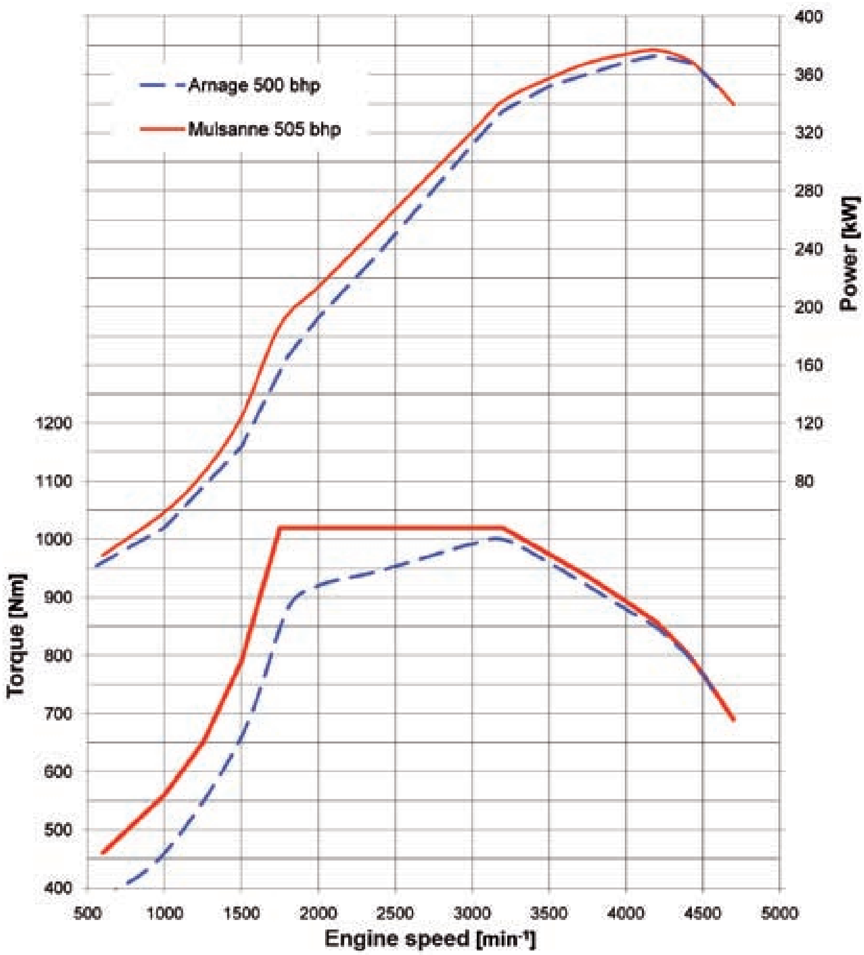

Figure 14: Performance and torque

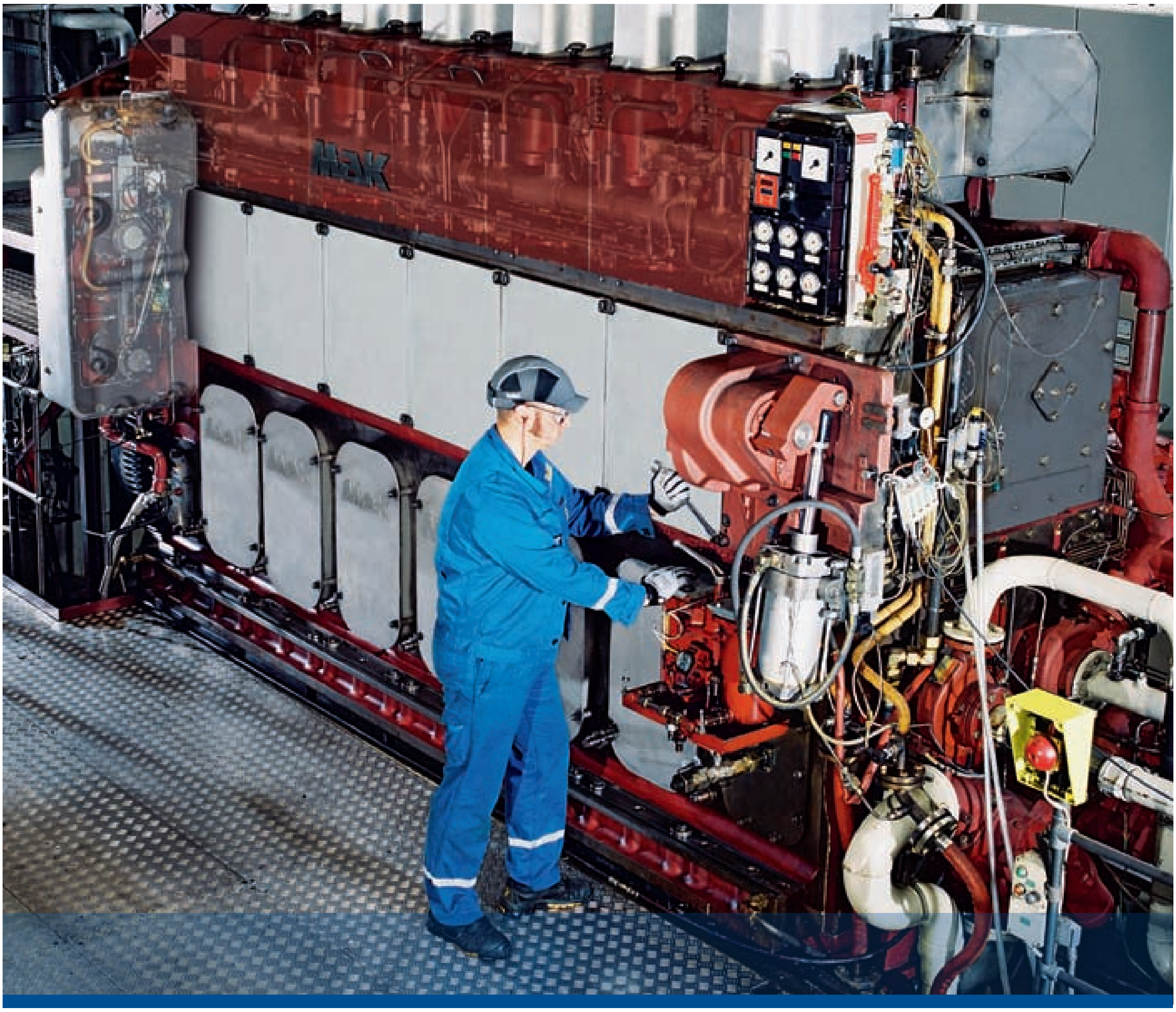

personal buildup for Force Motors Ltd.

Reduction of Nitrogen Oxide Emission from Maritime Diesel Engines in Common Rail Operation

In the framework of the joint EMI-MINI II project, research activities on how to meet the future IMO limits for maritime diesel engines have been performed over a period of 3 years. A reduction of NO_x emission by approximately 40 % could be reached by a combination of the Miller cycle with the common rail injection technology, while keeping the efficiency factor constant and an acceptable smoke behaviour.

1 Introduction

Since 2000, the nitrogen oxide emission from ocean-going ships has been limited according to a regulation from the International Maritime Organisation IMO [1]. In October 2008, a new multi-stage model for a further drastic reduction of NO_x emission was agreed on [2]. **Figure 1** shows the limit value trend and the state of today's maritime diesel engines.

The IMO II limit, which will come into force from 2011, requires a reduction by 20 % compared to IMO I. Additionally, from 2016, the IMO III limit will come into force for the so called Emission Control Areas, which requires a reduction of the NO_x emission by 80 % compared with the current level. While some engines already achieve the IMO II level, with in-cylinder measures and enhanced combustion processes, today, additional measures or an exhaust gas after-treatment will be required for the IMO III level.

In regard to these developments, experimental and theoretical studies have been performed within the framework of the EMI-MINI II project subsidized by the Federal Ministry of Economics and Technology (BMWi). The objective of these activities was to study the potential of the Miller cycle in combination with a direct-controlled common rail injector suitable for heavy fuel oil for the pollutant reduction within maritime diesel engines. To cover the entire chain of effects of the fuel injection, the combustion process and the formation of pollutants up to pollutant emission, five specialised partners established a research network. A heated high-pressure injection chamber was available at the chair of piston and combustion engines of the Rostock University for the analysis of the injection process with respect to injection jet dispersion and fuel evaporation. Fundamental studies of pollutant formation and reduction were performed on a single-cylinder diesel engine for research purposes at WTZ Roßlau gGmbH. These experimental activities were supplemented by computational simulations of the injection process, combustion process and pollutant formation at AVL Deutschland GmbH, Munich. The research results were implemented in practice on the maritime diesel engine M 32 CR of Caterpillar GmbH & Co. KG, Kiel. L'Orange GmbH from Stuttgart developed a single-circuit common rail injector suitable for heavy fuel oil opening new possibilities to deal with the problems associated with the Miller cycle.

2 Development Tools

2.1 Simulation Models

The CFD code FIRE was used for the modelling of the injection, scavenging, combustion and pollutant formation. Therefore, a combined simulation method was used to compute the cavitating mul-

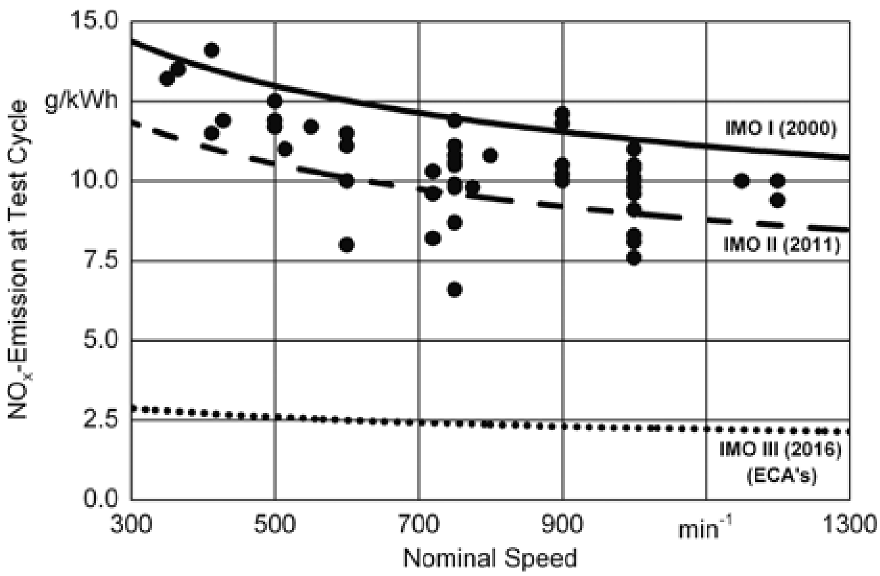

Figure 1: NO_x emission limiting by the IMO regulation

The Authors

Dipl.-Ing.
Christian Fink
is Scientific Assistant at the Chair of Piston and Combustion Engines of the University Rostock (Germany).

Dr.-Ing.
Moritz Frobenius
is Manager of the Advanced Simulation Technologies Department of AVL Deutschland GmbH in Munich (Germany).

Dr.-Ing.
Roland Pittermann
is Manager of the Environmental Laboratory of WTZ Roßlau gGmbH in Dessau-Roßlau (Germany).

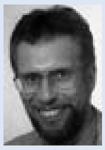

Dr.-Ing. Udo
Schlemmer-Kelling
is Manager of New Technology Introduction at Caterpillar GmbH & Co. KG in Kiel (Germany).

Dipl.-Ing.
Hartmut Schneider
is Senior Manager of Advanced Development at L'Orange GmbH in Stuttgart (Germany).

tiphase flow within the nozzle. The flow variables determined on the nozzle outlet are used as a boundary condition for the simulation of the fuel spray within the high-pressure chamber or engine. In a first step, for the spray simulation, the model parameters for droplet decomposition and evaporation were set in a way to reach a good match between calculated and experimentally determined values for the droplet penetration depth and the droplet spectrum [3]. Based on this, the combustion and pollutant formation models were adjusted. These were validated on the basis of studies on the FM 16/1 single-cylinder research diesel engine [4]. These models were used to perform the CFD simulations of the scavenge and combustion process for the M 32 CR maritime diesel engine.

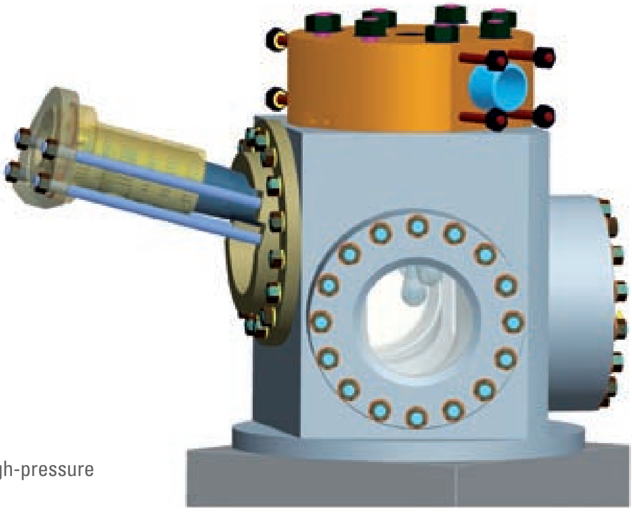

Figure 2: Heated high-pressure injection chamber

2.2 High-pressure Injection Chamber

For studies on the mixture formation and for the validation of the simulation models mentioned above diesel and heavy fuel oil injection sprays were optically analyzed in a heated high-pressure injection chamber, **Figure 2**. This chamber is specifically designed for large injectors and temperatures up to 900 K at a pressure of 60 bar. Using several scattering light and laser methods, characteristic parameters such as jet penetration length, jet cone angle, droplet sizes and droplet velocities were measured on injection jets reaching a length of up to 130 mm.

For the simultaneous analysis of the jet penetration and evaporation behaviour, a special combined Schlieren/scattering light bypass method in combination with a high-speed camera was used [5]. Compared to other combined methods of this sort, scattered light separated from the Schlieren light is routed past the Schlieren diaphragm and later superimposed again. This ensures a high quality of the scattered light signal in spite of a comparatively low output from the scattering light source.

2.3 Test Engines

For the basic studies on the Miller cycle, the externally charged direct-injection single-cylinder diesel research engine FM 16/1 was available, **Figure 3**. In the cylinder liner, optical windows are applicable at several locations through which the combustion process can be analyzed [6].

Fuel was injected using a common rail system. By default, the engine is operated at a compression ratio of 15.8 and a charge air temperature of 40 °C. To study the effects of the Miller cycle, the charge air temperature was reduced to 10 °C using an additional charge air cooler. This corresponds to an advancement of inlet valve closing by approximately 60 °CA to 20 °CA before bottom dead centre. In other test series, the compression ratio was increased from 15.8 to 17.3 by the use of a flatter piston bowl.

The results gained on the research diesel engine were verified on the maritime diesel engine 6 M 32 CR which is based on the 6 M 32 LEE (Low Emission Engine). By an increase of the compression ratio and charge pressure and the use of Miller cycle valve timing, this LEE design already allows a considerable NO_x reduction compared to IMO I. **Table** shows some characteristic values of the used test engines.

Within this research, the 6 M 32 LEE engine was equipped with a common rail injection system from L'Orange. A system test stand was available for the purpose of rating, adjusting and testing the common rail system outside the engine. For this, a 3-cylinder section of the engine was emulated. All cylinder heads

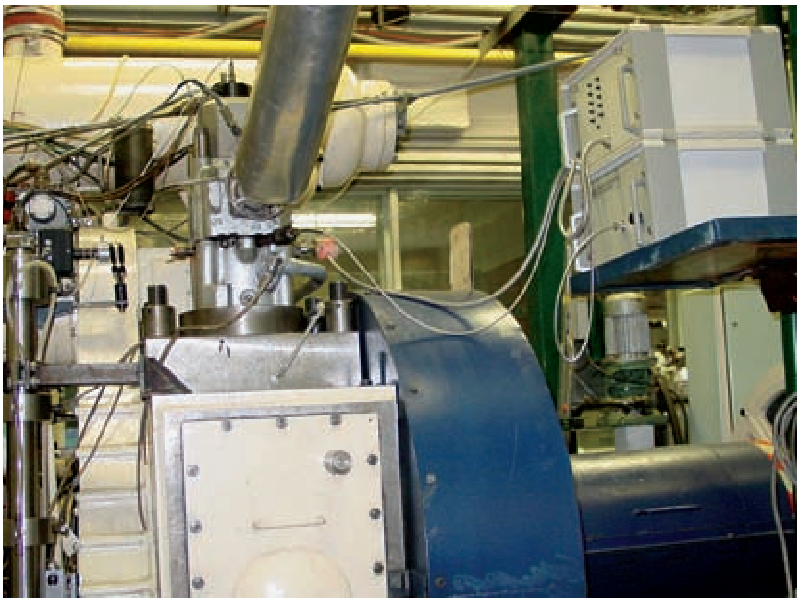

Figure 3: One-cylinder research diesel engine FM 16/1 with optical measuring equipment

Table: Characteristics of the test engines

Engine designation	FM 16/1	6 M 32 CR
Stroke [mm]	240	480
Bore diameter [mm]	160	320
Number of cylinders	1	6
Nominal output [kW]	96	3000
Nominal speed [rpm]	1200	600
Mean effective pressure [bar]	20	25
Max. ignition pressure [bar]	160	200
Max. injection pressure [bar]	1500	1500

were preheated so that the heavy fuel oil operation could also be represented realistically. The high pressure pump was electrically driven.

3 Results

3.1 Heavy Fuel Oil Common Rail Injection System

The developed injection system for the maritime diesel engine 6 M 32 CR is a heavy fuel oil capable common rail system with system pressures up to 1500 bar. Two high-pressure pumps (redundancy) lift fuel into a common high-pressure rail consisting of several partial segments. Flow control valves are fitted at the branches to the injectors. They prevent a permanent injection in the case of nozzle needle jamming in open position. Pressure and temperature sensors as well as a safety valve are fitted on one rail end. A pneumatically actuated flushing valve is integrated to keep the operating temperature of the injection system for a short-time standby operation with heavy fuel oil. The injection valve, **Figure 4**, is an electrically controlled single-circuit injector. That means, the injector is hydraulically controlled by fuel.

Although the basic design of the injector was adopted from the diesel application, some adjustments were necessary to ensure its suitability for heavy fuel oil, in particular due to a significantly higher fuel temperature. So, the injector solenoid, which operates the pilot valve, was moved out of the area of hot fuel and was additionally cooled using engine oil. A long elastic rod was used to transmit the actuating forces. It also compensates the thermal expansion and tolerances. The pilot valve itself with its controlling hydraulic throttles is designed as a separate module which allows its replacement if worn while continuing to use the injector housing with actuator. Also the nozzle element featuring 12 spray holes in two rows is cooled with engine oil to prevent coking.

Before it was used on the engine, the common rail injection system was tested on the system test stand over a longer period of time. During this, mechanical and hydraulic adjustments were made and the system behaviour in case of faults and malfunction of components as well as emergency programs and fuel effects (diesel, heavy fuel oil) were studied. After these preliminary studies, the common rail injection system was applied on the 6 M 32 CR engine. The spray design of the injection nozzles could be adopted from the mechanical system almost without any changes. Only the spray holes were reduced in diameter due to the higher injection pressure. A basic setup of the engine with respect to thermodynamics and pollutant emission by variation of rail pressure and start of injection was followed by tests with multiple injections for fine adjustment.

3.2 Injection Jet Propagation

Studies with the heated high-pressure chamber were carried out with respect to the effects of the injection pressure on the injection jet propagation. These studies have concentrated on part load operating points with increased filter smoke number, which are taken as reference points for the validation of the simulation. The upper part of **Figure 5** shows an example of the development of an injection jet over time. The use of the bypass method for the Schlieren/scattered light allows the simultaneous evaluation of the liquid and gaseous fuel phases. It can be seen that the penetration depth of liquid fuel stagnates at a certain length as there is a balance between the enthalpy of evaporation needed and the energy introduced by the air intake. At a chamber temperature of 800 K, a gas density of 12.5 kg/m^3 and an injected quanti-

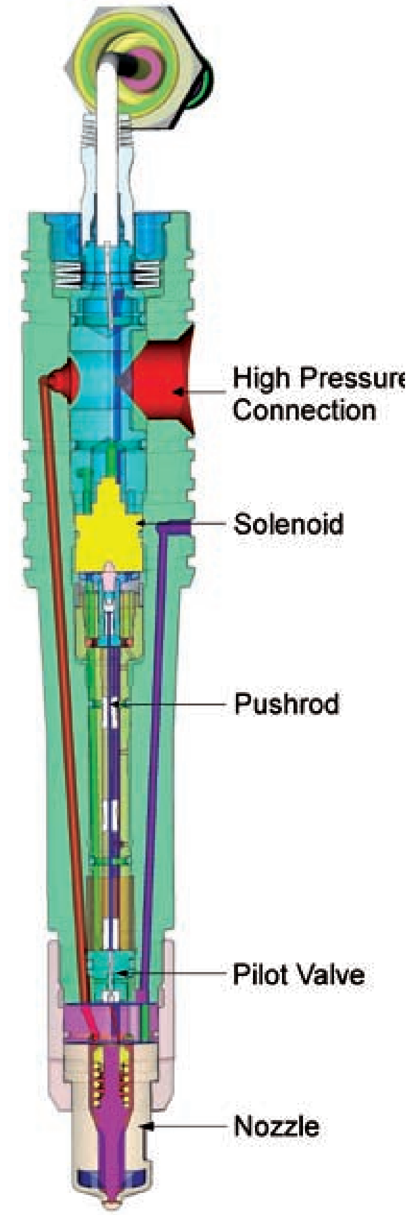

Figure 4: Single-circuit common rail injector

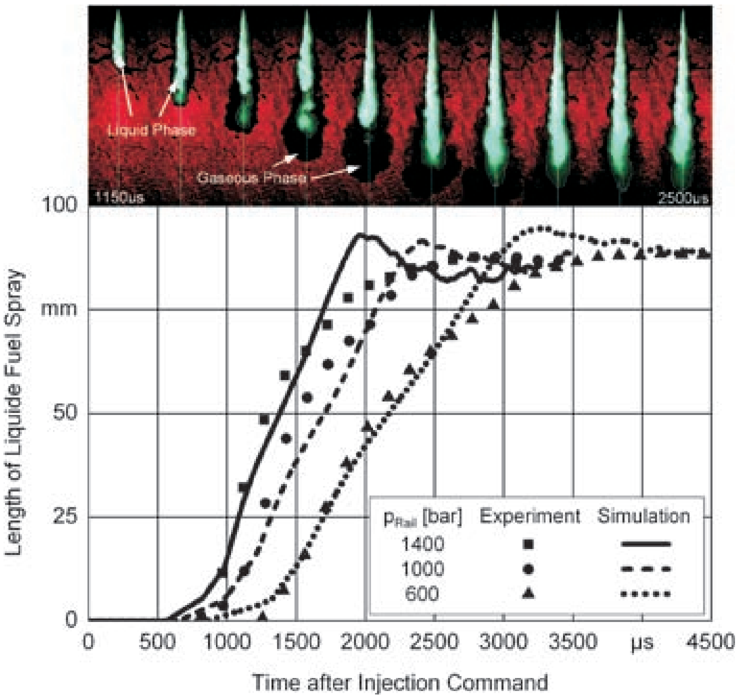

Figure 5: Injection jet propagation within the heated high-pressure chamber

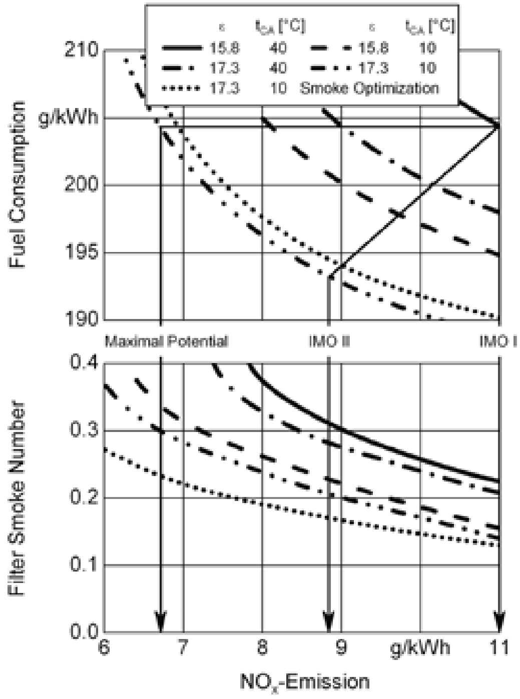

Figure 6: Test results on the FM 16/1

ty of 500 mg the increase of rail pressure p_{Rail} from 600 to 1400 bar shows significant influence on the jet velocity, though it shows almost no influences on the liquid penetration length of the liquid phase of the fluid. This aligns with findings from other authors [7, 8, 9] on injection nozzles of car and truck engines.

The lower part of the Figure 5 shows the experimentally determined length of liquid fuel spray at different rail pressures and the results from the CFD simulations. The simulations substantiate the independency of the liquid stagnation length of the rail pressure. This good match confirms the basic suitability of the simulation models used which is an essential prerequisite for further simulations of carburetion, combustion and pollutant formation.

3.3 Pollutant Emissions

First the results of the fundamental studies on the Miller cycle with the single-cylinder research diesel engine FM 16/1 shall be discussed. **Figure 6** shows the cycle values of fuel consumption, filter smoke number and NO_x emission for the test cycle E2 acc. to ISO 8178-4. The curves for constant parameters of charge air temperature t_{vZ} and compression ratio ε were gained by variations of the injection timing. For the starting condition with a compression ratio of 15.8 and a charge air temperature of 40 °C, rail pressure and injection timing were adjusted in order to reach the IMO I NO_x emission limit, which is at approx. 11 g/kWh at an engine speed of 1200 rpm. The trade-off between NO_x emission and fuel consumption can be significantly improved by a reduction of the charge temperature or by an increase of the compression ratio. The combination of both measures is most efficient. Thus, a reduction of the NO_x emission to 6.7 g/kWh could be achieved at constant fuel consumption, which is a reduction by 40 % compared to the starting condition. However, at the same time, the filter smoke number increases from 0.23 to 0.30 in the test cycle, meaning that the smoke visibility limit is exceeded at part load. So, in a further step, for a compression ratio of 17.3 and a charge air temperature of 10 °C the rail pressure was increased and the injection delayed. This resulted in a significant improvement of the smoke behaviour. The baseline of the filter smoke number could be nearly reached again, but at the cost of a slightly increased NO_x emission. With respect to IMO II, the combination of a higher compression ratio and a low charge air temperature is especially good. A 20 % NO_x reduction can be achieved with a 5 % reduction of the fuel consumption at a slightly improved smoke behaviour. Studies on the Caterpillar engine confirmed the results achieved on the single-cylinder research diesel engine.

The emission reduction concept of Caterpillar's LEE engines includes the application of Miller cycle in addition to the increase of the compression ratio. Due to the reduced combustion temperature caused by the Miller cycle operation and the obtained high ignition pressure both measures complement each other. When choosing an appropriate balance between both parameters the NO_x emission can be reduced without any impact on the fuel consumption, **Figure 7**. However, the limits of a single-stage charging and of the maximum permissible ignition pressure are reached at a NO_x emission of 8 g/kWh. A further NO_x reduction requires fundamental modifications on the engine.

The basic LEE variant with a compression ratio of 16.9 and a Miller cycle of 30 % achieves a NO_x reduction by approx. 30 %. A further reduction of the NO_x emission to 50 % of the IMO I limit would require a compression ratio of 18.2 at 40 % Miller cycle. For the time being, a proof of that could only be provided by simulation because a two-stage charging system would be necessary for an implementation.

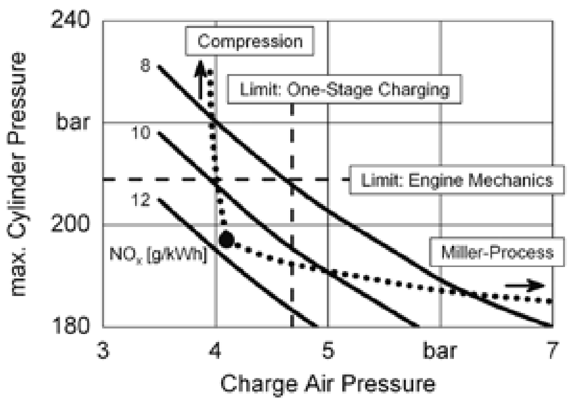

Figure 7: Engine-internal NO_x reduction at a mean pressure of 25 bar

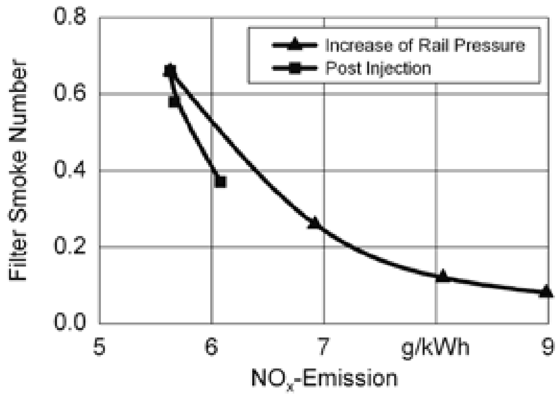

Figure 8: Smoke reduction at partial load

3.4 Smoke Optimization at Part Load

Generally, there is a smoke problem at part load with the introduction of the Miller process and an increase of the compression ratio, in particular in generator mode. A reason for this is the low temperature within the combustion chamber, which delays the soot oxidation. This problem can be solved by a special mode of operating in the part load ranges where the capabilities of the common rail injection system are used in particular. **Figure 8** shows the trade-off between filter smoke number and NO_x emission for the measures post-injection and rail pressure increase.

Post-injection was found to be a measure with little impact on the NO_x emission. With this, a reduction of the filter smoke number by 50 to 70 % over the whole operating range is possible. Post-injection is made with approx. 10 to 20 % of the total injected quantity and a timing of 5 to 10° CA after the main injection. A good dynamic behaviour of the common rail injector and the optimization of the post-injected fuel quantity at each load point are preconditions.

Also an increase of rail pressure causes a significant soot reduction, but increases the NO_x emission. **Figure 9** exemplarily shows the impact of the rail pressure p_{Rail} on the flame temperature and soot concentration within the combustion chamber. The maximum flame temperature within the combustion chamber increases. A quicker soot oxidation occurs at the end of the combustion which leads to lower filter smoke numbers. The tendency of the curves determined by optical methods is also revealed in the simulations.

The smoke blow at load pickup is another problem. While for driving applications a load pickup within 1 to 2 minutes is typical, for generator systems, this has to occur over several stages within 20 s. In the framework of this project, therefore, the potentials for smoke re-

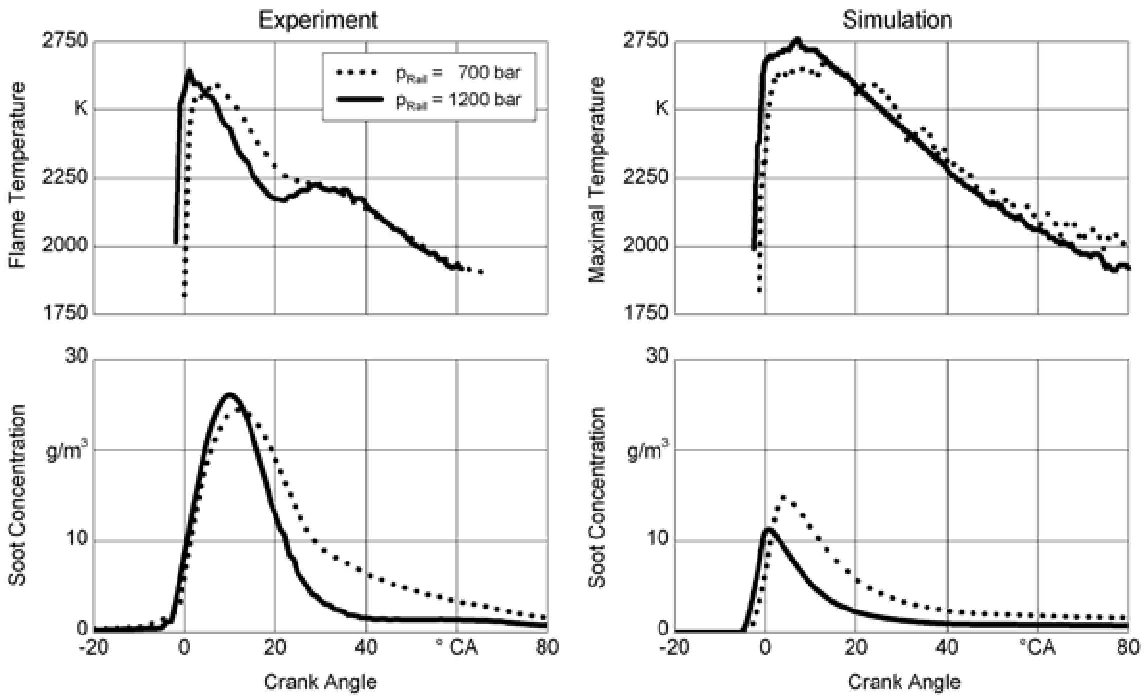

Figure 9: Impact of rail pressure increase on the flame temperature and soot oxidation

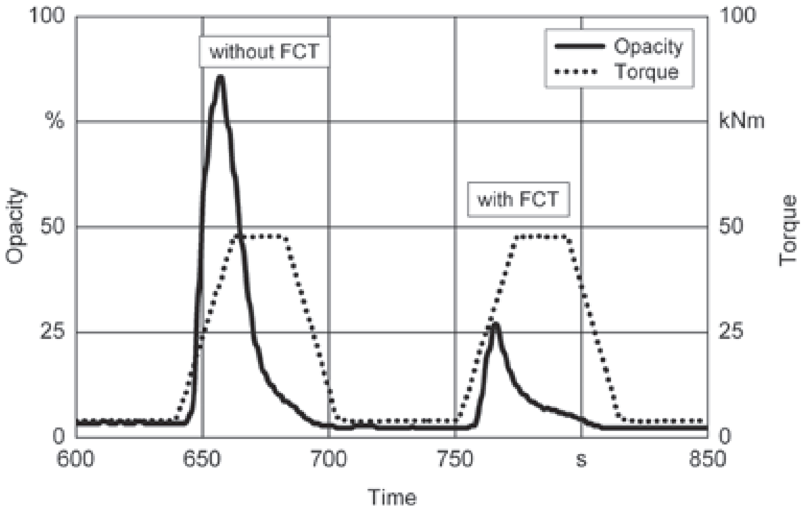

Figure 10: Smoke behaviour at load pickup

Acknowledgement

This research project was subsidized by the Federal Ministry of Economics and Technology. We thank for the financial support and the inspiring accompaniment through the project management of PTJ Jülich.

duction at load pickup of both sides, fuel side and air side, were studied. Characteristic fields of large diesel engines with common rail injection systems are typically configured for the stationary operation. In the instationary case, the switching to a start-up mode can be demonstrated, at which the load pickup occurs with as little as possible smoke emission. As the acceleration of highly charged engines with a mean pressure at full load of 25 bar heavily depends on the air supply, characteristic field settings are possible which either generate charging pressure or improve the air utilization. Tests on engines have shown that the second way is more promising.

An efficient measure is a variable valve actuator which switches off the Miller process in the case of acceleration. In this way, an air supply which is suddenly increased by 30 % is available for combustion. For the studies, a system known as FCT was used, which is able to shift the profile of the inlet cam by 15° CA. **Figure 10** shows the impact on the smoke behaviour during the load pickup. With identical torque response, FCT can reduce the opacity to approx. a third of the value without the use of FCT.

4 Summary and Perspective

In the framework of this joint project, research work on pollutant reduction of maritime diesel engines was performed. The Miller cycle in combination with an increase of the compression ratio offers the opportunity to meet the NO_x limit IMO II, which will come into force from 2011, without efficiency losses. A deterioration of the exhaust gas smoke behaviour can be avoided by an optimization of the combustion process using a common rail system capable of multiple injections. A further NO_x reduction down to the IMO III level requires the development of new combustion processes, where the reduction of the oxygen content in the charge air in combination with a two-stage charging and the improvement of the fuel atomization might be key technologies.

References

[1] MARPOL 73/78: Annex VI: Regulations for the Prevention of Air Pollution from Ships and NOx Technical Code. International Maritime Organization, London, 1998

[2] MEPC 58/23/Add. 1, Annex 13: Resolution MEPC.176(58), Adopted on 10 October 2008

[3] Frobenius, M.; Buchholz, B.; Brack, W.; Harndorf, H.: Interaktion von Injektorströmung und Spraybildung in mittelschnelllaufenden Common-Rail Dieselmotoren – Simulation und experimentelle Validierung. HdT-Tagung Diesel- und Benzindirekteinspritzung, Berlin, 2008

[4] Frobenius, M., Pittermann, R.: Untersuchung der Wirksamkeit von Rußminderungsmaßnahmen bei mittelschnelllaufenden Schiffsdieselmotoren mittels optischer Methoden und CFD. Symposium für Verbrennungsdiagnostik, Baden-Baden, 2008

[5] Fink, C.; Niendorf, M.; Buchholz, B.; Harndorf, H.: Einspritzanalyse an modernen Einkreis-CR-Injektoren für schwerölbetriebene, mittelschnelllaufende Großmotoren. HdT-Tagung Diesel- und Benzindirekteinspritzung, Berlin, 2008

[6] Pittermann, R.: Untersuchung der dieselmotorischen Verbrennung mittels multispektraler Messverfahren. Dissertation Universität Magdeburg, 1996

[7] Siebers, D.: Scaling Liquid-phase Fuel Penetration in Diesel Sprays Based on Mixing-Limited Vaporization. SAE 1999-01-0528

[8] Blessing, M.: Untersuchung und Charakterisierung von Zerstäubung, Strahlausbreitung und Gemischbildung aktueller Dieseldirekteinspritzsysteme. Dissertation, Universität Stuttgart, 2004

[9] Pauer, T.: Laseroptische Kammeruntersuchungen zur dieselmotorischen Hochdruckeinspritzung – Wirkkettenanalyse der Gemischbildung und Entflammung. Dissertation, Universität Stuttgart, 2001


Career
Archive
Events
E-Magazines
Top Stories
News Updates
1500 m
www.ATZonline.com
Options
NAVIGON

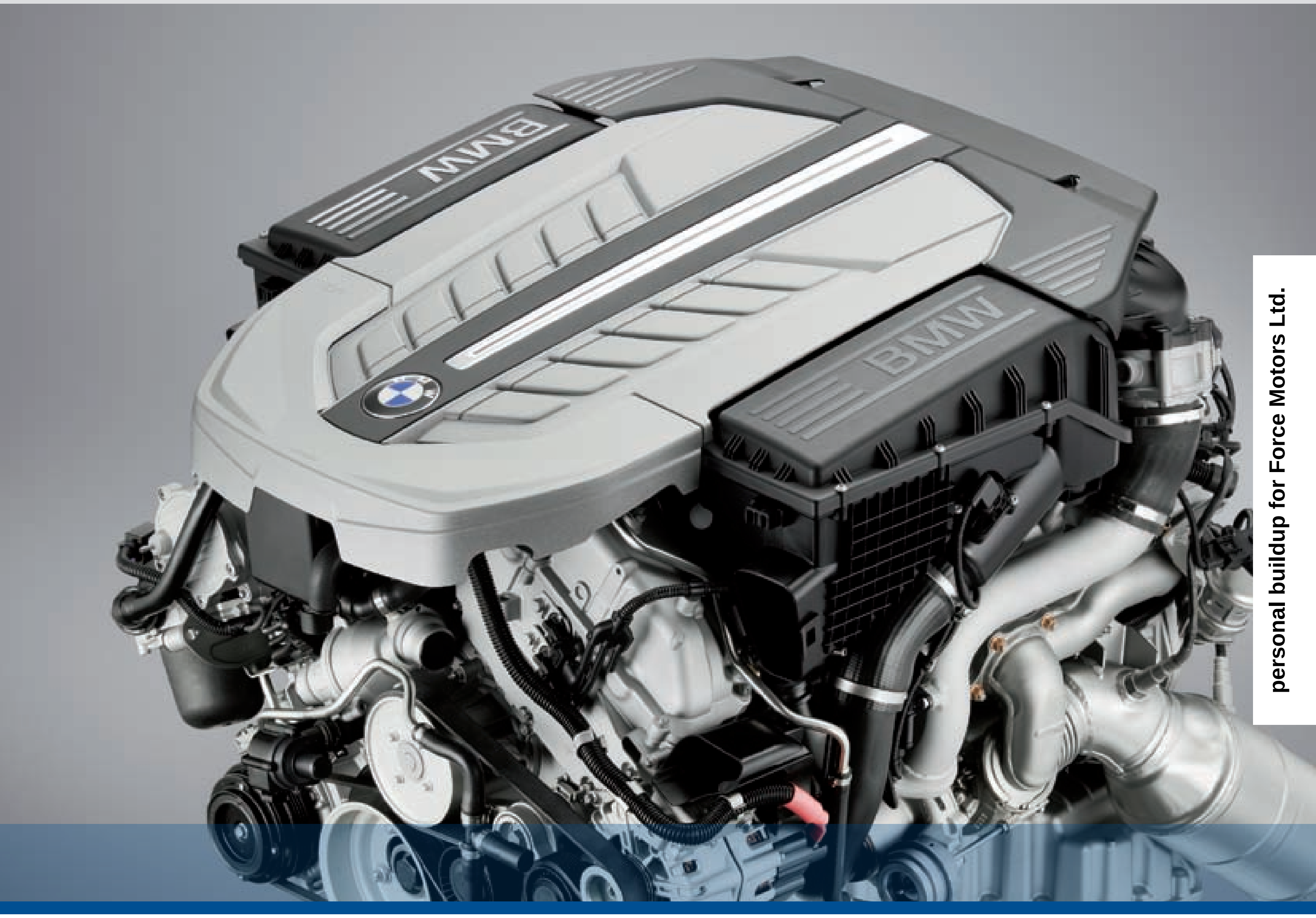

The New BMW V12 Gasoline Engine

The combination of High Precision Injection and twin turbocharger constitutes a unique, ground-breaking amalgamation. BMW's new-generation 7-series will continue to hold its leading position in the market with the new V12 engine. Superior power development with a unique sound and smooth running give this vehicle its own, very special character. The new V12 engine celebrated its debut together with another innovation, the new 8-speed automatic transmission, in the BMW 760i, which was launched this summer.

1 Introduction

BMW's outstanding competence in the development and production of twelve-cylinder engines is based on a long-standing tradition. It goes back to 1918, when the company first drew attention to itself by building an aircraft engine of this type. Presented in 1987, the BMW 750i was the first twelve-cylinder limousine to be produced in post-war Germany. BMW combined GDI (gasoline direct injection) with Valvetronic for the first time in the predecessor engine in 2003, setting a new milestone for efficient engine concepts with the most powerful, lowest-consumption, naturally aspirated V12 engine [1]. A new generation of turbocharged engines was introduced with the six-cylinder in-line engines in 2006 [2, 3], continued with the market launch of the eight-cylinder engine with exhaust-gas turbocharger in the V space of the engine block in 2008 [4, 5] and is now being supplemented by the new V12 engine.

BMW's approach to meeting the multifarious requirements of its customers goes by the name EfficientDynamics. Innovative engine concepts offer the only means of achieving the objective of combining a high level of driving pleasure with environmentally compatible, low consumption and emission values. The new V12 engine is the latest implementation of the EfficientDynamics ideal at the top end of the exclusive luxury class.

2 Objectives

The requirements specification for development of the new engine centred on the following requirements:

- a noticeable improvement in engine performance with the emphasis on a full-bodied torque characteristic and high customer value for clear positioning at the forefront of the BMW engine portfolio
- outstanding responsiveness, superior ease, smoothness and refinement
- a significant reduction in fuel consumption
- design of a convincing V12 engine sound
- worldwide usability
- compliance with all currently applicable emission standards (EU5, ULEV II) and the potential to meet the requirements of future standards.

After analysing alternative engine concepts, a decision was finally made in favour of a V12 twin turbo engine with a 60° cylinder bank angle, second-generation high-precision direct fuel injection, indirect charge-air cooling and 6 litres displacement, **Figure 1**.

3 Technical Description of the Basic Engine

There is a high level of component communality between the newly developed twelve-cylinder engine and the V8 engine

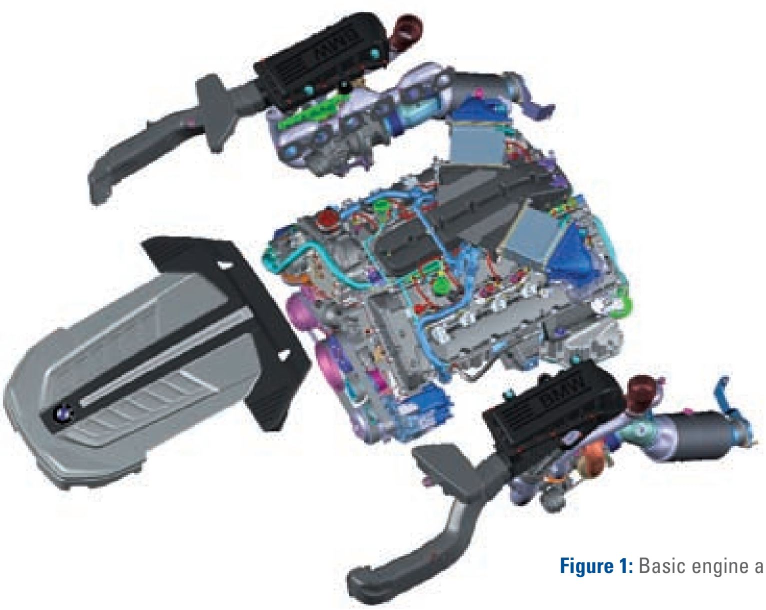

Figure 1: Basic engine and periphery

The Authors

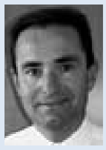
Dipl.-Ing. Hans-Stefan Braun is Head of Drivetrain Performance for Small Inline Engines and V Engines at BMW Group in Munich (Germany).


Dipl.-Ing. Thomas Brüner is Head of Calculations and Testing for Motor Engineering and Heat Management at BMW Group in Munich (Germany).


Dipl.-Ing. Klaus Hirschfelder is Head of V Engine Projects at BMW Group in Munich (Germany).


Dipl.-Ing. Uwe Hoyer is Head of Air Guidance and Exhaust Systems at BMW Group in Munich (Germany).


Dr.-Ing. Horst Kellerer is Manager of V12 Engine Project at BMW Group in Munich (Germany).


Dipl.-Ing. Johann Schopp is Head of Design for V Engines and Cooperation Engines at BMW Group in Munich (Germany).


Dr.-Ing. Christian Schwarz is Head of Development of Thermodynamics at BMW Group in Munich (Germany).

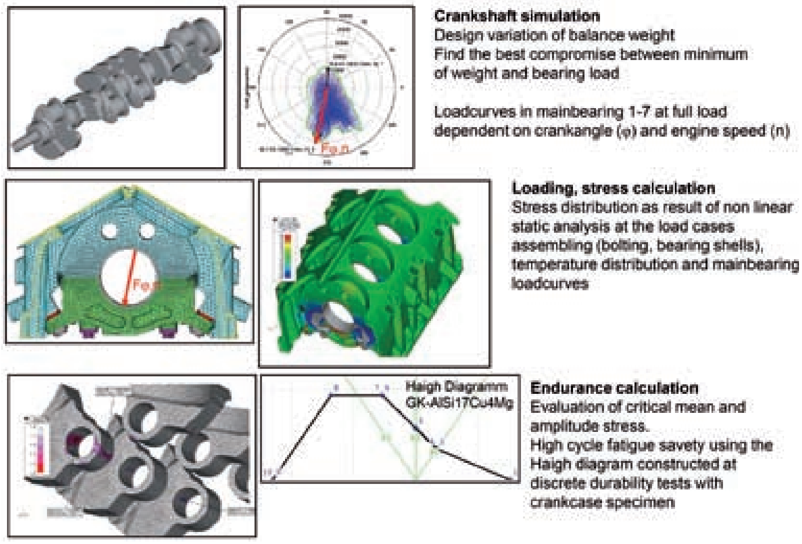

Figure 2: Computational dimensioning of the basic engine

within the framework of the V-engine building blocks. This resulted in a considerable reduction in design and validation expenditure as early as the development phase.

3.1 Cylinder Crankcase and Crank Drive System

The all-aluminium Alusil engine block has been realised as a closed-deck construction in order to take advantage of the greater rigidity offered by this technology. Together with the cylinder head arrangement bolted into the base plate of the deep-skirt cylinder crankcase, this design ensures that the bearing surfaces, which have undergone a honing process with exposure stage, are only distorted to a minor degree. The webs between the cylinders are cooled by drilled ducts in the hot zone. The engineers were able to produce a lightweight, but highly rigid construction thanks to the intensive use of FEM modelling, particularly with respect to the dimensioning of the main bearing bolting arrangement carried over from the V8 engine design, rigidity optimisation of the cylinder liners and gearbox flange, as well as the auxiliary equipment interfacing concept, **Figure 2**.

Holes have been drilled lengthwise through thrust bearings 1 to 3 in order to reduce ventilation losses in the crankshaft drive system. A means of shortening the engine block was created by driving the oil pump fitted on the outlet side directly. The proportion of oil in the blow-by gas was also reduced by drilling oil return holes that extend below the level of the oil and using separate gas channels.

The rugged iron-coated aluminium piston was designed as an easily assembled common component for both cylinder banks. It features a shape-optimised piston ring in a hard-anodised groove. Each forged cracked con rod with trapezoidal piston pin lug has a ternary sputter bearing shell at the rod side. Ternary bearing shells are fitted at the cover side, with binary bearing shells in the main bearings. The forged and twisted crankshaft has induction-hardened bearing surfaces, as well as oblique con-rod journal holes and a central main bearing hole to reduce its weight. 1st and 2nd order inertial forces are balanced out completely, as in the predecessor engine.

3.2 Cylinder Head

The main purpose of redesigning the cylinder head was to produce a rugged overall concept for high performance on the basis of the V8 combustion method with a central arrangement of injector and spark plug in the combustion chamber. Another objective was to integrate the cylinder head into the existing production line. A high level of rigidity with excellent fatigue strength was achieved as a result of intensive computational dimensioning of the cylinder head structure and coolant routing during the early concept phase. The vacuum pump driven by the exhaust camshaft is fitted on cylinder bank 1 to 6 on the control side. A gravity casting technique is used to produce the cylinder head castings in the BMW foundry. The cylinder head covers with integrated cyclone filters are made of die-cast aluminium.

3.3 Timing Gear and Chain Drive

The thermally joined camshafts feature forged cams, a steel flange for the sprockets and a sintered sensor gear for VANOS signal acquisition. A directed oil spray

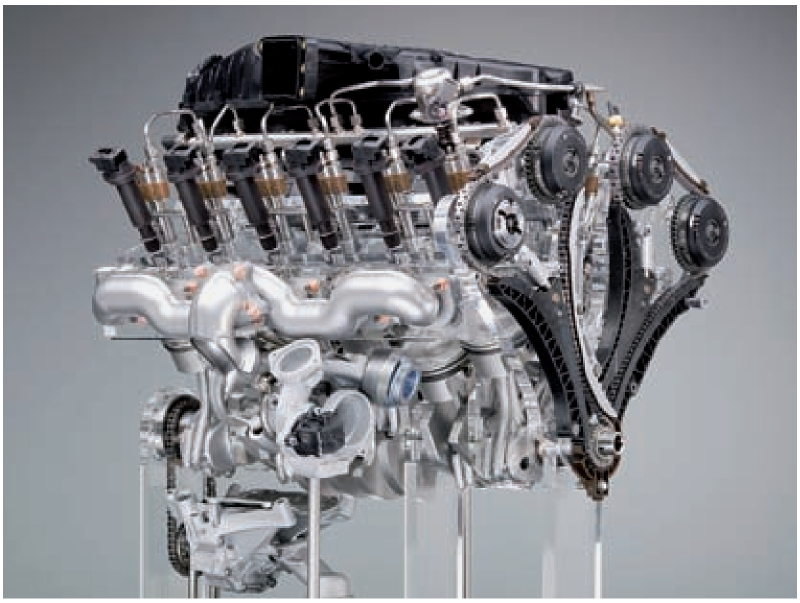

Figure 3: Skeletal engine

hole in the calotte of the roller cam follower ensures that oil is supplied to the rocker arm roller and cams for cooling and lubrication purposes. A supplementary 3-way cam is fitted on the intake side to drive the high-pressure fuel pumps. The timing gear and chain drive system is essentially derived from the V8 building blocks, **Figure 3**.

3.4 Oil Circuit

The 6-chamber pendulum-vain oil pump is also identical to the V8 oil pump in many respects. The volumetric flow control system only delivers the amount of oil actually required by the engine in its respective operating state and therefore contributes towards reducing CO_2 emissions. Made of die-cast aluminium, the upper and lower sections of the oil pan have been optimised in terms of strength and acoustic properties. The oil cooler thermostat and oil filter element have been integrated into the oil pan. A two-part oil scraper and a baffle reduce oil foaming and ensure an adequate supply of oil, even under extreme driving conditions.

3.5 Belt Drive System

The seven-ribbed primary belt that drives the power steering pump is also used to drive the 210 A alternator and the mechanical water pump. It has been possible to reduce belt wear throughout the entire life cycle by using a profile-free pulley to drive the water pump. The four-ribbed secondary belt that drives the refrigerant compressor no longer requires a tensioning roller or any other assembly aids thanks to the use of a patented, innovative revolver tensioning system. The belt drive system is driven by the primary side of the damper in order to reduce torsional vibration.

4 Technical Description of the Periphery

4.1 Air Intake Guide and Intake Manifold

A dual-flow intake air duct with engine-mounted silencers was used to optimise the package and the gas-exchange cycle. Central routing of the charge air into the intake manifold provides the optimum solution with respect to acoustics and the gas-exchange cycle. The throttle valves are fitted upstream of the charge-air coolers, Figure 1. The crankcase ventilation system has been realised according to a compound ventilation concept for the first time. In naturally aspirated mode, air is blown into the engine and the blow-by gases are only routed into the plenum chamber via one cyclone filter. In charged mode, the engine is vented via both cyclone filters upstream of the compressor without being aerated.

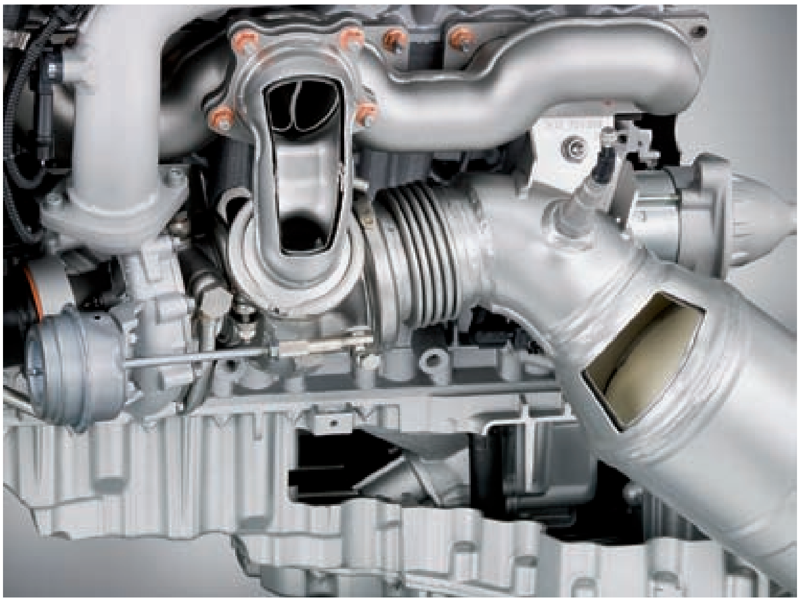

Figure 4: Turbocharger assembly

4.2 Fuel System

High Precision Injection is a 2nd generation direct injection system with a central arrangement of piezo injectors and spark plugs. With its precise spray preparation, this system constitutes the essential basis for the attained engine performance and the spontaneous response of the turbocharger, compliance with ambitious emission limits and low fuel consumption.

Line management within the fuel system has been optimised to minimise line distances. The rail and lines are made of stainless steel to meet the stringent requirements for the gastightness of the system imposed by the system pressure, Figure 3.

4.3 Exhaust Manifold and Turbocharger

The lateral positioning of the two exhaust-gas turbochargers produces a very compact and therefore ideal arrangement for a 60° V12 engine. Specially developed for this engine, the mono-scroll turbochargers are characterised by a high level of efficiency. With 2 times 3 into 1 routing, the aerodynamically favourable exhaust manifolds have been optimised for the firing order. Together, they provide the basis for excellent responsiveness and superior power and torque values, **Figure 4**.

4.4 Catalytic Converters and the Exhaust System

The ceramic monoliths combined into two elements, one fitted immediately behind each turbine, ensure that the operating temperature is reached as quickly as possible by means of short exhaust gas routing in conjunction with the latest generation of exhaust gas sensors. Compliance with the stringent requirements of the EU5 and ULEV II emissions legislation has already been assured by SOP with an identical version of these (monoliths, coating, loading) in conjunction with a secondary air system.

The decoupling elements integrated between turbine outlet and catalytic converter inlet provide acoustic and thermomechanical isolation. The lengths and cross-sections of the pipes used in the exhaust system and crossover point have been selectively optimised for the gas-exchange cycle and acoustic properties.

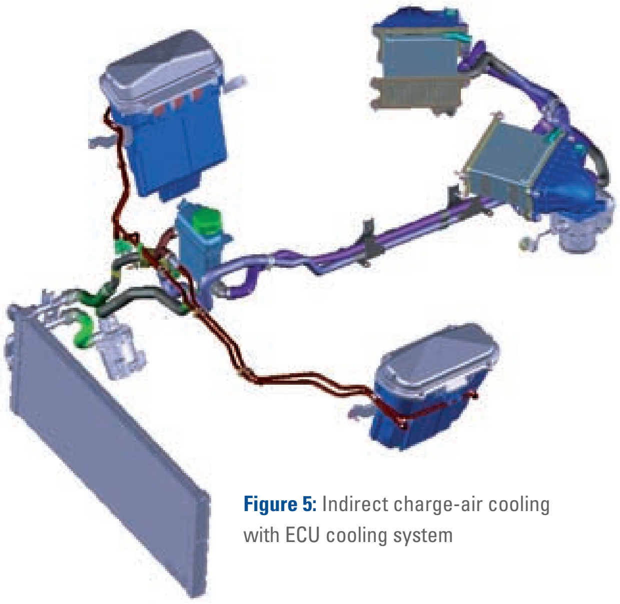

Figure 5: Indirect charge-air cooling with ECU cooling system

Figure 6: High precision injection

4.5 Coolant Circuit

4.5.1 Engine

By integrating all coolant ducts into the crankcase, it has been possible to do without external lines to a great extent in the basic engine. It has also been possible to achieve a significant reduction in the amount of short-circuited coolant and shorten the warming-up phase considerably compared with the predecessor engine by optimising cross-sections and concentrating the flow of coolant on surface structures that are expedient in terms of heat exchange properties. The coolant flows in parallel with the main oil gallery, but in the opposite direction from the oil, to the rear. Oil flows through the cylinder heads diagonally, from outside rear to inside front. The outlet arrangement has been optimised to achieve an even distribution of heat. The turbocharger bearing seats have been integrated into the main coolant circuit.

4.5.2 Charge-air Cooling

The limited installation space available in the vehicle and the surfaces required to cool the water and oil do not permit direct cooling of the compressed air. An indirect charge-air cooling system with its own electric water pump is therefore being used. The cooling system for the control units has also been integrated into this circuit, **Figure 5**.

4.5.3 External Cooling

The heat exchanger for the low-temperature circuit of the charge-air cooling system was positioned on the first cooling level in the cooling module, upstream of the condenser for the automatic air-conditioning system, to ensure optimum recooling. Boosted by a 1000 W electric suction fan, the cooling module also accommodates the coolant cooler for the engine circuit, the transmission fluid/water heat exchanger, which is cooled by an additional supercooling section of the coolant cooler, and the cooler for the power assisted steering system. The engine-oil coolers are fitted into the wheel arches.

4.6 Engine Management

Two water-cooled MSD87-12 control units are fitted with the V12 engine. Developed on the basis of the six-cylinder control unit, the MSD87-12 uses the same components as the MSD85 fitted with the V8 engine in terms of chip set, connectors and the water cooling system connection. A two-ECU concept with automatic master/slave recognition has been implemented. The master is responsible for communicating with the vehicle as a whole and for defining the setpoint values for the engine functions. The ECU with up-to-date software has been designed for the BN2020 (FlexRay) bus system.

5 Engine Design

5.1 Combustion System

The combustion system constitutes a logical further development of the High Precision Injection system used in the six- and eight-cylinder engines. It is characterised by a central arrangement of spark plug and outward-opening piezo injector in the combustion chamber and, interacting with a coordinated charge movement, enables optimum carburetion, **Figure 6**. The intake ports include valve masking. The port shape (CFD) and the valve timing were optimized with respect to gas exchange and flow. A flexible multiple injection strategy ensures that only a small amount of fuel is sprayed onto the wall of the cylinder, offering a means of achieving extremely low HC raw emission levels and an excellent catalytic converter heating functionality.

5.2 Gas-exchange Cycle/Turbocharging

The conventional exhaust-gas turbocharger arrangement was found to be the most expedient solution for BMW's twin turbo V12 engine with 60° cylinder bank angle. As far as minimum pressure loss is concerned, the concept enables short air paths and generous dimensioning of the charge-air cooler, which is directly linked to the intake manifold, Figure 2. On the exhaust side, the components in the extremely compact LSI manifold were separated into groups according to firing order, resulting in a favourable incident flow at the turbine. Compressor and turbine were designed and dimensioned according to the specific requirements of the engine. This is reflected in the instantaneous build-up of torque, the broad torque plateau at 750 Nm and the superior 400 kW peak power. The full-load characteristics are shown in **Figure 7**. The turbocharging system is assisted by the generously dimensioned cross-sections of the backpressure-optimised catalytic converters and the exhaust system.

5.3 Emissions Concept

The compact arrangement of manifold, turbocharger and catalytic converter provides the basis for an efficient emissions concept. Combined with High Precision Injection, this arrangement with multiple injection enables stratified catalytic converter heating with extremely late ignition timing, which ensures that the catalytic converter heats up very quickly. A significant reduction in catalytic converter loading was achieved compared with eight-cylinder BMW engine by using an engine-mounted secondary air system, with some components integrated into the cylinder head. The emission levels will satisfy the requirements of the EU-5 standard in Europe and the ULEV II standard in the USA by SOP, whereby the values undercut the specified limits by more than 50 % when the engine is new.

5.4 Engine Functions

The engine functions of the new twelve-cylinder engine have been further developed according to the building-block principle on the basis of the V8 functions [5]. In this respect, the software structure established between BMW and supplier functions was maintained. The two-bank system of the eight-cylinder engine was divided between the two control units. ECU coupling was implemented for the first time within the framework of the software sharing concept. The coupling information is exchanged via the FlexRay bus and not via a separate CAN bus. Unlike the V8 function, a pressure-guided load detection and control system is used. This system eliminates the need for the hot-film air-mass meters, which had previously been required for load detection. Apart from reducing costs, other advantages of this technique include its ruggedness and reliability.

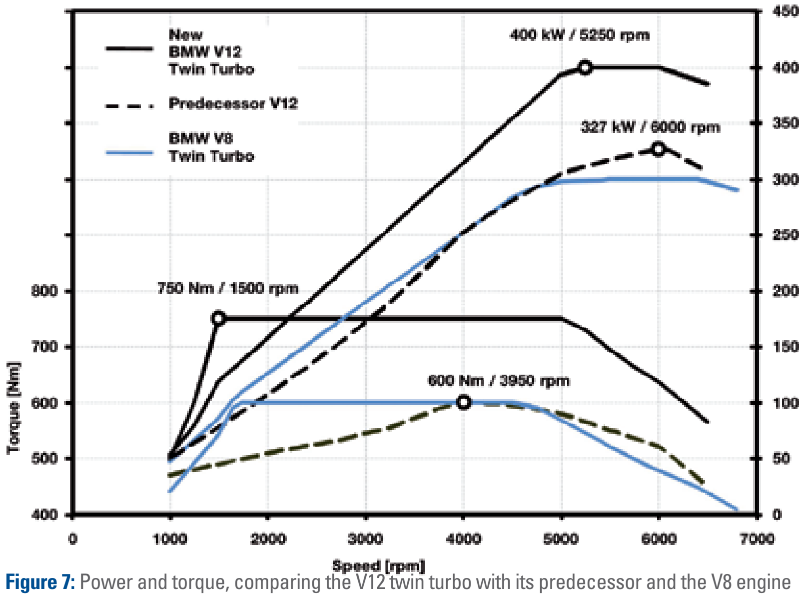

Figure 7: Power and torque, comparing the V12 twin turbo with its predecessor and the V8 engine

Table: Technical data, comparing the V12 twin turbo with its predecessor and the V8 engine

		V12 TwinTurbo	V8 TwinPower Turbo	V12 Predecessor
Engine	**Unit**	High Precision Injection (central)	High Precision Injection (central)	Valvetronic DI, swirl injector (side)
Displacement	**cm³**	5972	4395	5972
Compression ratio		10.0	10.0	11.3
Power (at ... rpm)	**kW**	400 (5250 – 6000)	300 (5500 – 6400)	327 (6000)
Specific power	**kW/l**	66,7	68,3	54,8
Torque (at ... rpm)	**Nm**	750 (1500 – 5000)	600 (1750 – 4500)	600 (3950)
Specific fuel consumption (optimum)	**g/kWh**	245	238	245

6 Functional Results

The data of the new V12 engine is summarised and compared with its predecessor and the new V8 engine in the **Table**.

6.1 Power and Torque

The twin turbo engine is characterised by an extremely wide useful rpm range. The 750 Nm maximum torque is already achieved at 1500 rpm and remains available right through to 5000 rpm. Used in conjunction with the automatic 8-speed transmission, this design guarantees ultimate powertrain superiority and constitutes the benchmark at the top end of the premium segment. The maximum power of 400 kW is reached between 5250 and 6000 rpm and the ceiling speed is reached at 6500 rpm.

6.2 Power Development

The engine already has a very high basic torque in naturally aspirated mode by virtue of its displacement and this is increased again significantly by the turbocharging concept right through to the full-load characteristic. This results in a responsiveness that is exceptional in a

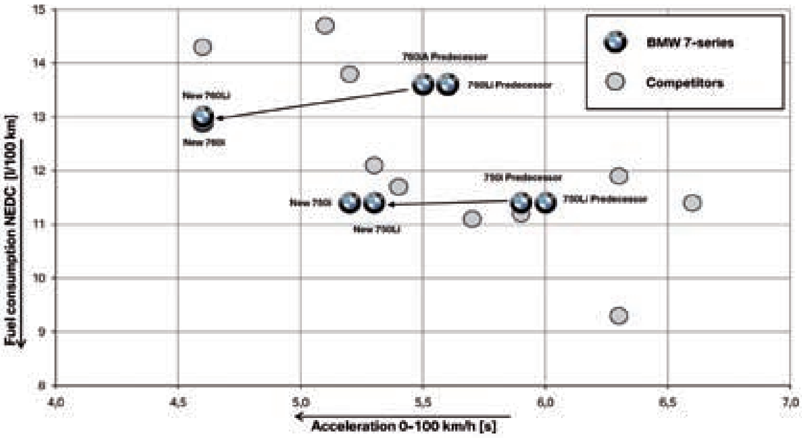

Figure 8: Driving performance and fuel consumption, comparing the new 7 series with V12 and V8 twin turbo with their predecessors and competitors

vehicle of this class. When coordinating power development, special attention was given to the transition from naturally aspirated mode via the charge-dominated load range through to full load. It was possible to achieve optimum transient behaviour throughout the entire rpm and load ranges by tuning all the parts involved in the gas-exchange and the boost-pressure control system. This harmonious development of power makes a vital impression on the character of the target vehicles.

6.3 Driving Performance and Fuel Consumption

The chart showing consumption as a function of driving performance in **Figure 8** compares the new 7-series with its predecessors and competitors. With considerably improved driving performance accompanied by a substantial reduction in fuel consumption, the 760i goes into the lead, ahead of its competitors, to represent BMW EfficientDynamics in the absolute premium segment. Its consumption and emission values are at a level that is not even achieved by some rival manufacturers' eight-cylinder models in the competitive environment of BMW's 7-series. Having increased engine power by 22 % and maximum torque by 25 % compared with the predecessor models, the fuel consumption of the new engine was reduced by 0.7 to 12.9 litres per 100 kilometres during the EU test cycle. The CO_2 emissions produced by the BMW 760i and the BMW 760Li amount to 299 g/km. These achievements were essentially made possible by combining the engine with a new eight-speed automatic transmission to produce an outstanding powertrain package. The eight-speed automatic transmission with its innovative gearset construction has been ideally matched to the performance characteristic of the twelve-cylinder engine. It unites easy shifting with sportiness and efficiency at an as yet unparalleled level.

6.4 Engine Acoustics

Balancing free inertial forces and moments of inertia and having excellent rotational nonuniformity, the V12 engine with classical 60° design offers an ideal basis for outstanding smoothness and refinement. By implementing targeted structural measures on the basic engine, the engineers were able to minimise the emission of mechanical noise components and produce a rigid integrated composite structure with the new eight-speed transmission. The excitation of the engine structure brought about by the polygon effect of the chain was reduced significantly by using the roller timing chain developed for the new generation of V engines, which is also highly resistant to wear. The exhaust and intake systems were tuned in such a way as to ensure appropriate idle and slow driving comfort for a vehicle of its class on the one hand, while underlining the impression of capacity and dynamic performance with a perceptible but non-intrusive, sonorous load sound on the other. The measures taken to achieve this included the use of map-controlled exhaust flaps on the rear silencers.

7 Summary

The new V12 engine with twin turbocharger and High Precision Injection constitutes a new apogee in BMW engine development. In the new 760i it combines superior driving performance with favourable consumption and minimal emission values to produce exclusive smoothness and refinement. In conjunction with the new eight-speed automatic transmission, the engine represents BMW's EfficientDynamics powertrain strategy in the absolute luxury segment. The engine is being assembled on the newly built, highly flexible manufacturing assembly line "Manufaktur" at the Munich facility.

References

[1] Jägerbauer, E.; Fröhlich, K.; Fischer, H.: Der neue 6,0-l-Zwölfzylindermotor von BMW. In: MTZ 63 (2003), Nr. 7
[2] Welter, A.; Bruener, T.; Unger, H.; Hoyer, U.; Brendel, U.: Der neue aufgeladene Reihensechszylinder-Ottomotor von BMW. In: MTZ 67 (2007), Nr. 2
[3] Mährle, W.; Krauss, M.; Luttermann, C.; Klauer, N.: High Precision Injection in Verbindung mit Aufladung am neuen BMW-TwinTurbo-Ottomotor. In: MTZ 67 (2007), Nr. 4
[4] Langen, P.; Brox, W.; Brüner, T.; Fischer, H.; Hirschfelder, K.; Hoyer, U.: Der neue V8-Ottomotor von BMW mit zwei Turboladern. Teil 1: Konstruktive Merkmale. In: MTZ 68 (2008), Nr. 11
[5] Bock, C.; Hirschfelder, K.; Ofner, B.; Schwarz, C.: Der neue V8-Ottomotor von BMW mit zwei Turboladern. Teil 2: Funktionale Eigenschaften. In: MTZ 68 (2008), Nr. 12

WWW.VIEWEGTEUBNER.DE

Gasoline Engines are the answer to the challenges of future

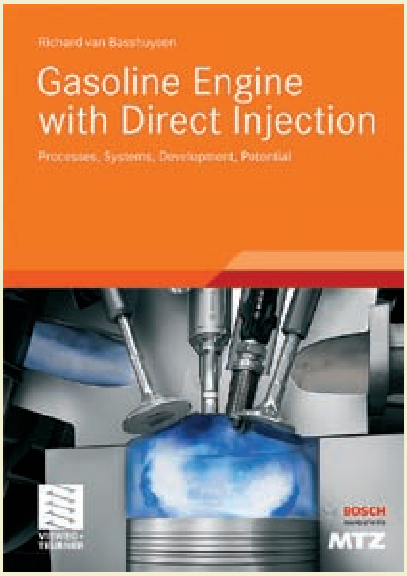

Richard van Basshuysen
Gasoline Engine with Direct Injection
Processes, Systems, Development, Potential
2009. xviii, 437 pp. With 399 Fig. Hardc. EUR 49,00
ISBN 978-3-8348-0670-3

Direct injection spark-ignition engines are becoming increasingly important, and their potential is still to be fully exploited. Increased power and torque coupled with further reductions in fuel consumption and emissions will be the clear trend for future developments. From today‘s perspective, the key technologies driving this development will be new fuel injection and combustion processes. The book presents the latest developments, illustrates and evaluates engine concepts such as downsizing and describes the requirements that have to be met by materials and operating fluids. The outlook at the end of the book discusses whether future spark-ignition engines will achieve the same level as diesel engines.

authors | editors

Dr.-Ing. E. h. Richard van Basshuysen was Head of Development for premium class vehicles and for engine and transmission development at Audi. Today, he is editor of the magazines ATZ and MTZ. The editor was supported by a distinguished team of authors consisting of 22 experts and scientists from industry and universities.

Please send me

____ Copies
Gasoline Engine with Direct Injection
ISBN 978-3-8348-0670-3
EUR 49,00
(+ shipping and handling)

Fax +49(0)611.7878-420

Company | Last name | First name | 321 09 001

Department

Street name | Postcode/Zip | City, Country

Date | Signature

Please supply at retail price via bookshop or directly from Vieweg+Teubner Verlag. Subject to change without notice. 1|2009.
Managing Directors: Dr. Ralf Birkelbach, Albrecht F. Schirmacher. AG Wiesbaden HRB 9754

TECHNIK BEWEGT.

VIEWEG+TEUBNER

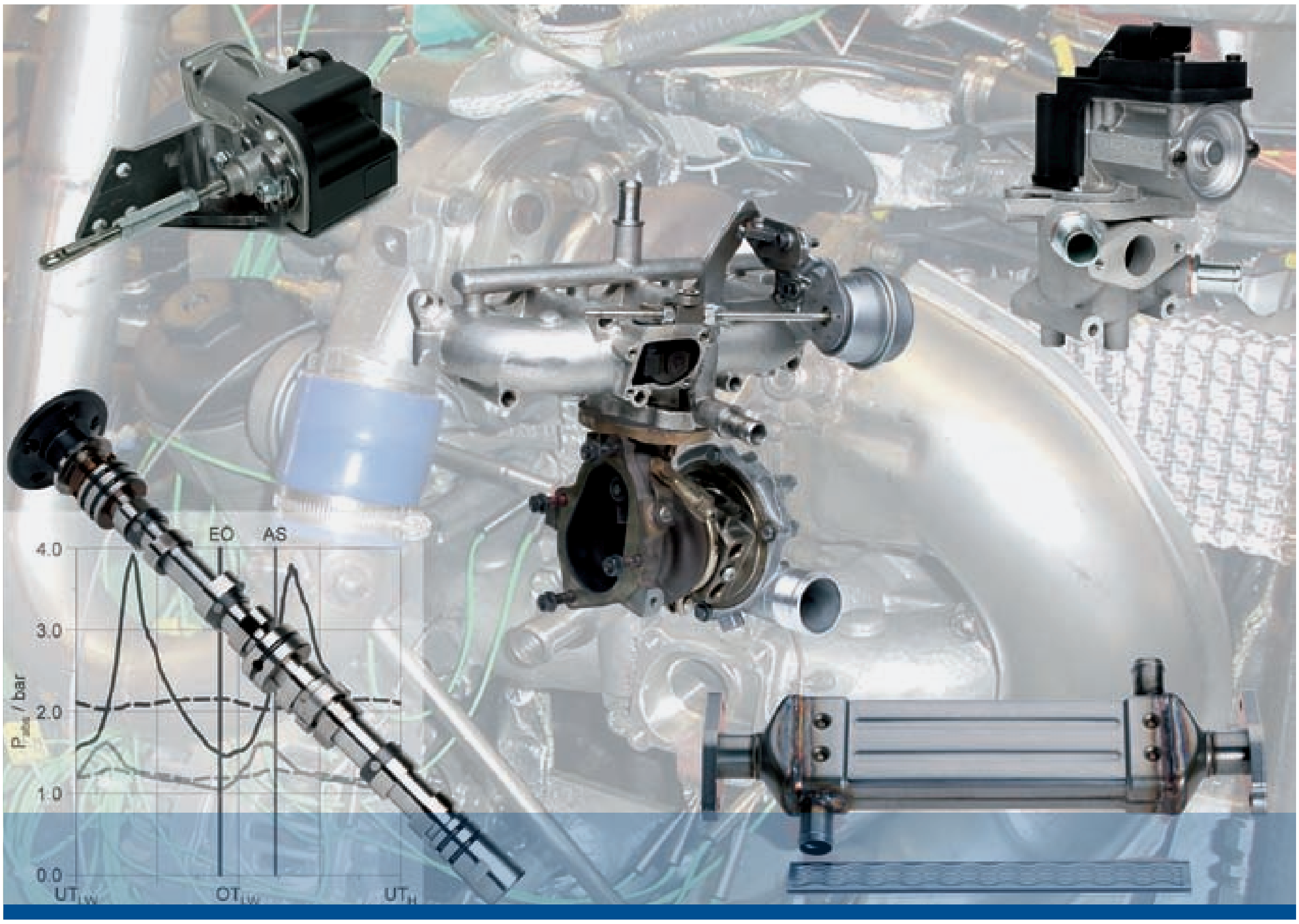

Optimisation of Gasoline Engine Performance and Fuel Consumption through Combination of Technologies

The gasoline engine has undergone intensive development in recent history with the introduction of technologies such as turbocharging and direct fuel injection. In addition to the reduction of part load fuel consumption, there is also significant optimisation potential for avoiding full load overfuelling and increasing low speed torque. Mahle will demonstrate in this paper that the introduction of technologies, used individually as well as in combination, can bring about an increase in torque at low engine speeds as well as reducing the requirement for over-fuelling.

1 Introduction

Whilst operating at higher engine speeds and loads the gasoline engine has traditionally been over-fuelled for component protection. The engine over-fuelling requirements increase respectively with a lower exhaust temperature limit (due to component material requirements) or octane number of the fuel. As a consequence both the engine fuel consumption and the tail pipe emissions increase, because the three-way catalyst is rendered effectively useless due to the non-stoichometric operating conditions. In order to achieve a load neutral reduction in high load over-fuelling, exhaust gas cooling, either through a water-cooled exhaust manifold (WCEM) or by integration of the exhaust manifold in the cylinder head [1, 2, 3], can be implemented. Furthermore a reduction in over-fuelling is enabled through the use of external cooled Exhaust Gas Recirculation (EGR) [5, 7]. This paper shows to what extent these technologies can be used and how they can be combined. Additionally, if the reduction in exhaust gas temperature is large enough, the use of a variable geometry turbine (VGT) with typical diesel engine turbine entry temperatures of up to 830 °C might be advantageous in comparison to a conventional wastegated turbocharger (t/c) in order to increase the engine torque at low engine speeds [2]. It also might reduce the exhaust backpressure in the mid-speed region compared to a conventional t/c. This increase in low speed engine torque enables a reduction in fuel consumption through the lengthening of the overall vehicle gear ratio and the associated shift in engine operating point to higher load. Because inlet and exhaust camshaft phasers have become state of the art of current direct injection, turbocharged gasoline engines and with this significant gains in engine torque can be realised due to scavenging strategies [8, 9, 10] this paper will present the potential of an operational point optimised exhaust valve opening duration. The continuously variable exhaust opening duration is realised with a relatively simple and cost effective solution using a "CamInCam" (CIC) exhaust camshaft in a DOHC application [4].

2 Experimental Engine and Equipment

The experimental engine used is a 1.4 l production unit with two stage charging capabilities (turbocharger and mechanical supercharger). An overview of the tested technologies is presented in the **Table**. In order to achieve external exhaust gas cooling the standard series production exhaust manifold with integrated turbine housing has been replaced with a water-cooled exhaust manifold (WCEM) complete with a flange mounted, but uncooled, turbine housing, **Figure 1**. The water-cooled manifold is made using a twin walled aluminium construction with an additional integrated wastegate (which can also serve as a place to draw EGR gas from). A centrally fed coolant rail divides the coolant flow to the respective manifold sections. The use of the WCEM enables the fuelling to be enleaned for a given turbine inlet temperature, thus the thermal loading on the in-cylinder components, most notably the piston and exhaust valve, also increases. Because of this not only a pre-turbine temperature limit of 980 °C is set, but also an exhaust port temperature limit of 950 °C. For the testing the original turbocharger is used with a flange applied and also a VGT turbocharger from a 2.0 l diesel engine. With the VGT unit the specific output of 90 kW/l of the production unit can be maintained. Without a wastegate the VGT would create an unacceptable level of boost pressure at high engine speeds even with the turbine inlet guide vanes fully open, therefore the boost pressure is controlled by the manifold integrated wastegate. In order to carry out the full load EGR testing the test engine setup is modified to accommodate an externally cooled EGR circuit. In this instance the exhaust gas is removed from the manifold pre-turbine using the wastegate and re-circulated down stream of the compressor, before the throttle blade. The temperature of the EGR gas is not controlled, however the use of an EGR cooler keeps the re-circulated gas temperature under 100 °C. As an alternative to the WCEM configuration, the original baseline engine is fitted with an exhaust "CamInCam" (CIC) camshaft and an exhaust cam phaser. This configuration requires valve cut outs in the piston crown, which are achieved whilst maintaining

The Authors

Dr.-Ing. Peter Wieske
is Project Leader at Corporate Advanced Engineering at Mahle GmbH in Stuttgart (Germany).

Bernhardt Lüddecke
is Development Engineer at Corporate Advanced Engineering at Mahle GmbH in Stuttgart (Germany).

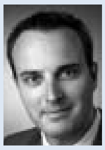

Sebastian Ewert
is Development Engineer at Corporate Advanced Engineering at Mahle GmbH in Stuttgart (Germany).

Dr.-Ing. Alfred Elsäßer
is Head of Testing at Corporate Advanced Engineering at Mahle GmbH in Stuttgart (Germany).

Hermann Hoffmann
is Head of Design at Corporate Advanced Engineering at Mahle GmbH in Stuttgart (Germany).

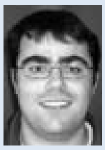

James Taylor
is Principal Development Engineer at Mahle Powertrain in Northampton (Great Britain).

Neil Fraser
is Senior Principal Research & Development Engineer at Mahle Powertrain in Northampton (Great Britain).

Table: Overview of the various experimental setups (WCEM: water-cooled exhaust manifold, CIC: CamInCam)

Variant Hardware	Baseline with supercharger	Baseline	WCEM	WCEM + EGR	WCEM + Diesel-VGT	Baseline + Exhaust-CIC
Exhaust Manifold	Series Production	Series Production	WCEM	WCEM	WCEM	Series Production
Turbocharger	Series Production	Series Production	Series production, flange mounted + un-cooled	Series production, flange mounted + un-cooled	Diesel-VGT from 2,0 l + wastegate	Series Production
Supercharger	Series Production	–	–	–	–	–
EGR Circuit	–	–	–	Pre-turbine, post compressor	–	–
Exhaust Camshaft	Series Production	Series Production	Series Production	Series Production	Series Production	Cam-In-Cam
Exhaust Camphaser	–	–	–	–	–	60° CA
Piston	Series Production	Series Production	Series Production	Series Production	Series Production	Modified, production CR

compression ratio by modification of the piston crown profile. The CIC enables a variation in the total valve-opening period, defined as the time period between the opening of the first exhaust valve and closing of the second exhaust valve, by phasing the two valve lifts relative to each other. The air temperature post intercooler is controlled to 30 °C, fuel used is 98 RON and the standard EMS system has been replaced with an open ECU.

3 Results

3.1 Effect of the Water-cooled Exhaust Manifold

Figure 2 shows the relative air to fuel ratio and the fuel consumption as a function of engine speed for the baseline setup (without supercharger) and the variant with the water-cooled exhaust manifold (with the original turbocharger) for the minimum amount of over-fuelling before the temperature limits are reached. Stoichometric running conditions can be achieved using the water-cooled manifold at an engine speed of 3500 RPM. At higher engine speeds, where the exhaust port temperature limit is reached, lambda still can be increased by 0.05 to 0.1 over the baseline. However, the possible total fuel consumption savings only show half of the potential of the leaner conditions. The introduction of exhaust manifold cooling reduces the amount of exhaust thermal energy available; consequently the turbine pressure ratio increases. In order to maintain torque, boost pressure is increased, which increases the pumping work. This leads to a higher internal EGR rate, which promotes knocking conditions that retards the combustion phasing. With the retarded combustion phasing the boost pressure requirement increased further, leading to a cycle of negative effects.

For a given value of lambda and effective load the required boost pressure for the engine with the water-cooled exhaust manifold is higher than the baseline by around 40 mbar to 80 mbar. Furthermore maximum power for a gasoline engine is reached at operating conditions just below stoichometry. Enleaning the mixture beyond $\lambda \approx 0.9$ at constant load means an additional increase in boost pressure requirement in the region of a further 100 mbar, that increases cycle averaged exhaust back pressure by a further

Figure 1: Water cooled exhaust manifold with original series production turbocharger, modified with a flange mounting

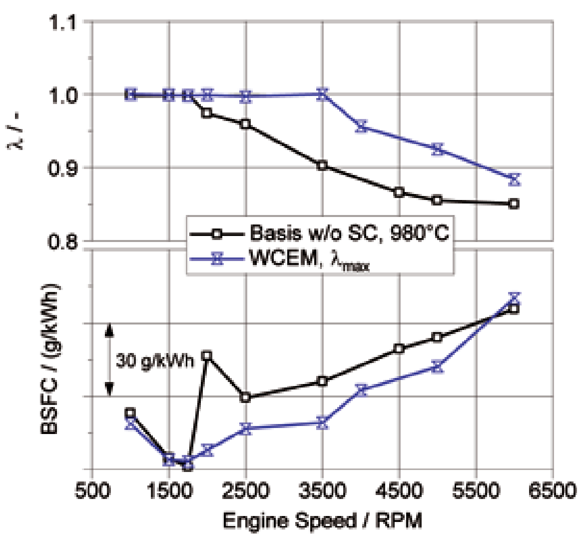

Figure 2: Over-fuelling requirement and fuel consumption with and without cooled exhaust manifold

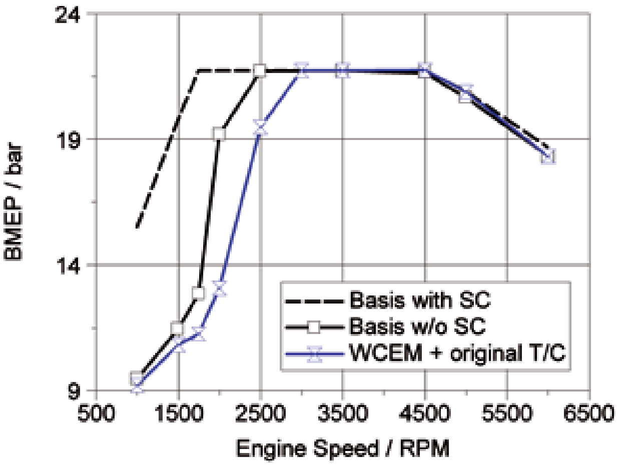

Figure 3: Effect of the water-cooled exhaust manifold on the achievable BMEP compared to the baseline variant w/o cooled exhaust manifold

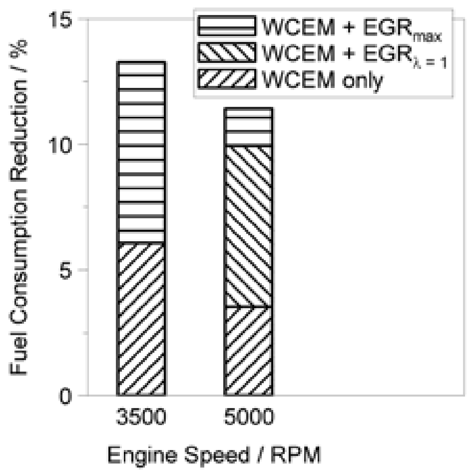

Figure 4: Fuel consumption savings with the cooled exhaust manifold (WCEM), WCEM + EGR (λ = 1) and WCEM with maximum possible EGR rate (λ = 1, wastegate closed)

200 mbar. This means that the potential savings from enleaning the air fuel mixture are not completely converted to savings in fuel consumption. This is especially noticeable at 6000 RPM, where the fuel consumption is higher than baseline with the water-cooled manifold setup despite the fact that it is being run with a leaner air fuel mixture (0.88 compared to 0.85). **Figure 3** shows the effect of running the water-cooled manifold on the Brake Mean Effective Pressure (BMEP) compared with the baseline engine with and without the supercharger. Here the BMEP losses due to the exhaust cooling are particularly evident in the area up to 3000 RPM (after which the three curves converge) when compared to the baseline setup with no super charger. On the basis of these results a reduction in the cooling surface area of the manifold looks sensible.

3.2 Combination of Water-cooled Exhaust Manifold and Full Load EGR

As a development from the previous results, showing that at high engine speeds and loads a leaner, but not stoichiometric operation is possible within the given boundary conditions of the WCEM, the engine is equipped with an additional external EGR circuit. **Figure 4** shows the BSFC improvements with the water-cooled manifold running with and without the external EGR. At 3500 RPM the fuel consumption potential increases from 6 % (WCEM only) to 13 % (WCEM and EGR) in combination with external EGR, whilst maintaining stoichiometric operation. At 5000 RPM the fuel consumption is improved by 10 % over the baseline (3 % due to WCEM, 7 % by EGR). Additional fuel consumption improvements (circa 1 %) can be realised at this operating condition by further increasing the EGR rate. For the operating points shown the EGR rate is not limited by the combustion process but by the turbocharger (wastegate fully closed), **Figure 5**. This figure shows the spark angle as well as 10 %, 50 % and 90 % MFB points as a function of mixture dilution either by EGR or fuel at full load and at an engine speed of 3500 RPM. Reducing the overfuelling causes the combustion phasing to be retarded by 4.6° CA due to knock limit, however through the addition of EGR it can be advanced by 7° CA (thus an overall improvement of 2.4° CA).

Figure 6 shows a detailed loss analysis for the four engine configurations ("baseline", "WCEM with maximum enleanment (λ=0.93, port temperature limited)", "WCEM plus EGR (λ = 1)" and "WCEM plus maximum EGR") at 5000 RPM, WOT. Comparing the "baseline" and "WCEM with maximum enleanment" it is clear that the losses from incomplete combustion (HC and CO) can be reduced with

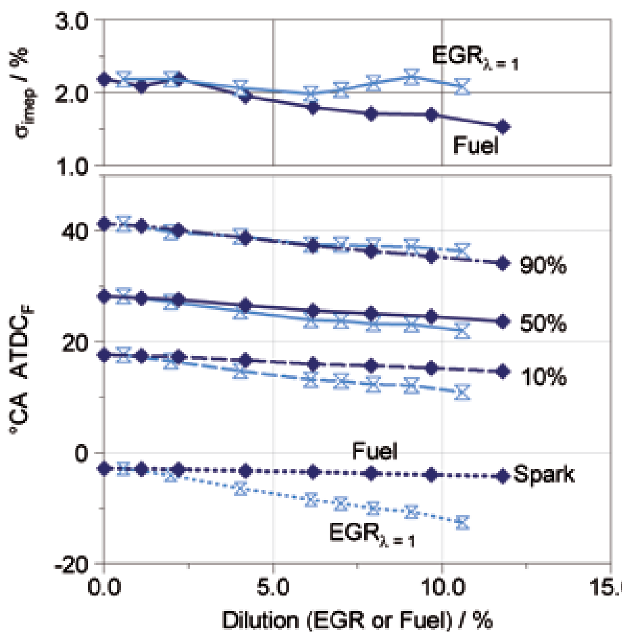

Figure 5: Standard deviation of IMEP (σ_{imep} in %) as well as % MFB as a function of the dilution of the combustion mixture with EGR or fuel at 3500 RPM (0 % fuel dilution equal to λ = 1, 10 % fuel dilution λ = 0,9)

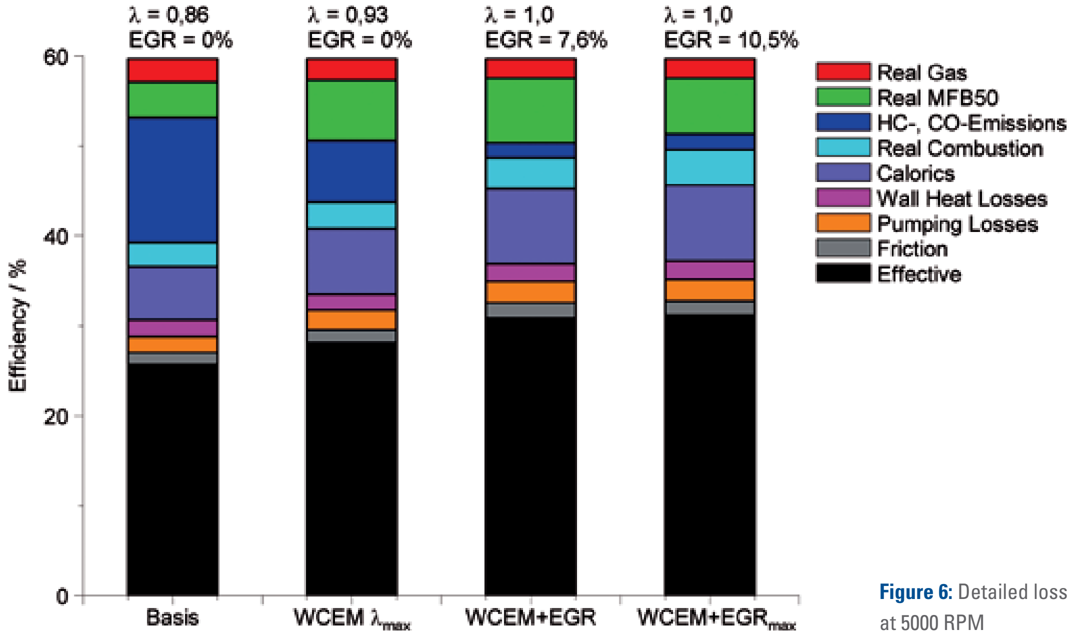

Figure 6: Detailed loss analysis of WCEM + WOT EGR at 5000 RPM

the leaner mixture. This advantage however has to be considered against the disadvantage of a later 50 % MFB angle and the accompanying longer burn duration of the leaner mixture. As a consequence of the higher boost pressure requirements the pumping losses also increase when compared to the baseline setup.

With the introduction of EGR the HC and CO losses can be further reduced without changing the 50 % MFB point. In raising the EGR rate even higher whilst maintaining stoichometry it is also possible to further reduce the combustion phasing losses, "WCEM + EGR_{max}" in Figure 6. At this operating point the combustion phasing loss is the second highest and demonstrates the potential that could be achieved without influencing the compression ratio through the use of an optimised charging device. If the turbocharger can provide the increased boost pressure requirements caused by the exhaust gas cooling, the enleanment as well as the full load EGR, then the combination of water-cooled manifold and full load EGR is sensible.

3.3 Potential Comparison of the Different Combinations

The water-cooled manifold, as well as the full load EGR circuit, both enable a reduction in the exhaust gas temperature. If the exhaust gas temperature reduction is significant, then the use of a turbocharger with variable geometry inlet vanes might be also beneficial for a gasoline engine. Whilst variable turbine geometry (VGT) technology is state of the art of current diesel engines, there is only one gasoline application in the premium market segment [11], due to their higher exhaust gas temperatures. Despite this there is a current example of an application that uses both cooled exhaust manifold and a variable flow turbine technology (VFT) [12]. When compared to a fixed geometry turbine a VGT turbine can achieve higher boost pressures at lower engine speeds by closing its inlet vanes. On the other hand as a general rule it has the turbine efficiency reduced when the inlet vanes are either fully opened or closed. Thus, contrary to a fixed geometry turbine, it might be possible at lower engine speeds that there is no positive pressure ratio across the engine during the valve overlap period. In addition, increasing turbine power by closing the inlet vanes might cause compressor surge issues. As an alternative to the combination of WCEM and VGT how far the low speed torque can be optimised by scavenging is investigated. Therefore, with the baseline engine (without the cooled exhaust manifold and w/o supercharger) the standard exhaust cam-

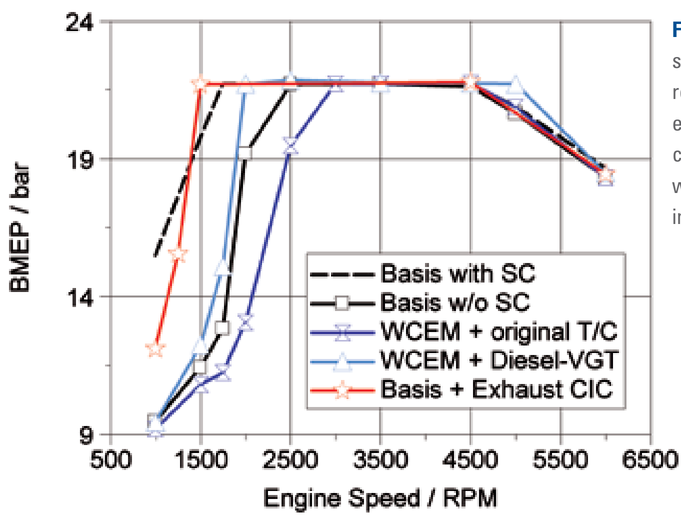

Figure 7: Steady state BMEP results for different technology combinations whilst maintaining 90 kW/l

shaft is replaced by a "CamInCam" camshaft. This will allow for phasing the exhaust valve lifts relative to each other. In comparison to the baseline the exhaust opening duration is reduced in order to achieve pulse separation with synchronised exhaust valve lift events.

Figure 7 shows the steady state BMEP versus engine speed for the five possible test engine configurations: "WCEM plus VGT", "baseline plus CIC" as well as "WCEM plus the original turbocharger". These are compared against "baseline with supercharger" and "baseline without supercharger". All tested engine configurations are single stage turbocharged (operation without the supercharger) except baseline with supercharger. Figure 7 highlights the significant increase in the BMEP at low engine speeds that is achievable with the "WCEM plus VGT" configuration (maximum BMEP is reached at 2000 RPM instead of 3000 RPM) when compared with the "WCEM plus the original turbocharger". This shows that the BMEP losses due to the exhaust gas cooling can be compensated for with the VGT. In addition it shows further downspeeding potential as 125 kW can be achieved at 5000 RPM instead of 6000 RPM. However the increase in torque in comparison to the baseline without supercharger is actually quite moderate. **Figure 8** details the minimum over-fuelling requirements and fuel consumption performance of the "baseline" and "WCEM plus VGT" variants. For completeness the results of reduced turbine inlet temperature of 780 °C are presented; this temperature limit may be used where component life is a concern. Despite using the maximum allowable turbine temperature limit of 830 °C as well as exhaust gas cooling both the over-fuelling requirements and fuel consumption are greater with the VGT variant than the baseline at high engine speeds and loads. On the other hand the VGT test variant, despite requiring a richer mixture, achieves a lower fuel consumption than the baseline in the mid engine speed range. This is due to the fact that the VGT works much more efficiently than a fixed geometry turbocharger (with open wastegate) in this region.

As can be seen in Figure 7 of the tested engine variants the combination of the baseline engine plus the CIC provides the

IMPRINT

MTZ WORLDWIDE

www.MTZonline.com

11|2009 · November 2009 · Volume 70
Springer Automotive Media | GWV Fachverlage GmbH
P.O. Box 15 46 · 65173 Wiesbaden · Germany
Abraham-Lincoln-Straße 46 · 65189 Wiesbaden · Germany

Managing Directors Dr. Ralf Birkelbach, Albrecht Schirmacher
Advertising Director Thomas Werner
Senior Production Christian Staral
Sales Director Gabriel Göttlinger

EDITORS-IN-CHARGE

Dr.-Ing. E. h. Richard van Basshuysen
Wolfgang Siebenpfeiffer

EDITORIAL STAFF

Editor-in-Chief
Johannes Winterhagen (win)
Phone +49 611 7878-342 · Fax +49 611 7878-462
E-Mail: johannes.winterhagen@springer.com

Vice-Editor-in-Chief
Dipl.-Ing. Michael Reichenbach (rei)
Phone +49 611 7878-341 · Fax +49 611 7878-462
E-Mail: michael.reichenbach@springer.com

Chief-on-Duty
Kirsten Beckmann M. A. (kb)
Phone +49 611 7878-343 · Fax +49 611 7878-462
E-Mail: kirsten.beckmann@springer.com

Sections

Electrics, Electronics
Markus Schöttle (scho)
Phone +49 611 7878-257 · Fax +49 611 7878-462
E-Mail: markus.schoettle@springer.com

Engine
Dipl.-Ing. (FH) Moritz-York von Hohenthal (mvh)
Tel. +49 611 7878-278 · +49 611 7878-462
E-Mail: moritz.von.hohenthal@springer.com

Heavy Duty Techniques
Ruben Danisch (rd)
Phone +49 611 7878-393 · Fax +49 611 7878-462
E-Mail: ruben.danisch@springer.com

Online
Dipl.-Ing. (FH) Caterina Schröder (cs)
Phone +49 611 78 78-190 · Fax +49 611 7878-462
E-Mail: caterina.schroeder@springer.com

Production, Materials
Stefan Schlott (hlo)
Phone +49 8191 70845 · Fax +49 8191 66002
E-Mail: Redaktion_Schlott@gmx.net

Service, Event Calendar
Martina Schraad
Phone +49 212 64 235 16
E-Mail: martina.schraad@springer.com

Transmission, Research
Dipl.-Ing. Michael Reichenbach (rei)
Phone +49 611 7878-341 · Fax +49 611 7878-462
E-Mail: michael.reichenbach@springer.com

English Language Consultant
Paul Willin (pw)

Permanent Contributors
Richard Backhaus (rb), Christian Bartsch (cb), Prof. Dr.-Ing. Peter Boy (bo), Prof. Dr.-Ing. Stefan Breuer (sb), Jörg Christoffel (jc), Jürgen Grandel (gl), Ulrich Knorra (kno), Prof. Dr.-Ing. Fred Schäfer (fs), Roland Schedel (rs), Bettina Seehawer (bs)

Address
P.O. Box 15 46, 65173 Wiesbaden, Germany
E-Mail: redaktion@ATZonline.de

MARKETING | OFFPRINTS

Product Management Automotive Media
Sabrina Brokopp
Phone +49 611 7878-192 · Fax +49 611 7878-407
E-Mail: sabrina.brokopp@springer.com

Offprints
Martin Leopold
Phone +49 2642 9075-96 · Fax +49 2642 9075-97
E-Mail: leopold@medien-kontor.de

ADVERTISING | GWV MEDIA

Ad Manager
Britta Dolch
Phone +49 611 7878-323 · Fax +49 611 7878-140
E-Mail: britta.dolch@gwv-media.de

Key Account Manager
Elisabeth Maßfeller
Phone +49 611 7878-399 · Fax +49 611 7878-140
E-Mail: elisabeth.massfeller@gwv-media.de

Ad Sales
Frank Nagel
Phone +49 611 7878-395 · Fax +49 611 7878-140
E-Mail: frank.nagel@gwv-media.de

Display Ad Manager
Susanne Bretschneider
Phone +49 611 7878-153 · Fax +49 611 7878-443
E-Mail: susanne.bretschneider@gwv-media.de

Ad Prices
Price List No. 53 (10/2009)

SUBSCRIPTIONS

VVA-Zeitschriftenservice, Abt. D6 F6, MTZ
P. O. Box 77 77, 33310 Gütersloh, Germany
Renate Vies
Phone +49 5241 80-1692 · Fax +49 5241 80-9620
E-Mail: SpringerAutomotive@abo-service.info

SUBSCRIPTION CONDITIONS

The eMagazine appears 11 times a year at an annual subscription rate of 269 €. Special rate for students on proof of status in the form of current registration certificate 124 €. Special rate for VDI/ÖVK/VKS members on proof of status in the form of current member certificate 208 €. Special rate for studying VDI members on proof of status in the form of current registration and member certificate 89 €. The subscribtion can be cancelled in written form at any time with effect from the next available issue.

PRODUCTION | LAYOUT

Heiko Köllner
Phone +49 611 7878-177 · Fax +49 611 7878-464
E-Mail: heiko.koellner@gwv-fachverlage.de

HINTS FOR AUTHORS

All manuscripts should be sent directly to the editors. By submitting photographs and drawings the sender releases the publishers from claims by third parties. Only works not yet published in Germany or abroad can generally be accepted for publication. The manuscripts must not be offered for publication to other journals simultaneously. In accepting the manuscript the publisher acquires the right to produce royalty-free offprints. The journal and all articles and figures are protected by copyright. Any utilisation beyond the strict limits of the copyright law without permission of the publisher is illegal. This applies particularly to duplications, translations, microfilming and storage and processing in electronic systems.

Springer Automotive Media is part of the specialist publishing group Springer Science+Business Media.

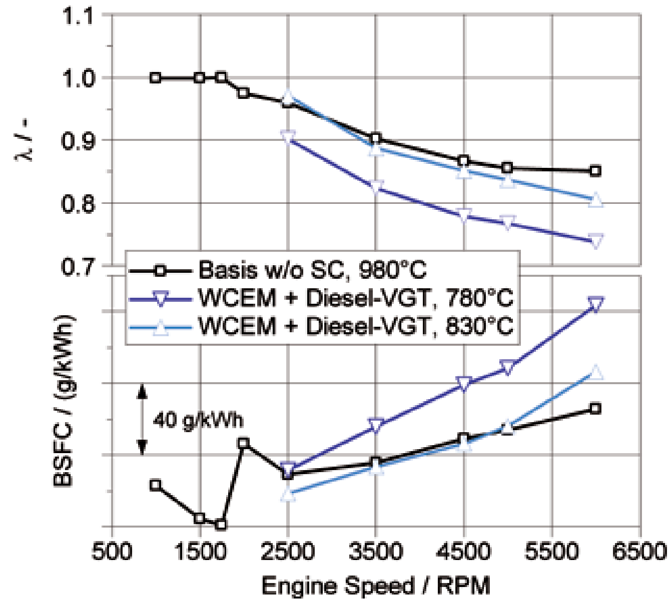

Figure 8: Over-fuelling requirements and fuel consumption of the baseline without supercharger vs. WCEM + VGT

best BMEP potential at lower engine speeds. The blowdown pulse separation in conjunction with the exhaust cam phasing leads to an increase in the mass flow of the scavenged air, which enables the turbine and compressor to work in a much more efficient manner. With the CIC set to a similar opening duration as the baseline at high speeds (i.e. from the opening point of the first valve to the closing point of the second valve) the fuel consumption is fractionally higher than the baseline variant. With a further valve timing optimisation taking the exhaust cam and event phaser as well as the intake cam phaser functionality into account the BSFC of the baseline at 6000 RPM, WOT, can be achieved within 2 %. Whilst maintaining 90 kW/l the combination of WCEM plus VGT offers no significant advantages over an uncooled exhaust manifold with standard turbocharger configuration. The large heat transfer area of the water cooled exhaust manifold leads to a significant loss of BMEP at low engine speeds, however the over fuelling requirement is also high due to the low temperature limit of 830 °C.

4 Summary and Outlook

Through using exhaust gas cooling (WCEM) the over-fuelling requirements of a charged gasoline engine can be significantly reduced, although this does not necessarily translate to a corresponding reduction in fuel consumption as it intensifies problems associated with knock. The combining with full load EGR has proven to be advantageous, as this helps to compensate for the implications of using exhaust gas cooling at high engine speeds and loads. Due to the significant enthalpy losses at low engine speeds when using exhaust gas cooling, a reduction in the heat transfer area is necessary which for example can be achieved by integrating the exhaust manifold into the cylinder head. Furthermore the BMEP losses associated with exhaust gas cooling can be balanced by using a VGT turbocharger, although this leads to a greater over-fuelling requirement due to a lower turbine entry temperature limit. Reducing the over-fuelling requirements by further expanding the cooling circuit (e.g. by cooling the turbine housing [2]) would not be advantageous due to the greater exhaust enthalpy losses at lower engine speeds. More favourable would be the combination of exhaust gas cooling with full load EGR. However this combination of technologies (diesel VGT, wastegate, full load EGR) offers only moderate performance advantages at high system costs. Taking the cost aspects into account a VGT combined with a gasoline engine does not make sense. A more favourable alternative would be to further optimise the gas exchange process through a variable exhaust valve opening duration [13].

References

[1] Borrmann, D.; Kuhlbach, K.; Friedfeldt, R.; Mehring, J.; Fritsche, R.: Zylinderkopf mit integriertem Abgaskrümmer als Beitrag zu ottomotorischen Downsizing Konzepten. 17. Aachener Kolloquium Fahrzeug- und Motorentechnik, 2008
[2] Sorger, H.; Zieher, F.; Sauerwein, U.; Schöffmann W.: Hochbelastete Zylinderköpfe für Otto- und Dieselmotoren. In MTZ 69 2008 Nr. 2
[3] Balding, A.; Coltman, D.: The Lotus integrated exhaust manifold. Industry newsletter of Lotus engineering, issues 22, 2007
[4] Schneider, F.; Lettmann, M.: MAHLE CamInCam, die neue Lösung für variable Ventilsteuerzeiten. 16. Aachener Kolloquium Fahrzeug- und Motorentechnik, 2007
[5] Müller, R.; Feldhaus, G.; Pantow, E.; Edwards, S.; Finkeldei, T.; Trapp, R.; Neubauer, M.; Kapus, P.: Reduzierung der CO_2-Emissionen eines Turbo-DI-Ottomotors durch gekühlte AGR und optimierte Regelung des Kühlsystems. 16. Aachener Kolloquium Fahrzeug- und Motorentechnik, 2007
[6] Potteau, S.; Lutz, P.; Leroux, S.; Vogel, J. B.; Moroz, S.; Tomas, E.: Cooled EGR for a Turbo SI Engine to Reduce Knocking and Fuel Consumption, SIA Congress, 2007
[7] Cairns, A.; Fraser, N.; Blaxill, H.: Pre versus post compressor supply of cooled EGR for full load economy in turbocharged gasoline engines, SAE 2008-01-425, 2008
[8] Böhme, J.; Müller, H.; Ganz, M.; Marques, M.: Der neue 2,5 Liter TFSI Fünfzylinder Motor für den Audi TT RS, 30. Wiener Motorensymposium, 2009
[9] Lückert, P.; Kreitmann, F.; Merdes, N.; Weller, R.; Rehberger, A. Bruchner, K.; Schwedler, K.; Ottenbacher, H.; Keller, T.: Der neue 1,8l 4-Zylinder Turbo Direkteinspritz Ottomotor für alle PKW mit Standardantrieb von Mercedes Benz, 30. Wiener Motorensymposium, 2009
[10] Andriesse, D.; Comignaghi, E; Lucignano, G.; Oreggioni, A.; Quinto, S.; Sacco, D.: Der neue 1.8l DI Turbo Jet Ottomotor von Fiat Powertrain Technologies, 17. Aachener Kolloquium Fahrzeug- und Motorentechnik, 2008
[11] Sterner, A.; Hofstetter, M; Kerkau, M.; Beer, M.; Ronneburger, R.; Knirsch, S.: Die variable Turbinengeometrie für die ottomotorische Anwendung beim neuen 3,6 l Biturbo Motor des Porsche 911 Turbo.11. Aufladetechnische Konferenz, 2006
[12] Ito, N.; Ohta, T.; Kono, R.; Arikawa, S.; Matsumoto, T,: Development of a 4-Cylinder Gasoline Engine with a Variable Flow Turbo-charger. SAE Technical Papers 2007-01-0263, 2007
[13] Wieske, P.; Lüddecke, B.; Ewert, S.; Elsäßer, A.; Hoffmann, H.; Rückauf, J.; Taylor, J.: Neue Konzepte zur Optimierung des transienten Drehmomentaufbaus und zur Verbrauchsoptimierung von aufgeladenen Ottomotoren. 18. Aachener Kolloquium Fahrzeug- und Motorentechnik, 2009

TÜV SÜD

Automotive

Choose certai
Add value.

tank.tech 2009

Congress with accompanying technical exhibition

November 10 – 11, 2009

The Monarch Hotel, Bad Gögging near Munich, Germany

Information online: www.ATZlive.com

In cooperation with

ATZ

TÜV SÜD Automotive GmbH

TÜV®

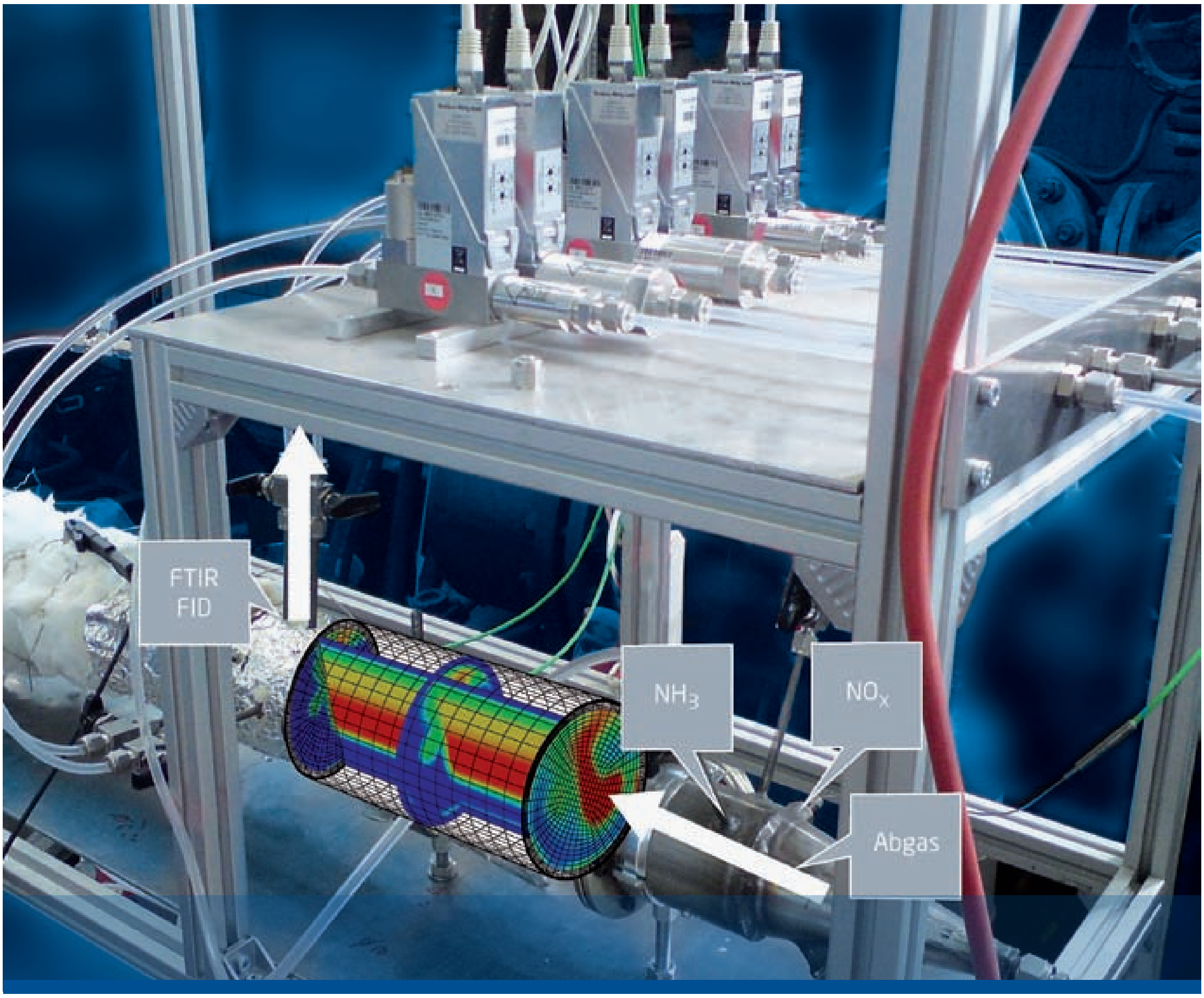

personal buildup for Force Motors Ltd.

KATsim – A Tool for Numerically Simulating Exhaust-gas Catalysts

The demands placed on numerically simulating exhaust-gas aftertreatment components are manifold. In addition to laying out the process engineering of exhaust-emission systems, the focus also rests on concept studies for their configuration as well as on 3-D simulations. Increasingly, simulations are also being used for developing and calibrating algorithms for engine control units. To meet these different requirements, IAV is developing the KATsim modular numeric simulation system.

1 Introduction and Objective

In addition to measures inside the engine, developing suitable exhaust-gas aftertreatment strategies is indispensable for meeting emission limits prescribed in law. Particular significance is attached to the numeric simulation of exhaust-gas aftertreatment components, such as catalytic converters and diesel particulate filters, throughout the development process. As part of the preliminary layout process, decisions must be made on how to configure the exhaust system in relation to the prescribed emission ceilings and anticipated engine emissions. Studying the way in which different components interact within the exhaust system, such as the effects regenerating the particulate filter has on downstream SCR or NO_x adsorption catalysts, is also of interest.

In addition to configuring the process engineering of exhaust systems, 3-D computations can also be used for assessing local temperatures and conversion rates on the basis of inhomogeneous distributions of thermodynamic state variables both upstream of the catalyst as well as inside it.

Complex numeric simulation models are being used on an increasing scale in the process of developing and calibrating algorithms for control units. Not only can they be employed as complex controlled-system models for laying out control and diagnostic strategies but also for deriving simple algorithms suitable for application in control units. Necessitating real-time capability, the use of models in SiL or HiL simulators places high demands on the numeric algorithms implemented.

The following article presents a modular system for simulating exhaust-gas catalysts based on numerically solving transient, thermodynamic conservation equations for mass and energy. The models can be linked with 3-D simulation programs, such as OpenFOAM. Linking them to ASCET SD and MATLAB/Simulink additionally opens up ways of using the models as "virtual test benches" within the algorithm development process and for basic control-unit algorithm calibration.

2 Model Basics and Numeric Realization

Modeling the chemico-physical processes taking place in the catalytic converter [1] involves convective and diffusive mass and energy transfer processes within a channel representative of the catalyst monolith shown in **Figure 1**. The heterogeneous, catalyzed chemical reactions within the wash-coat are linked to the mass and energy balances by means of extend-

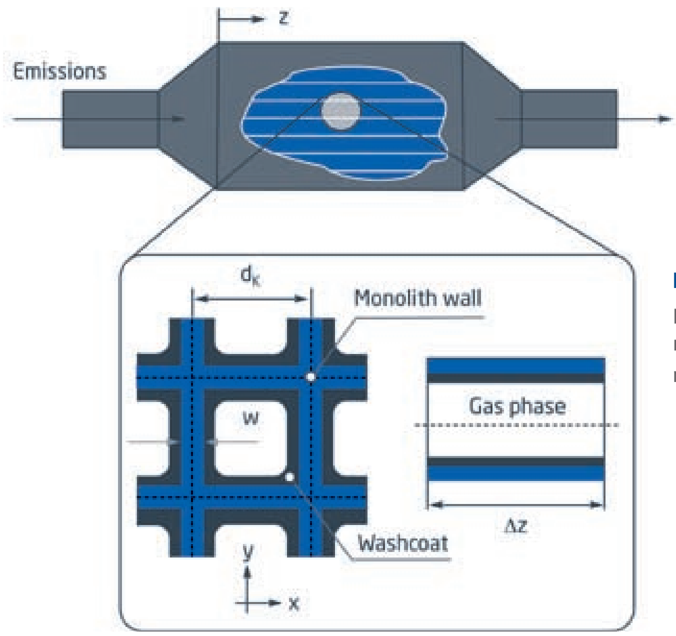

Figure 1: Schematic presentation of the reference channel model

The Authors

Dipl.-Math.
Sandra Dusemund
is Development Engineer for Diesel Engine Functions in the Business Area of Powertrain Mechatronics at IAV GmbH in Gifhorn (Germany).

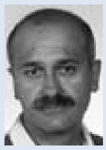

Dr.-Ing.
Hellfried Schneider
is Development Engineer for Diesel Engine Functions in the Business Area of Powertrain Mechatronics at IAV GmbH in Gifhorn (Germany).

Dr.-Ing.
Kay Langeheinecke
is Head of the Diesel Engine Functions Team in the Business Area of Powertrain Mechatronics at IAV GmbH in Gifhorn (Germany).

Dipl.-Ing.
Robert Bank
is Member of the Scientific Staff at the Chair of Technical Thermodynamics at Rostock University (Germany).

Table: Model equations and reaction mechanism of SCR catalysts

Governing equations

energy equation gas phase, solid, isolation and canning

$$\frac{\partial}{\partial t}(\rho_g\, c_{p,g}\, T_g) + \frac{\partial}{\partial z}(\rho_g\, u_g\, c_{p,g}\, T_g) = \alpha_{m,innen}\,(T_s - T_g)\,\Psi_K$$

$$\rho_S c_S \frac{\partial T_S}{\partial t} = \frac{\partial}{\partial z}\left(\lambda_S \frac{\partial T_S}{\partial z}\right) + \sum_{j=1}^{n}\left\{q_{reak,j} + \frac{\Delta A_{w,j}}{\Delta V_{S,j}}\,\alpha_{m,innen}\,(Nu)\,(T_g - T_S)\right\}$$

continuity equation (gas phase bulk, gas phase washcoat, surface washcoat)

$$c_g \frac{\partial x_{i,g}}{\partial t} + \frac{\partial}{\partial z}(c_g\, u_g\, x_{i,g}) + c_g\, \beta_i\, (x_{i,s} - x_{i,g}) = 0$$

$$c_g \frac{\partial x_{i,s}}{\partial t} + c_g\, \beta_i\, (x_{i,g} - x_{i,s}) + \sum_j v_j\, r_j = 0$$

$$\frac{\partial \Theta_i}{\partial t} + \frac{\sum_j v_j\, r_j}{n_{ads,max}} = 0$$

chemical reaction kinetics (adsorption, desorption, chemical reaction)

$$\dot r_{k,ads} = \left(1 - \sum_j \Theta_{j,ads}\right) k_{k,ads} \exp\left(-\frac{E_{a,k}}{R_g T}\right) x_k^{y}\, \frac{1}{G_k}$$

$$\dot r_{k,des} = \Theta_{k,ads}\, k_{k,ads} \exp\left(-\frac{E_{a,k}}{R_g T}\right)$$

$$\dot r_{k,reak} = k_{k,reak} \exp\left(-\frac{E_{a,k}}{R_g T}\right) \frac{1}{G_k} \prod_j (x,\Theta)_j^{\gamma_j}$$

Nomenclature

A	area	q	heat current density	z	coordinate	Θ	surface configuration
c	heat capacity	$\dot r$	rate of reaction	α	heat transfer coefficient	Ψ	area volume parameter
c_g	molarity	R_g	gas constant	β	coefficient of diffusion	*ads*	adsorption
E_a	activation energy	t	time	γ	order of reaction	*des*	desorption
G	term of inhibition	T	temperature	φ	angle	*reak*	reaction
k	rate factor	u	velocity	λ	heat conduction coefficient	g	gas(-phase)
$n_{ads,max}$	number of active sites	V	volume	v	stoichiometric coefficient	i, j, k	indices
Nu	*Nusselt* number	x	concentration	ρ	density	m	mean
						S	monolith (*solid*)

Reaction mechanism SCR

hydrolysis / thermolysis	$HNCO + H_2O \rightarrow NH_3 + CO_2$	side reaction	$2NH_3(s) + 3NO_2 \rightarrow N_2 + 3NO + 3H_2O$
adsorption / desorption of ammonia	$NH_3 + s \leftrightarrow NH_3(s)$	reduction of nitrous oxide	$2NH_3(s) + 3N_2O \rightarrow 4N_2 + 3H_2O$
standard SCR reaction	$4NH_3(s) + 4NO + O_2 \rightarrow 4N_2 + 6H_2O$	oxidation of ammonia 1	$4NH_3(s) + 3O_2 \rightarrow 2N_2 + 6H_2O$
fast SCR reaction	$4NH_3(s) + 2NO + 2NO_2 \rightarrow 4N_2 + 6H_2O$	oxidation of ammonia 2	$2NH_3(s) + 2O_2 \rightarrow N_2O + 3_2O$
SCR reaction without oxygen	$8NH_3(s) + 6NO_2 \rightarrow 7N_2 + 12H_2O$	oxidation of ammonia 3	$4NH_3(s) + 5O_2 \rightarrow 4NO + 6H_2O$
slow SCR reaction	$4NH_3(s) + 6NO \rightarrow 5N_2 + 6H_2O$	adsorption / desorption water	$H_2O \leftrightarrow H_2O(s)$
formation of nitrous oxide	$2NH_3(s) + 2NO_2 \rightarrow N_2O + N_2 + 3H_2O$		

ed Arrhenius approaches using source and sink terms. Allowance is made for various reaction mechanisms for describing DOC, SCR, NO_x adsorption and 3-way catalytic converters. A list of the model equations and the reaction mechanism for SCR catalysts [2] is provided in **Table**.

The conservation equations are discretized using the finite-volume method, with an axial volume element being divided into gas phase, monolith wall und wash-coat. The areas are coupled in accordance with the principles of heat and mass transfer. The heterogeneous, catalyzed reactions only take place in the wash-coat zone. The resultant, rigid differential-algebraic system of equations is integrated by means of a modified solution algorithm to Bader and Deuflhard [3] with time step adaptation. With an axial resolution of 15 volume elements, the highly efficient solution algorithm provides the model with real-time capability on a modern-day standard PC (Intel 2.4 GHz Duo Core). The program code is written in the C programming language and integrated in a MATLAB GUI. In addition to this, interfaces are provided to MATLAB/Simulink by means of S functions and to ASCET SD.

3 Test-bench Investigations and Parameterization

The reaction-kinetic parameters (the extended Arrhenius approaches being shown in Table 1) are determined on the basis of experimental studies carried out on synthetic-gas test benches. The complex, interlinked reaction mechanisms can be split up into individual reactions, with the reaction parameters being ascertained separately. In a second step, interactions between exhaust-gas components, such as inhibition effects, are calibrated on a cross-reactional basis. Experiments with actual exhaust gas on the engine test bench are used for validating the parameters while allowing for the overall reaction mechanism.

Gas is metered on the synthetic-gas test bench by means of a mass-flow controller. Mineral-insulated and surface thermocouples are used for sensing temperatures. Exhaust-gas composition is analyzed using FTIR and FID systems.

The experimental data and model data provide the basis for defining target functions. As the target functions undergoing optimization are non-linear in the parameters being sought, using optimization methods, such as the Newton or the conjugated gradient method, harbors the risk of finding local minimum relating to the starting parameters instead of the global minimums being sought. This is why use is made of a hybrid method, a combination of genetic algorithm and conjugated gradient method. The genetic algorithm [4] works with many parameters and evaluates their quality using the conjugated gradient method. The best parameter sets pass on their parameters, with parameter recombinations and mutations taking place. In turn, this new parameter generation provides the basis for determining the best parameter sets until a breakoff criterion is met.

4 Applications

Based on the example of an SCR catalyst, the following illustrates the various uses of KATsim.

4.1 1-D Simulations: Analyzing Exhaust-gas Cycles

One-dimensional computations of standardized exhaust-gas cycles are carried out to validate the model and the quality of reaction-kinetic parameters. Radial distributions of the thermodynamic variables at the various axial positions are only taken into consideration as radially averaged variables. Compared with three-dimensional computations, the significantly shorter computing times are an advantage. The extent to which a real three-dimensional system can be justifiably simulated using a one-dimensional model follows from an analysis of the initial and boundary conditions.

Figure 2 shows the results of simulating the time-resolved and cumulated nitrogen-oxide emissions downstream of the SCR catalyst of a six-cylinder diesel engine in the NEDC cycle. Comparison with the experimental data reveals clear variations during the cold-starting phase as a result of water and hydrocarbon adsorption processes. Relevant reaction mechanisms are not calibrated in this model because detailed analysis of the cold-starting phase is not at the focus of the investigations presented here. Over the further course of time, excursions fall to approximately 10 ppm, corresponding to the accuracy required. Compared with the experimental data, the cumulated nitrogen-oxide masses show deviations of less than 5 %.

4.2 3-D Simulations: Effects of Inhomogeneous Mixture Formation

After coupling the 1-D simulation model with the OpenFOAM open-source CFD toolbox, it is possible to perform 3-D simulations of the processes taking place in the monolith. This provides the capability of allowing for radial distributions of input variables, such as speed and composition, as well as three-dimensional effects of heat transfer at the catalyst surface. To incorporate the 1-D simulation model into the 3-D simulation model, the monolith end face meshed with rectangular elements is extruded in the axial direction to form "cell stacks", with a reference channel being assigned to each stack. Each reference channel is based on the 1-D simulation model and subjected to differentiated starting conditions reflecting the distributions upstream of the catalyst. The reference channels are thermally coupled by solving the three-dimensional

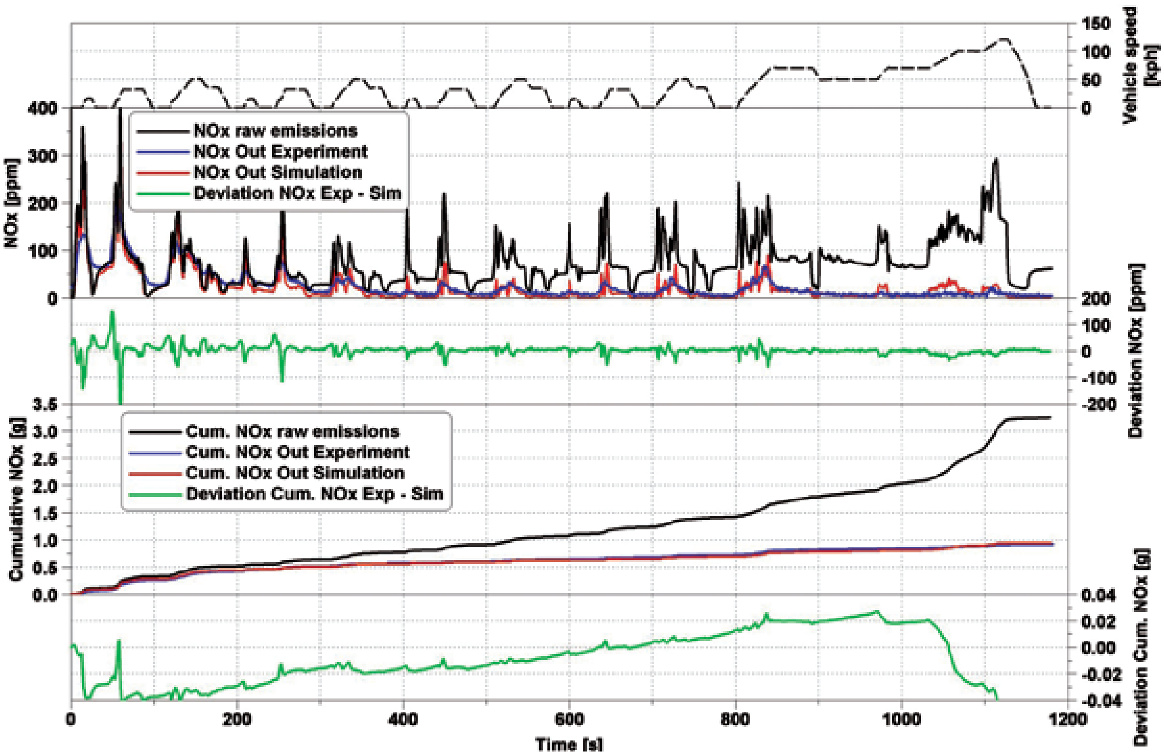

Figure 2: Simulation of a NEDC cycle and comparison with experimental data

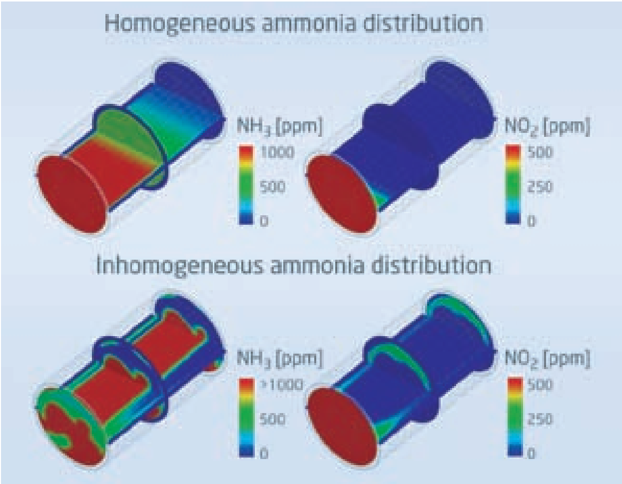

Figure 3: 3-D investigation of ammonia-distribution inside the SCR catalyst

thermal conduction equation for the entire monolith in OpenFOAM.

By way of example, **Figure 3** shows three-dimensional simulations for reducing NO_2 in the SCR catalyst for the cases of homogeneous and inhomogeneous ammonia distribution, with the quantity metered being the same. In the case of even distribution, ammonia and nitrogen oxide are fully converted in the monolith. Inhomogeneous ammonia distribution shows a clear breakthrough of ammonia and nitrogen oxides.

4.3 Dynamic Simulation in MATLAB/Simulink: Algorithm Development and Controller Layout

After integrating KATsim as a function block in MATLAB/Simulink, dynamic simulations of exhaust-gas cycles are carried out with the aim of developing and validating suitable ammonia metering strategies, **Figure 4**. Here, exhaust-gas measurement readings taken upstream of the catalyst are transferred to KATsim as boundary conditions. To control the quantity of metered-in ammonia on a model basis, the catalyst's ammonia charge is determined in an algorithm suitable for control-unit use while allowing for adsorption, desorption as well as various reduction reactions and compared with a setpoint ammonia charge demanded at a specific operating point. Resulting from this, the controller algorithm determines a quantity of ammonia that is to be metered in by the injector. In relation to the exhaust gas upstream of the catalytic converter (exhaust-gas mass flow, temperature, composition), the target charge takes into account a maximum nitrogen-oxide conversion rate with negligible ammonia slip under steady-state operating conditions.

Figure 5 shows the above-mentioned NEDC cycle. At the beginning of the cycle, the catalyst is uncharged. Metering is released as from an exhaust temperature of 100 °C, with ammonia being injected in accordance with the difference between target and actual catalyst charge. Dynamic changes in exhaust-gas variables during the cycle can result in ammonia breakthroughs downstream of the catalyst when using target charges determined under steady-state operating conditions. In addition to adjusting the controller parameters, it is also possible to reduce ammonia slip by dynamically adjusting the target charge. This is done by observing a safety margin and not by adjustment to the maximum charge specific to the operating point. Any associated reduction in the conversion rate is low in the NEDC cycle under analysis.

In addition to the simple metering strategy described here, there are further model-based, non-linear possibilities of controlling the metering rate. Using complex numeric models as "virtual test benches" provides the capability of comparing the various approaches on a reproducible basis, of evaluating control quality and, ultimately, of permitting basic calibration of the control and model parameters.

5 Summary and Outlook

IAV is developing a modular simulation system to meet the various demands in developing new exhaust-gas aftertreatment systems. In addition to one-dimensional simulations, three-dimensional in-

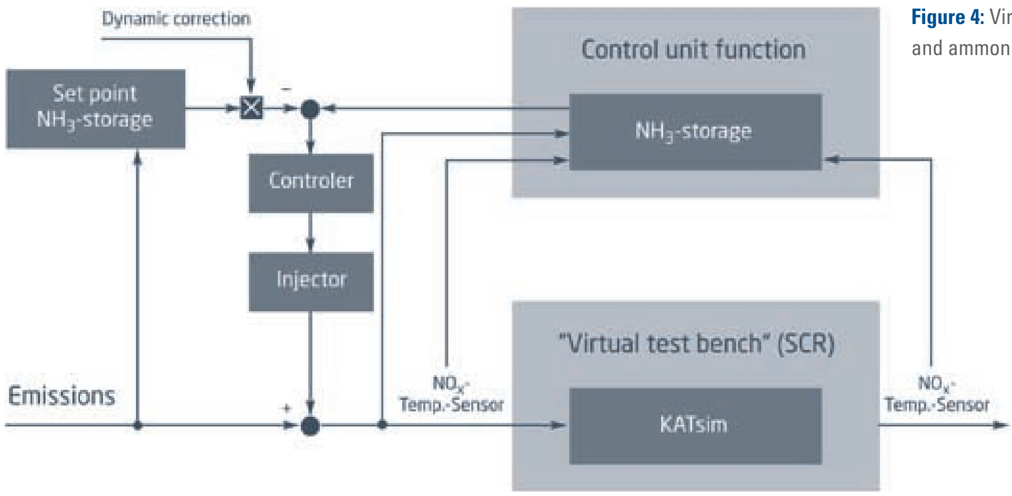

Figure 4: Virtual test bench and ammonia metering strategy

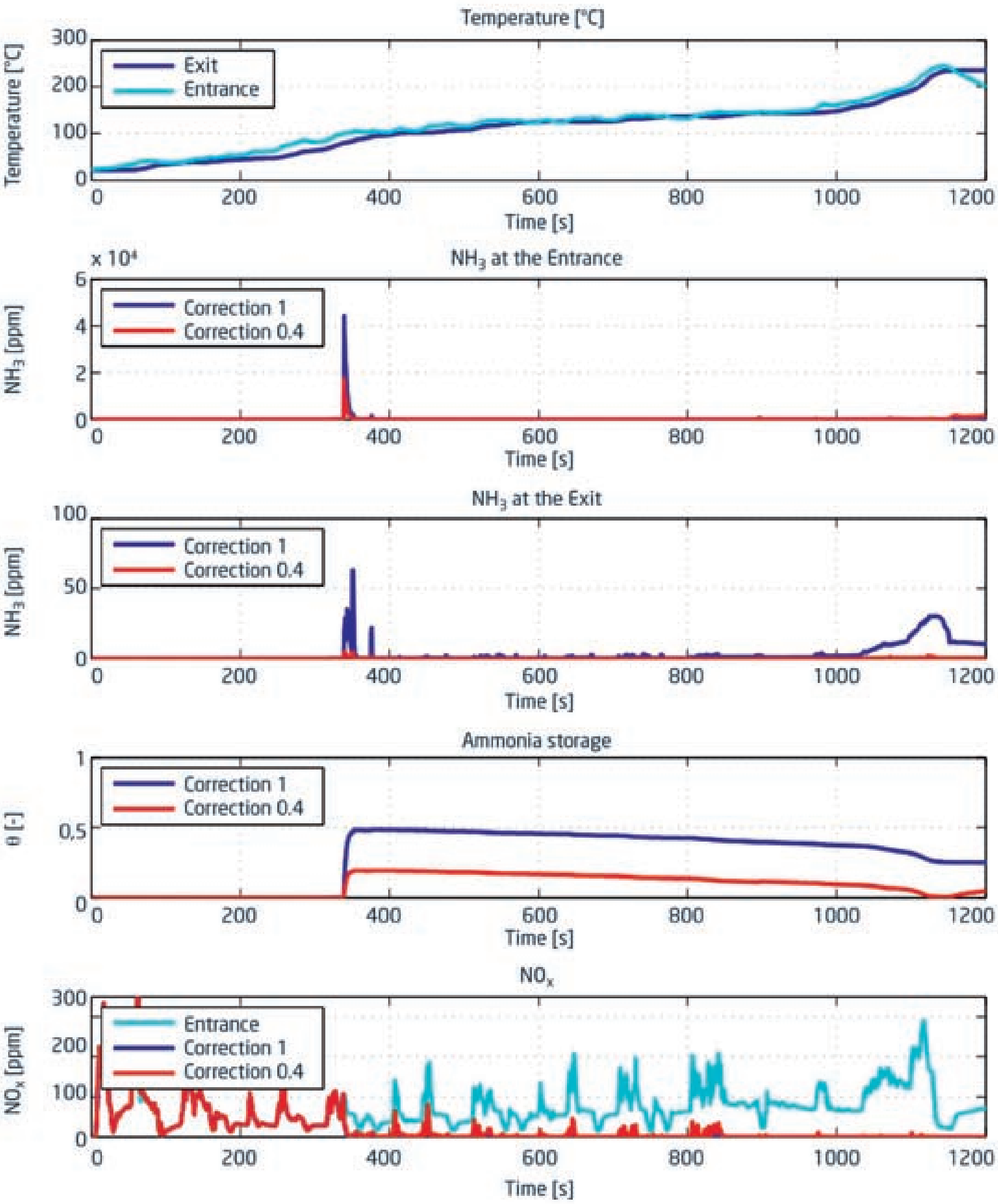

Figure 5: Comparison of different dynamic corrections in the NEDC cycle

vestigations are carried out to examine the physical processes taking place inside the catalyst. Doing do, it is possible to study the effects inhomogeneous flow, concentration and temperature distributions upstream of the catalytic converter have on local conversion rates. In combination with MATLAB/Simulink, KATsim can be used as a "virtual best bench" for the development and basic calibration of new control-unit algorithms.

Improvements currently being made to the "virtual test bench" include the integration of further exhaust-gas aftertreatment components, such as DPF, DOC and NO_x adsorption catalysts. To configure appropriate operating and control algorithms, it is necessary to influence exhaust-gas states directly downstream of the combustion chamber by altering engine operating points. By way of example, post-injection inside the combustion chamber can be used to increase the exhaust-gas temperature for thermally regenerating the diesel particulate filter or for optimizing cold-starting behavior. This involves adding engine models (e.g. zone models of combustion inside the engine) to the "virtual test bench" or linking appropriate simulation tools for simulating the engine process, such as THEMOS or GT-Power, with KATsim.

References

[1] Hayes, R. E.; Kolaczkowski, S. T.: Introduction to Catalytic Combustion. Gordon and Breach Science Publishers, 1997
[2] Käfer, S.: Trockenharnstoff-SCR-System und Betriebsstrategie für Fahrzeuge mit Dieselmotor (Dry Urea SCR System and Operating strategy for Diesel-Engined Vehicles). Kaiserslautern, University of Technology, Dissertation, 2004
[3] Press, W. H.; Teukolski, S. A.; Vetterling, W.T.: Numerical Recipes in C: The Art of Scientific Computing. Cambridge University Press, 1992
[4] Falkenauer, E.: Genetic Algorithms and Grouping Problems. John Wiley and Sons, 1998

Peer Review ATZ|MTZ

Peer Review Process for Research Articles in ATZ and MTZ

Steering Committee

Prof. Dr.-Ing. Stefan Gies	RWTH Aachen	Institut für Kraftfahrwesen Aachen
Prof. Dipl.-Des. Wolfgang Kraus	HAW Hamburg	Department Fahrzeugtechnik und Flugzeugbau
Prof. Dr.-Ing. Ferit Küçükay	Technische Universität Braunschweig	Institut für Fahrzeugtechnik
Prof. Dr.-Ing. Stefan Pischinger	RWTH Aachen	Lehrstuhl für Verbrennungskraftmaschinen
Prof. Dr.-Ing. Hans-Christian Reuss	Universität Stuttgart	Institut für Verbrennungsmotoren und Kraftfahrwesen
Prof. Dr.-Ing. Ulrich Spicher	Universität Karlsruhe	Institut für Kolbenmaschinen
Prof. Dr.-Ing. Hans Zellbeck	Technische Universität Dresden	Lehrstuhl für Verbrennungsmotoren

Advisory Board

Prof. Dr.-Ing. Klaus Augsburg	**Dr.-Ing. Markus Lienkamp**
Prof. Dr.-Ing. Bernard Bäker	**Prof. Dr. rer. nat. habil. Ulrich Maas**
Prof. Dr.-Ing. Michael Bargende	**Prof. Dr.-Ing. Martin Meywerk**
Dr.-Ing. Christoph Bollig	**Prof. Dr.-Ing. Klaus D. Müller-Glaser**
Prof. Dr. sc. techn. Konstantinos Boulouchos	**Dr. techn. Reinhard Mundl**
Prof. Dr.-Ing. Ralph Bruder	**Prof. Dr. rer. nat. Cornelius Neumann**
Dr. Gerhard Bruner	**Dr.-Ing. Lothar Patberg**
Prof. Dr. rer. nat. Heiner Bubb	**Prof. Dr.-Ing. Peter Pelz**
Prof. Dr. rer. nat. habil. Olaf Deutschmann	**Prof. Dr. techn. Ernst Pucher**
Dr. techn. Arno Eichberger	**Dr. Jochen Rauh**
Prof. Dr. techn. Helmut Eichlseder	**Prof. Dr.-Ing. Konrad Reif**
Dr.-Ing. Gerald Eifler	**Dr.-Ing. Swen Schaub**
Prof. Dr.-Ing. Wolfgang Eifler	**Prof. Dr. sc. nat. Christoph Schierz**
Prof. Dr. rer. nat. Frank Gauterin	**Prof. Dr. rer.-nat. Christof Schulz**
Prof. Dr. techn. Bernhard Geringer	**Prof. Dr. rer. nat. Andy Schürr**
Prof. Dr.-Ing. Uwe Grebe	**Prof. Dr.-Ing. Ulrich Seiffert**
Prof. Dr.-Ing. Horst Harndorf	**Prof. Dr.-Ing. Hermann J. Stadtfeld**
Prof. Dr. techn. Wolfgang Hirschberg	**Prof. Dr. techn. Hermann Steffan**
Univ.-Doz. Dr. techn. Peter Hofmann	**Dr.-Ing. Wolfgang Steiger**
Prof. Dr.-Ing. Günter Hohenberg	**Prof. Dr.-Ing. Peter Steinberg**
Prof. Dr.-Ing. Bernd-Robert Höhn	**Prof. Dr.-Ing. Christoph Stiller**
Prof. Dr. rer. nat. Peter Holstein	**Dr.-Ing. Peter Stommel**
Prof. Dr.-Ing. habil. Werner Hufenbach	**Prof. Dr.-Ing. Wolfgang Thiemann**
Prof. Dr.- Ing. Roland Kasper	**Prof. Dr.-Ing. Helmut Tschöke**
Prof. Dr.-Ing. Tran Quoc Khanh	**Dr.-Ing. Pim van der Jagt**
Dr. Philip Köhn	**Prof. Dr.-Ing. Georg Wachtmeister**
Prof. Dr.-Ing. Ulrich Konigorski	**Prof. Dr.-Ing. Jochen Wiedemann**
Dr. Oliver Kröcher	**Prof. Dr. techn. Andreas Wimmer**
Dr. Christian Krüger	**Prof Dr. rer. nat. Hermann Winner**
Univ.-Ass. Dr. techn. Thomas Lauer	**Prof. Dr. med. habil. Hartmut Witte**
Prof. Dr. rer. nat. Uli Lemmer	**Dr. rer. nat. Bodo Wolf**
Dr. Malte Lewerenz	

Scientific articles in ATZ Automobiltechnische Zeitschrift and MTZ Motortechnische Zeitschrift are subject to a proofing method, the so-called peer review process. Articles accepted by the editors are reviewed by experts from research and industry before publication. For the reader, the peer review process further enhances the quality of ATZ and MTZ as leading scientific journals in the field of vehicle and engine technology on a national and international level. For authors, it provides a scientifically recognised publication platform.

Therefore, since the second quarter of 2008, ATZ and MTZ have the status of refereed publications. The German association "WKM Wissenschaftliche Gesellschaft für Kraftfahrzeug- und Motorentechnik" supports the magazines in the introduction and execution of the peer review process. The WKM has also applied to the German Research Foundation (DFG) for the magazines to be included in the "Impact Factor" (IF) list.

In the ATZ|MTZ Peer Review Process, once the editorial staff has received an article, it is reviewed by two experts from the Advisory Board. If these experts do not reach a unanimous agreement, a member of the Steering Committee acts as an arbitrator. Following the experts' recommended corrections and subsequent editing by the author, the article is accepted. *rei*

MTZ Peer Review
The Seal of Approval for scientific articles in MTZ.
Reviewed by experts from research and industry.

Received ....
Reviewed ....
Accepted ....

Seal of Approval – this seal is awarded to articles in ATZ and MTZ that have successfully completed the peer review process

The reference book for adhesives practitioners

The Adhesive Technology Compendium for the trade magazine adhesion extra ADHESIVES & SEALANTS

Adhesive Technology Compendium 2009
304 pages. paperback.
Euro 25.90
ISBN 978-3-8348-0912-4

Content:

Topical background information on:

- Adhesives suppliers
- Equipment and plant manufacturing companies
- Research and development companies

Guide to German laws and regulations

Overview of European standards and test methods

Sources

Statistical overview: Production and markets

Order

Fax: +49(0)611.78 78-440 or at www.adhaesion.com

Yes, I wish to order ____ copies

Adhesive Technology Compendium 2009
304 p., paperback, € 25.90
ISBN 978-3-8348-0912-4

Subject to modifications.
Available from bookstores
or from the publishers.

Full name

Street (no PO box) Post code/City

Date Signature

Abraham-Lincoln-Str. 46 • D-65189 Wiesbaden • Phone: +49 (0) 611.78 78-0 • www.viewegteubner.de
CEO: Dr. Ralf Birkelbach. Company registered at AG Wiesbaden HRB 9754

VIEWEG+TEUBNER

Gas Sampling Probe for the Sampling of Engine Combustion Chamber Samples
in High Temporal Resolution

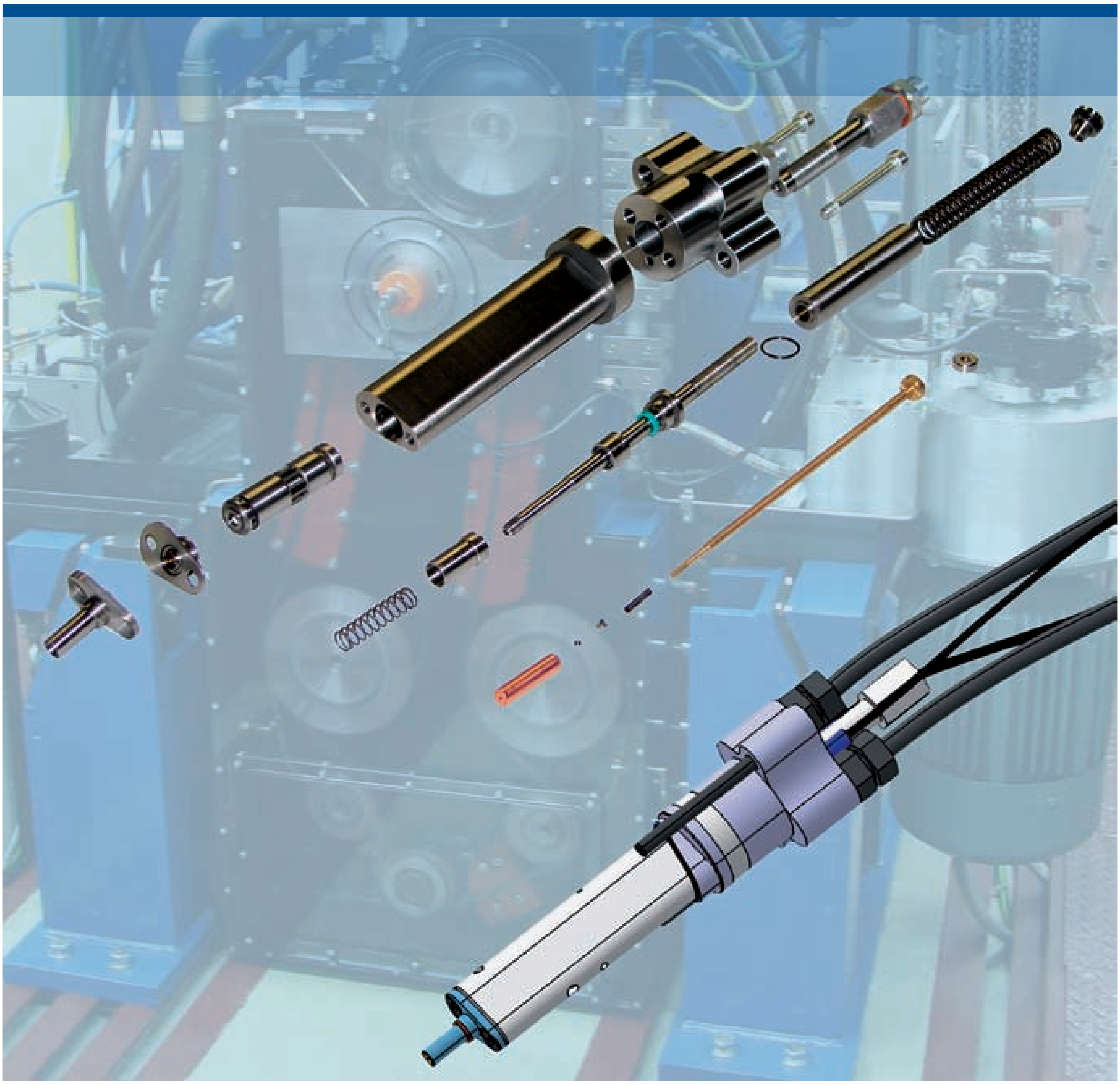

Despite extensive research, the formation and oxidation of soot in combustion engines still raises many questions. The Chair of Combustion Engines (LVK) at the Technische Universität München (TUM) developed a novel research tool, which allows the time-resolved sampling of soot from the combustion chamber.

1 Introduction

Due to the introduction of new emission limits, engine developers are challenged to develop more low-emission combustion processes, either by optimizing existing combustion processes, or through the conception of new ones. Although there are several process control alternatives, the influence of different combustion process parameters on the generation and post-oxidation of soot has so far not been adequately analyzed. Research has been done on the formation of soot within the combustion chamber, but up to now only the soot mass has been measured in a time-resolved manner. In order to research the temporally resolved soot formation in consideration of the soot structure, the Chair of Combustion Engines (LVK) at the Technische Universität München (TUM) developed a novel and innovative gas sampling probe. This probe allows the sampling of particles from the combustion chamber at different stages of combustion. These samples are a kind of snap-shot of the soot, at different points in the combustion cycle. Comparison of said snapshots shows the soot's generation, formation and the following post-oxidation in the combustion chamber, thus allowing for detailed research on the soot formation process. This article covers the entire development process of the new gas sampling probe by the LVK, including designing and simulation, as well as its initiation and initial results of the sampling.

2 Development

2.1 Goals and Challenges

The aim is the sampling of soot from the combustion chamber of an engine at a specified point of combustion. In order to depict the individual steps of the soot formation, it is necessary to extract samples in high time resolution, as shown in **Figure 1**. The sample particles specifically need to be collected and separated, taking special care not to alter their structure by mechanical action. The mixing of samples with earlier ones must be avoided. For significant conclusions about the soot's composition it is necessary to inhibit the sample's reaction after the sampling. To avoid condensation and precipitation in the sampling path, the distance between the sampling point and the collecting location have to be as short as possible.

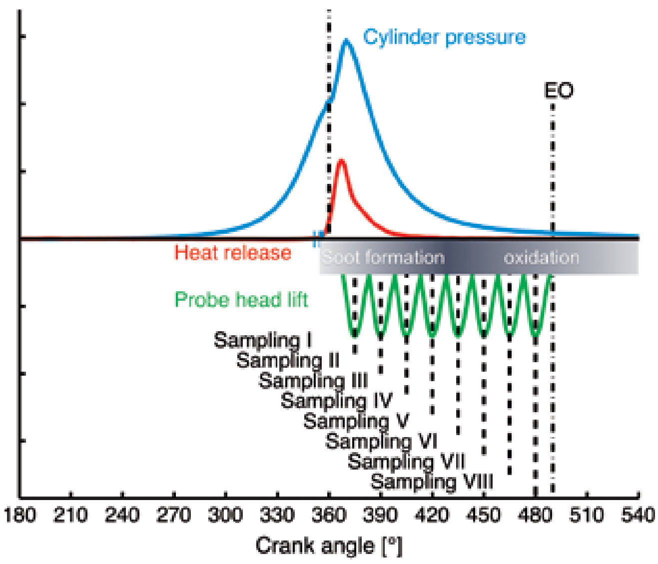

Figure 1: Gas sampling schematic; at the top: pressure curve, heat release and of particles (PM); at the bottom: gas sampling probe head strokes

The Authors

Dipl.-Ing.
Sebastian Pflaum
is Scientific Employee at the Chair of Internal Combustion Engines of the Technische Universität München (Germany).

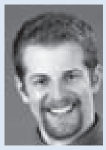

Dipl.-Ing.
Alexander Heubuch
is Scientific Employee at the Chair of Internal Combustion Engines of the Technische Universität München (Germany).

Prof. Dr.-Ing.
Georg Wachtmeister
is Director of the Chair for Internal Combustion Engines at the Technische Universität München (Germany).

MTZ Peer Review
The Seal of Approval for scientific articles in MTZ.
Reviewed by experts from research and industry.

Received .... 9 July 2009
Reviewed .... 9 July 2009
Accepted .... 27 July 2009

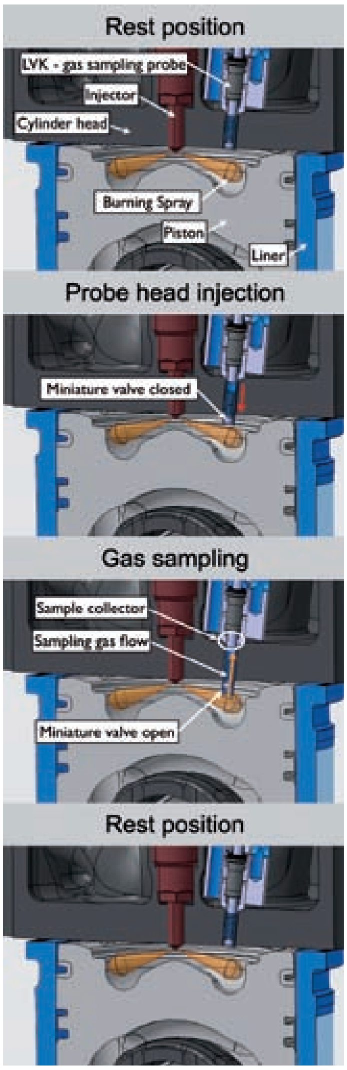

Figure 2: Gas sampling with the new LVK probe head

2.2 The Downsides to Conventional Gas Sampling Valves

Conventional probes described in literature [1] are commonly inserted via the cylinder head. They are fitted flushly with the combustion deck in the area between the valve seats and the gas exchange valves. Those valves are similar to small decompression valves or exhaust valves, measuring about 6 millimeters in diameter. For the gathering of gas samples the valves are usually activated magnetically. They are opened for 1-2 ms by about 0.1 mm. Due to the flush fitting with the cylinder head the samples are taken from the combustion chamber's temperature boundary layer, in which the flames have already been extinguished. Therefore the gases and particles coming from the area of the spray (responsible for most of the soot formation of diesel engines) cannot be studied. Theoretically it is possible to insert a conventional gas sampling probe deeper into the combustion chamber, as far as the injection area. Yet, because the valve head points statically into the spray zone, the injection spray will be highly affected. Furthermore, a valve extending into the combustion chamber will be subject to extremely high temperatures, reducing its durability and supporting the samples' post-reaction. Both alternatives do not allow the sampling of unaffected samples from the main combustion area, thus prompting the LVK to develop a novel probe.

2.3 Solution

At the LVK, a probe was developed and patented with several unique features beyond conventional probes inserted into the combustion chamber. Within 1 ms, a flushly mounted gas sampling probe head is shot through the boundary layer about 10 mm deep into the combustion chamber, **Figure 2**. A sample is taken via a synchronized miniature valve in the probe head. Afterwards, the probe head is withdrawn. Despite the large lift it is possible to reach sampling periods as short (1 ms) as conventional probes. (At 600 rpm 1 ms equals 3.6° CA).

3 Operating Mode and Design of the New Gas Sampling Probe

3.1 Actuation of the Probe Head

For the highly dynamic probe's actuation, three alternatives were extensively reviewed:

- electromagnetic drive: rejected due to large moving masses, long time-lags, large induction currents (electromagnetic compatibility with measurement equipment) and large space requirement
- camshaft drive with control element: rejected because of the barely scannable cam profile plus resulting extreme Hertzian stress
- hydraulic drive: small, lightweight pistons allow for miniature build; high dynamics with gas pressure reservoir and hydraulic pressure up to 400 bar; chosen drive.

3.2 Kinematics of the Sampling Process

In order to enable a probe lift that is as fast and harmonical as possible (comparable to the lift of a gas exchange valve) during the sampling process, the piston driving the probe (probe piston) is accelerated to maximum injection speed, for half of the maximum lift in the direction of the combustion chamber, **Figure 3** (phase 1). This is followed by a decelera-

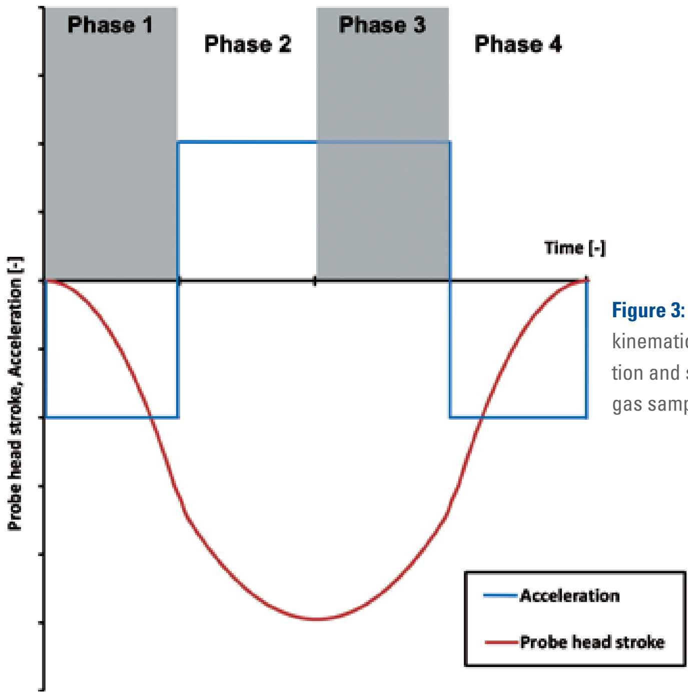

Figure 3: Probe head kinematics; acceleration and stroke while gas sampling

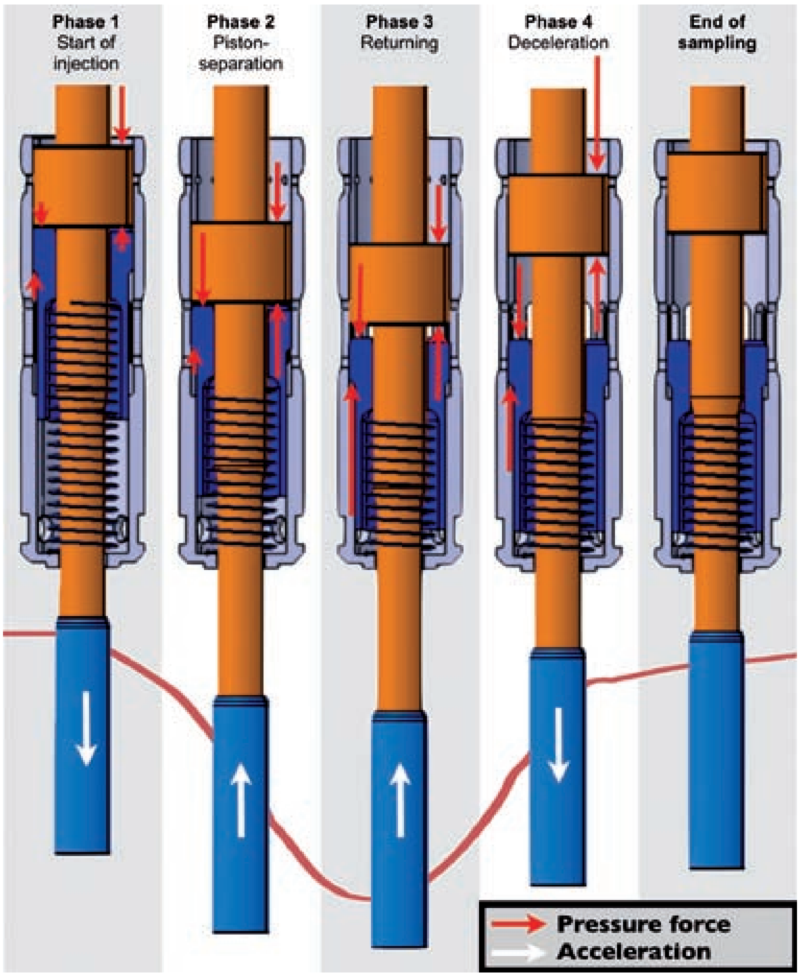

Figure 4: Hydraulic system with pressure forces and accelerations

tion phase (phase 2) with identical absolute acceleration up to the maximum probe lift. (In the area of the maximum lift the probe takes samples from the inner core of the flame. During the following retraction process (phase 3), the probe is accelerated initially and decelerated after half of the lift (phase 4). With an optimal design, the probe is retracted into the rest position at a "docking"-speed of almost zero. High "docking"-speeds would shatter the special gaskets as well as the probe's arrester.

The acceleration curve shows clearly that the resulting accelerating forces for the desired movement (pattern) are supposed to change abruptly after half of the lift. For conventional pistons working both ways with a 4/3-port valve control, this means that after half of the lift the valve control has to be switched from the final "extend" position over the neutral position into the "retract" position. For this action, conventional hydraulic valves of the necessary class of volume flow need about 30-60 ms. Complex high-speed valves still take up to 5 ms. As a sampling time of 1 ms is required, such cylinder controls must be discarded. Other conventional control principles, too, were tested and rejected within the framework of a concept study – mostly because of long switching times. This necessitated the development of a novel control principle for the gas sampling probe.

3.3 Differential Piston Principle

It was possible to find a design detached from conventional hydraulic controls, enabling the desired abrupt and automatic power reversal. For this the probe piston (orange) driving the probe head (light blue) is executed by means of a differential piston with dominating undersurface, **Figure 4**. A control piston running (dark blue) on the probe piston systematically controls the pressurization of the differential piston's lower and larger surface. If the system pressure only butts against the probe piston's upper surface, it will be accelerated in the direction of the pressure chamber (phase 1). A drain throttle, which was designed by means of the simulation, connects the piston clearance to the oil return. Due to the throttle balance, the buildup of only low pressures between the pistons is ensured during phase 1. After half of the lift, the piston clearance passes a control edge, and the system pressure builds up fully between both pistons. At the probe piston, now pressurized on the upper side and on the lower side, the acceleration force now reverses and the piston is being decelerated (phase 2). Shortly before reaching the maximum lift, the gas sampling is triggered for 1 ms. After reaching the point of reversal, the probe piston and the probe are accelerated in the direction of the cylinder head (phase 3) in order to be decelerated via hydraulic damping for the "docking" to the rest position. The entire movement pattern is executed – depending on the hydraulic pressure – in about 3 ms. After the sampling the probe piston has returned to the rest position. Only the control piston still is in the bottom dead center. After the pressure release it is pushed back upwards to the piston's rear side by a spring. There is a need for a resetting break of about 2 seconds. As one sampling already supplies enough particles for the desired analyses, this resetting break does not affect the research in any way.

3.4 Gasket Concept of the Piston Gaskets

As the probe head is propelled with speeds of up to 20 m/s and hydraulic pressures of up to 400 bar occur, the pistons' axial gaskets are presented with enormous challenges. Regarding the gaskets, in general, the tolerated specific friction at the gasket edge is the limiting element. As the sliding speed at the sealing edge is determined by the high injection speed, it is essential to limit the pressure difference to close to zero. This is made possible by a special gasket system combining one annual gap with one axial face seal

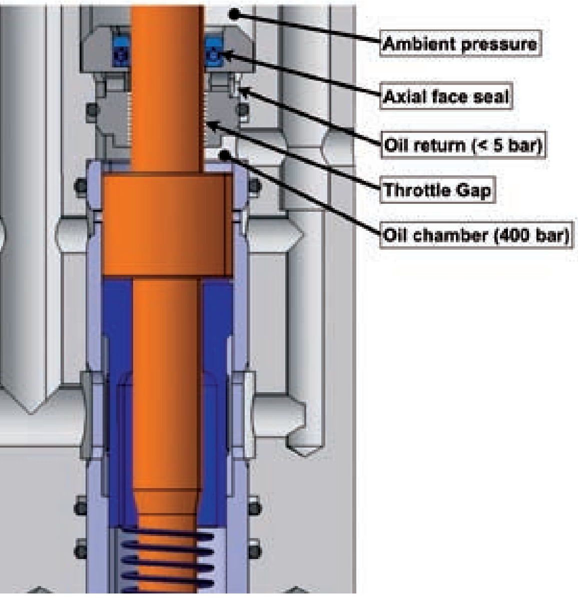

Figure 5: Piston seal combined of split ring an slip ring sealing

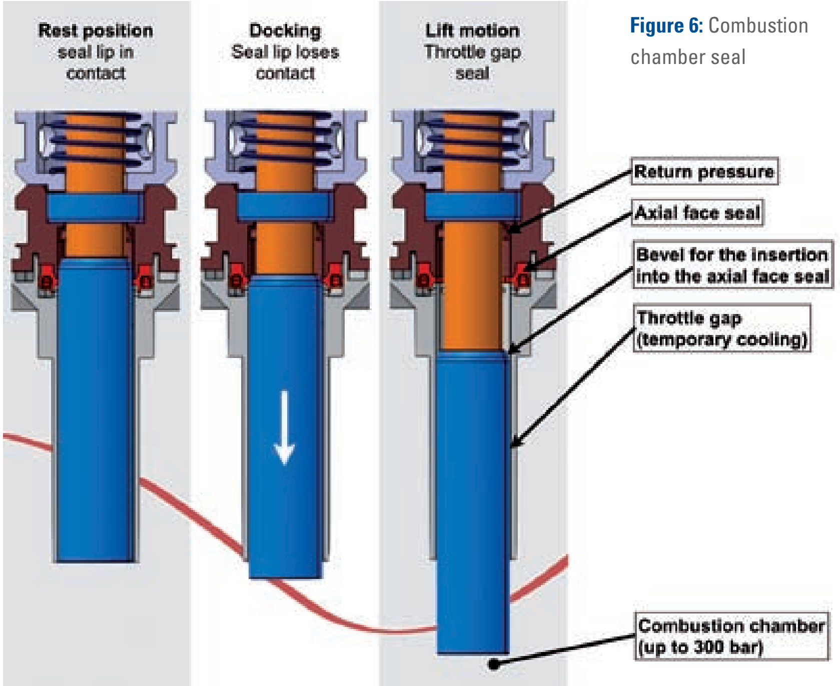

Figure 6: Combustion chamber seal

respectively, **Figure 5**. A slot between the gaskets, which is connected to the oil return, comprises a boundary condition of the pressure, according to which the hydraulic pressure is released via the seal gap to the level of the return pressure. Therefore, only the difference between return pressure and ambient pressure applies to the axial face seal, and high sliding speeds can be tolerated.

3.5 Gasket Concept of the Combustion Chamber Seal

Due to high maximum pressures in the combustion chamber (up to 300 bar) in combination with hot, sooty gases, the combustion chamber's sealing poses the biggest challenge for the probe head's sealing towards the combustion chamber. A valve seat lining for the probe, known from gas exchange valves, was rejected due to its sensitivity to the "docking" speed. A gasket system as described above would be susceptible to contamination and overheating because of the continuous blowby of combustion gas via the gap. The solution was found in a lift-dependent, combined gasket system, **Figure 6**, developed in cooperation with the German company GFD, situated in Brackenheim. For this, at low speeds of the probe within the lift range of 0 to 1 mm, the combustion chamber pressure is sealed off by an axial piston seal between the probe head and the casing. For higher speeds in the lift range of 1 to 10 mm, a throttle gap seal measuring about 15 mm in length was used to seal the combustion chamber pressure. This way, in the rest position, the probe's sealing is absolutely leakproof, protecting the axial gasket which is located behind the throttle gap from the hot combustion chamber gases. Only during the sampling phase of a few milliseconds, hot, sooty blowby gas is discharged in inconsiderable amounts. As the gas cools off in the long throttle gap, it no longer endangers the sensitive axial seal.

3.6 Sampling Valve System in the Probe's Head

For the control of the sampling the LVK specifically developed a highly dynamic miniature valve system to be built into the probe's head. Its opening characteristics are variable for every sampling process and are adjustable to the range. In experimental operation, the extracted combustion gas is expanded and cooled immediately and mixed with inert gas, in order to avoid the sample's post-reaction. Shortly after the sampling valve in the probe head, extracted soot particles are segregated on an easily retractable inwardly cooled specimen holder.

4 Simulation

4.1 Modeling

The desired probe dynamics necessitate an acceleration average of 40.000 m/s². In order to define the required geometry of pistons, control edges and deceleration elements, a simulation model depicting the probe's essential mechanical and hydraulic characteristics, was created by means of MatLab-Simulink, **Figure 7**. For this only one-dimensional equations were used; the gas sampling probe was modeled as a spring-mass-damper-system.

The simulation model's constituting elements are both pistons, onto which acting forces are balanced and integrated. Newton's equations of motion apply accordingly for

acceleration $= \frac{1}{m} * \Sigma_i F_i$,

speed $v = \int \frac{1}{m} * \Sigma_i F_i$ and

path $s = \iint \frac{1}{m} * \Sigma_i F_i$.

Pistons and valves are considered as point masses. The acting forces consist of the built-in springs' reset forces, the contact forces between the pistons, and the pistons and the damping respectively, and the fluid forces and loss terms. All of the parts' elastic characteristics are modeled

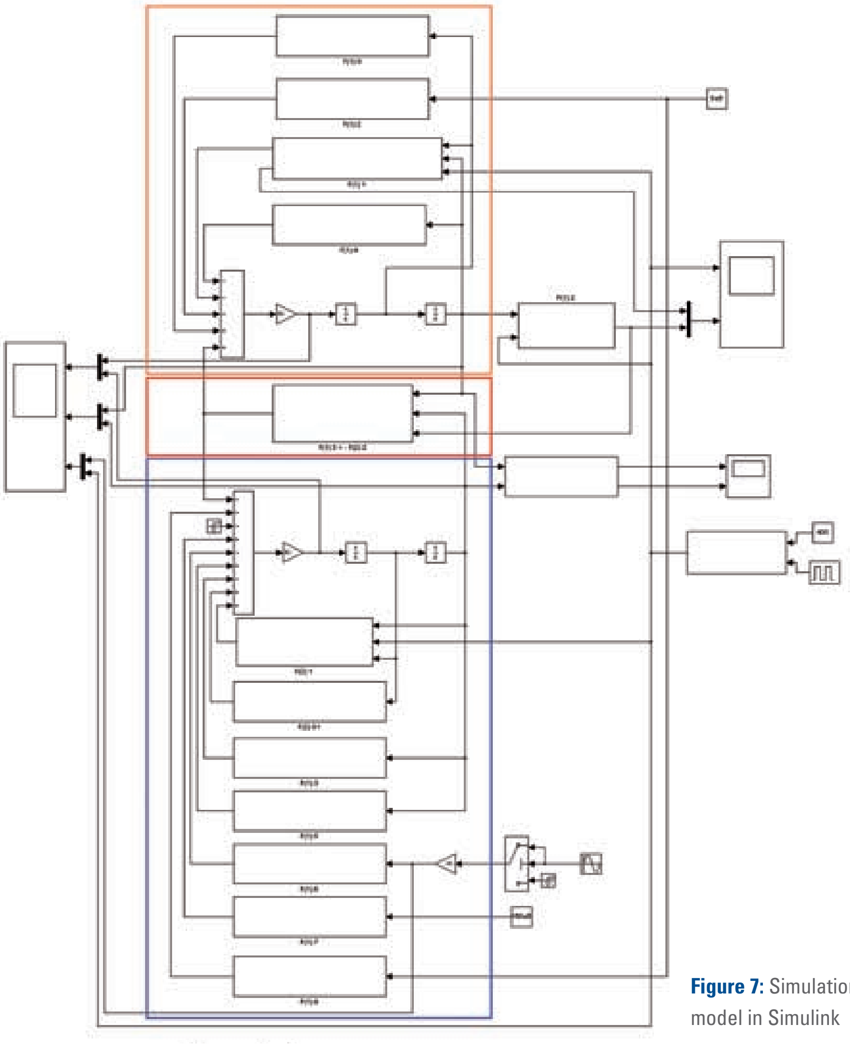

Figure 7: Simulation model in Simulink

as spring elements, whereas respective compensatory spring stiffness was determined according to geometry and material law. This allows the path-dependent calculation of the contact forces, resulting in a steady force path, which can be processed by means of conventional integration methods. Losses caused by friction in the slide face and similar effects were captured in the form of damping terms. A linear, speed-dependent correlation was chosen accordingly:

$$F_D = -K * v$$

For the estimation of suitable damping constants, the LVK was able to fall back on experience with simulations of the needle lift of injectors, where similar conditions apply.

The fluid forces consist of the applied hydraulic pressure and the combustion chamber pressure applying to the combustion chamber probe. That pressure acts on the probe's face surface and has a considerable influence on the probe's behavior. The hydraulic system is depicted by the Bernoulli equation for pipe flows with friction:

$$\Delta p = \zeta \frac{\rho}{2} q^2 + \lambda \frac{l}{d} \frac{\rho}{2} q^2 + \frac{\rho}{2} q^2$$

For this, the fluid is considered ideally incompressible; constant volume as well as constant viscosity is assumed. This allows a simple coupling of piston position and fluid flow in order to calculate the volume of the acceleration- and deceleration chambers. Loss coefficients were estimated according to literature. It was necessary to make allowance for the fact that the equations used apply to stationary, fully formed streams, whereas in this case highly dynamic processes were studied. Due to the large diameters of the supply holes and the drain holes, combined with fairly small volume flows, the flow speed is low, usually under 10 m/s. Given the distinctly larger uncertainties regarding other parts of the simulation, errors can be contained within reasonable parameters. For the flow condition within the sealing gaps and the deceleration gaps, a laminar slot flow is assumed. This allows for the appliance of

$$\Delta p = \frac{12\eta}{d\pi\delta^3} \frac{lQ_L}{1 + 1.5\varepsilon^2} ; \quad \delta = \frac{D - d}{2}$$

4.2 Results and Validation

Figure 8 depicts the probe's calculated and measured lift paths. As can be seen, the short sampling times calculated in the simulation (unverified), as well as

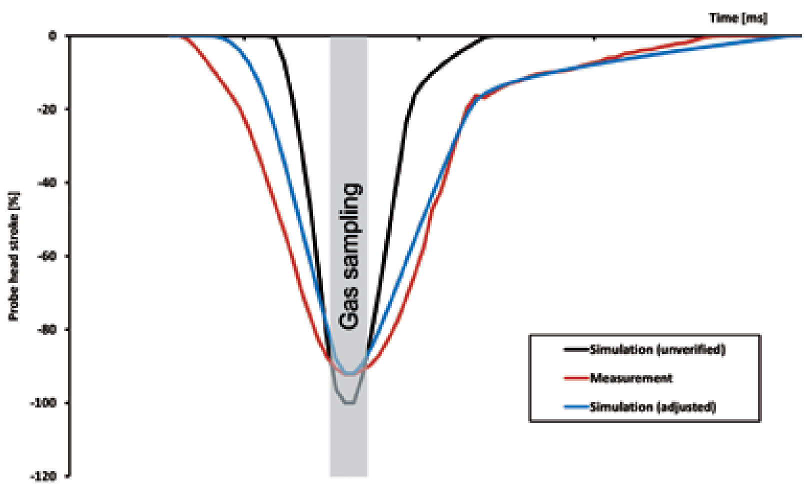

Figure 8: Probe head lifts in comparison: simulation unverified, measurement, simulation adjusted

Table: Model adjustments

	Simulation Parameter	Validated Parameter	Cause
Rate of pressure rise in probe feed	$\frac{dp}{dt} = 2000 \frac{bar}{ms}$	$\frac{dp}{dt} \approx 500 \frac{bar}{ms}$	Long switching time of high-speed valve
Damping coefficient at probe	$K_{Sondenkolben} = -60 \frac{l}{s}$ $K_{Steuerkolben} = -40 \frac{l}{s}$	$K_{Sondenkolben} = -100 \frac{l}{s}$ $K_{Steuerkolben} = -60 \frac{l}{s}$	Increased friction at the axial piston and control piston. Piston seals due to deviations in the rings' surface pressure

the harmonic path of motion, are confirmed by the lift measuring, even though the lift curve lags behind the simulation with regard to its dynamics.

This lag is caused by the switching time of the high-speed valve that triggers the sampling process, resulting in a low rate of pressure rise. If the rates of pressure rise and the damping coefficients are adjusted according to the measured values, the model provides the blue path (Simulation adjusted), which reflects reality most accurately. The **Table** depicts the required model adjustments.

5 Assembly

The German company GFH GmbH in Deggendorf carried out the assembly of all miniature parts, applying novel manufacturing techniques, such as quasi distortion-free plasma-vacuum hardening, as well as plasma polishing. Their products were extremely accurate, allowing for the probe to be installed and initiated straight after assembly, without any reworking. We would like to thank Mr. Preis and Mr. Pauli at the GFH who coordinated the assembly.

6 Test Execution and Initial Results

6.1 Installation of the Gas Sampling Probe and Initial Tests

After its initiation and tests in an external pressure vessel, the probe was installed in the cylinder head of the LVK's 1.8l single cylinder test engine, which has been specifically developed, assembled and set up for research purposes at the LVK, **Figure 9** [2, 6, 7]. The initial gas samplings were undertaken at an engine speed of 600 rpm and a maximum combustion chamber pressure of 110 bar. Fortunately, in its rest position, the probe proved to be sealed tight even during the engine run – no combustion chamber gas was extracted unintentionally.

6.2 Initial Gas Samplings from the Running Combustion Engine

The desired sampling of particles at high combustion chamber pressures was an immediate success. Yet, initially, due to an oversized throttle in the probe's sampling valve it was not possible to extract sample gas at a later phase of the combustion, when the pressure in the combustion chamber has already subsided to about 30 to 40 bar. After the adjustment of the throttle that supplies inert gas to the sampling chamber, it was possible to gather a sufficient amount of particles with a single sampling at every point of the cycle. So the soot structure's analysis with transmission electron microscopy (TEM) was secured.

6.3 Initial Results of Soot Sample Analyses

Within the framework of the research project "Niedrigst-Emissions-Lkw-Dieselmotor (NEMo)" (Low emission truck diesel engine), under patronage of the Bayerische Forschungsstiftung (Bavarian Research Foundation), particle samples are studied at the Lehrstuhl für Mikrocharakterisierung (Department of Materials Science and Engineering Institute of Microcharacterisation and Laboratory for High-resolution Electron Microscopy; IMC) at the University Erlangen-Nuremberg. Soot formation, post-oxidation and the resulting change in the soot structure is studied, depending on combustion process parameters. Initial engine tests produced particle samples from different points of the combustion. **Figure 10** shows the development of the gas concentration during combustion, according to the pres-

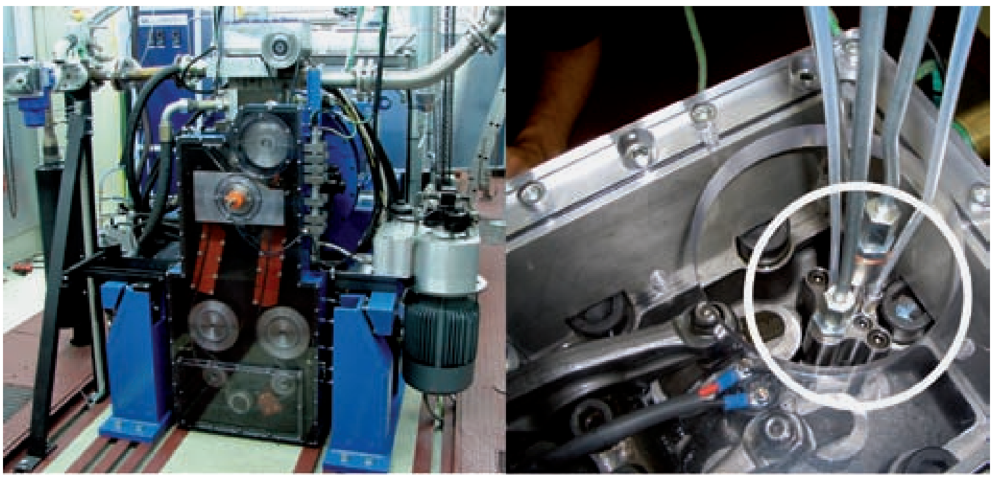

Figure 9: left: LVK research engine; right: gas sampling probe mounted in cylinder head

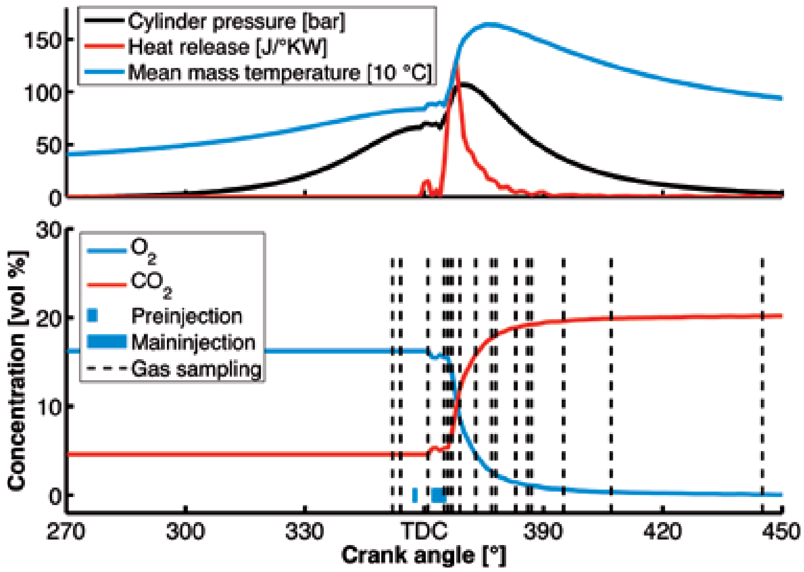

Figure 10: Combustion chamber gas sampling; top: cylinder pressure and heat release; bottom: concentrations and gas sampling

sure curve and rate of heat release. Sampling times are depicted in vertical, dashed lines. The study of particles that were extracted very early proved to be extremely demanding, as unburned fuel vapor is always extracted during gas sampling. This vapor is deposited on the sample and may evaporate during electron bombardment in the microscope (see dark areas in **Figure 11**).

During analysis of the particle samples, the Department of Materials Science and Engineering Institute of Microcharacterisation and Laboratory for High-Resolution Electron Microscopy (IMC) at the University Erlangen-Nuremberg, succeeded in finding formed primary particles even at early points of the combustion. Over the rate of heat release, their increase, their agglomeration and their structural change can be monitored.

The authors apologize for not being able to publish our project partner's extensive results of the analyses at this point.

7 Summary and Outlook

The LVK succeeded in developing and implementing a novel gas sampling probe for research purposes. The probe allows for the sampling of gas and particle samples from the flame core of a running engine at defined points of the cycle. Even during initial testing it was possible to gather samples of the soot particles from the burning spray. The sample analysis via transmission electron microscopy (IMC, Erlangen) showed the primary particles' formation during combustion, as well as their agglomeration, structural changes and post-oxidation effects. The new probe's functionalities by far exceed those of gas sampling valves conventionally used in research, facilitating novel research results. Conventional valves only allow for the sampling of gases from the temperature boundary layer of the combustion chamber.

Further research will be done using the new LVK gas sampling probe, in order to study the formation and post-oxidation of soot during combustion, as a function of process parameters.

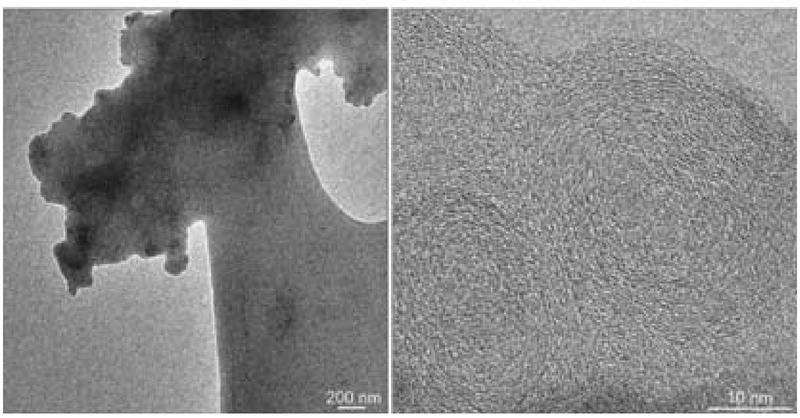

Figure 11: Extracted particles under transmission electron microscope; left: burned fuel spots on sample; right: soot Particles with distinctive structure

Acknowledgement

This investigation was performed in the context of a research project "Niedrigst-Emissions-Lkw-Dieselmotor (NEMo)" (Low emission truck diesel engine), under patronage of the Bayerische Forschungsstiftung (Bavarian Research Foundation). The authors would like to express their thanks to the BFS for supporting this project.

References

[1] Hansen, J.: Untersuchung der Verbrennung und Rußbildung in einem Wirbelkammer-Dieselmotor mit Hilfe eines schnellen Gasentnahmeventils. Dissertation, RWTH Aachen, 1989
[2] Wachtmeister, G.; Pflaum, S.: Motorenentwicklung am Lehrstuhl für Verbrennungskraftmaschinen der TU München. Automobiltechnologie in Bayern, 2007
[3] Bignion, E.: Untersuchung der Kohlenwasserstoff-Emission hubraumkleiner Motoren. Dissertation, Universität Karlsruhe, 2001
[4] Jodocy, B.: Der Einfluss motorischer Parameter auf die Ladungshomogenität im Ottomotor. Dissertation RWTH Aachen, 1990
[5] Wölfle: Untersuchung der Schadstoffbildung im Zylinder eines direkteinspritzenden PKW-Dieselmotors. Dissertation, Universität Aachen
[6] Wloka, J.; Pflaum, S.; Wachtmeister, G.: 3000 bar Common-Rail Einspritzung als Beitrag zur innermotorischen Emissionsreduzierung. Vortrag, 1. Münchner Automobiltechnisches Kolloquium, München, 17.04.09
[7] Pflaum, S.; Wachtmeister, G.: Dieselmotor im Grenzbereich. Vortrag, ATZ / MTZ Konferenz, Heavy Duty Engines. Bonn, 19.11.2008